Report No. FHWA-RD-76-117

URBAN STORM RUNOFF INLET HYDROGRAPH STUDY

Vol. 2. Laboratory Studies of the Resistance Coefficient for Sheet Flows over Natural Turf Surfaces

March 1976
Final Report

This document is available to the public
through the National Technical Information
Service, Springfield, Virginia 22161

Prepared for
FEDERAL HIGHWAY ADMINISTRATION
Offices of Research & Development
Washington, D.C. 20590

NOTICE

This document is disseminated under the sponsorship of the Department of Transportation in the interest of information exchange. The United States Government assumes no liability for its contents or use thereof.

The contents of this report reflect the views of the Utah Water Research Laboratory, which is responsible for the facts and accuracy of the data presented herein. The contents do not necessarily reflect the official views or policy of the Department of Transportation. This report does not constitute a standard, specification, or regulation.

The United States Government does not endorse products or manufacturers. Trade or manufacturers' names appear herein only because they are considered essential to the object of this document.

TECHNICAL REPORT STANDARD TITLE PAGE

1. Report No. FHWA-RD-76-117	2. Government Assession No.	3. Recipient's Catalog No.
4. Title and Subtitle URBAN STORM RUNOFF INLET HYDROGRAPH STUDY: Vol. 2. Laboratory Studies of the Resistance Coefficient for Sheet Flows Over Natural Turf Surfaces		5. Report Date March 1976 6. Performing Organization Code
7. Author(s) C. L. Chen		8. Performing Organization Report No. PRWG 106-2
9. Performing Organization Name and Address Utah Water Research Laboratory Utah State University Logan, Utah 84322		10. Work Unit No. 11. Contract or Grant No. DOT-FH-11-7806
12. Sponsoring Agency Name and Address Office of Research and Development Federal Highway Administration U.S. Department of Transportation Washington, D.C. 20590		13. Type of Report and Period Covered Final Report 14. Sponsoring Agency Code

15. Supplementary Notes

FHWA contract manager: D. C. Woo

16. Abstract

The main objective of this study is to develop an accurate design method for computing inlet hydrographs of surface runoff, with average recurrence intervals of 10, 25, and 50 years, from typical urban highway by flood routing technique.

Resistance to sheet flows over natural turf surfaces is experimentally investigated. The formulation of a functional relationship between the resistance coefficient and controlling parameters for shallow flows over various turf surfaces is essential to the mathematical modeling of surface runoff from urban highway sideslopes covered with different species of turf. An analysis of results obtained from laboratory experiments for laminar flow on Kentucky Blue grass and Bermuda grass reveals that a relationship exists between the Darcy-Weisbach friction coefficient, Reynolds number, and bed slope. Time did not permit tests to be performed on all species of turf other than Kentucky Blue grass and Bermuda grass which can be sodded. However, a general trend of the resistance relationship for shallow flows over such dense turf surfaces as affected by raindrop impact and roughness is qualitatively determined.

This volume is the second in a series. The others in the series are:

Vol No.	FHWA No.	Short Title	NTIS(PB) No. (if available)
1	76-116	Computer Analysis of Highway Runoff	(not yet available)
3	76-118	Hydrologic Data for Highway Watersheds	(not yet available)
4	76-119	Synthetic Storms for Urban Highways	(not yet available)
5	76-120	Parametric Infiltration Models for Sideslopes	(not yet available)

17. Key Words	18. Distribution Statement
Flow resistance, Friction, Laboratory tests, Roughness coefficient, Sheet flow, Soil surfaces, Surface runoff, Testing facilities, Turf grasses	No restriction. This document is available to the public through the National Technical Information Service, Springfield, Virginia 22161.

19. Security Classif. (of this report)	20. Security Classif. (of this page)	21. No. of Pages	22. Price
Unclassified	Unclassified	107	

PREFACE

The work described in this report was performed under contract DOT-FH-11-7806, entitled ''Urban Storm Runoff Inlet Hydrograph Study'' between the Federal Highway Administration and Utah State University. This research contract aimed at the development of an accurate design method for computing inlet hydrographs of surface runoff under intense rainstorms on urban highways. One of the major tasks in this research project was the laboratory determination of the flow resistance on various paved and turf surfaces during and after rainfall. This information is essential to the accurate computation of flow variables at any point and time on the surfaces. A functional relationship between the resistance coefficient and controlling parameters for shallow flows on various turf surfaces was experimentally determined and then incorporated in a mathematical model of surface runoff from a highway sideslope. The mathematical model was formulated in the analytical phase of the project. The work reported herein was part of the laboratory phase of the project.

This report is a summary of important results obtained from the flow-resistance tests on Kentucky Blue grass and Bermuda grass which were sodded. Experiments were not conducted on other species of turf which could not be sodded. Investigations on some species of turf directly seeded on the test bed are still underway, and if any meaningful results can be obtained, they will be reported later. Tests on synthetic turf and paved surfaces were not performed in the present study, but can be done in the future, if time and funds are permitted.

The research was conducted under the general supervision of Dr. Cheng-lung Chen, Professor of Civil and Environmental Engineering at Utah State University. During this research, Messrs. Frank W. Haws and Duard S. Woffinden helped design the stormflow experimentation system. Drs. Neil W. Morgan and Leon A. Huber helped develop the computer control and data acquisition program for operation of the whole system. Professor Duane G. Chadwick helped calibrate the modules of the rainstorm simulator. Mr. I. Wayne Noble helped repair and fix electronic troubles in the system during the experiments. Mr. Gilbert Peterson and his laboratory shop personnel helped build the system. All of the mentioned are, or at one time were, professional staff at the Utah Water Research Laboratory. Without their help, this study could not have been successfully carried out. Gratitude is also due many students who helped fabricate, test, and calibrate the system that consists of thousands of hydraulic and electric components as well as to those who helped collect, reduce, and analyze experimental data in the course of the investigation.

The contract was monitored by Dr. D. C. Woo, Contract Manager, Environmental Design and Control Division, Federal Highway Administration. The author is indebted to him for his ideas to initiate this study and overall research plan, detailed discussions of research conduct of all phases, and critical reviews and comments of the results during the course of the work.

TABLE OF CONTENTS

LIST OF FIGURES

LIST OF FIGURES (CONTINUED)

LIST OF TABLES

LIST OF TABLES (CONTINUED)

LIST OF ABBREVIATIONS AND SYMBOLS

a,b	=	coefficients
C	=	constant
d	=	raindrop size
d_m	=	manometer tube reading of flow depth
$F_1,F_2,\ldots$	=	functional relationships
F	=	Froude number
f	=	Darcy-Weisbach friction coefficient
g	=	acceleration of gravity
h	=	depth of flow in the vertical direction
k	=	roughness size
n	=	Manning's roughness coefficient
Q	=	total discharge
q	=	discharge per unit width
R	=	hydraulic radius of flow
R	=	Reynolds number
R_d	=	raindrop Reynolds number
r	=	rainfall intensity
S_o	=	bed slope
V	=	average velocity of flow section; voltage
V_r	=	average velocity of flow section on rough surface
y_o	=	depth of flow section
y_r	=	depth of flow section on rough surface
θ	=	angle of inclination of bed with respect to horizontal plane
λ	=	roughness concentration
ν	=	kinematic viscosity of water
ρ	=	mass density of water
τ_o	=	boundary shear

INTRODUCTION

In the application of the Saint-Venant equations to the computation of free surface flow, difficulties are encountered in the evaluation of the friction coefficient for flow over a surface when starting with a completely dry condition at the onset of rain. For other conditions, it may not be known what it should be, but it can be evaluated from the known equations. The value of the friction coefficient varies among many other factors with the surface roughness, such as the relative roughness (smooth or rough), roughness concentration (e.g., maximum density for the surface of a sand-grain or turf roughness), roughness mobility or erodibility (fixed or movable), and roughness stiffness (rigid or flexible). The values of the friction coefficient for laminar shallow flows over various practical surfaces can vary over an order of magnitude, of course, depending upon the roughness characteristics of the surfaces under study. A big error in the evaluation of the friction coefficient will result in the unrealistic values of the flow variables computed, if there ever exists a solution of the equations at all. Suffice it to say that success in the mathematical modeling of the surface runoff hinges greatly on the accurate evaluation of the friction coefficient and hence that of the friction slope, aside from many other considerations such as a numerical technique used for solution. The present study is thus directed to investigate, by using unique laboratory equipment, the friction coefficient for flow over various natural turf surfaces which have the maximum density of typical rough, movable, and flexible roughness.

Four flow regimes are known to exist in an open channel, namely, subcritical-laminar, supercritical-laminar, supercritical-turbulent, and subcritical-turbulent [Robertson and Rouse, 1941]. Among them, the first two regimes (laminar) are not commonly encountered in applied open-channel hydraulics except for the place where there is very shallow depths of flow (i.e., sheet flow) and erosion control for such flow [Chow, 1959]. All the four flow regimes are expected to occur in the case of flow over a natural turf surface. However, limitations in the flow capacity of the laboratory equipment does not permit the high range of turbulent flow. Also, lack of time did not permit experiments on all the species of turf originally specified by the Federal Highway Administration. Only two species of turf, Bermuda grass and Kentucky Blue grass, which can be sodded, were tested. (At the time of writing this report, tests are still planned on Crested Wheat grass which is being planted by direct seeding on a test bed.) Despite these limitations and other inherent problems associated with such experiments, laboratory observations reveal a relationship between the friction coefficient and some significant parameters at least qualitatively, if not quantitatively, in the range of subcritical-laminar flow. The experimental results reported herein agreed surprisingly well with those obtained from previous investigators such as Ree and Palmer [1949]. No attempt was made, however, to develop similar relationships in the other flow regimes such as for supercritical-laminar flow because of its inherent instability and degeneration into roll waves [Robertson and Rouse, 1941].

Fixed-bed, open-channel resistance formulas are well known to hydraulicians. These formulas [see, e.g., Chow, 1959; ASCE Committee, 1963; Rouse, 1965] can form the theoretical basis for the development of resistance formulas for movable-bed and vegetated channels. The early investigations of flow resistance in grassed channels can be traced back to the work of the U.S. Soil Conservation Service [Palmer, 1946; Stillwater Outdoor Hydraulic Laboratory, 1947; Ree, 1949; Ree and Palmer, 1949]. Because of the ever-increasing interest in the mathematical modeling of the rainfall-runoff process and sediment yield from a watershed, in which overland flow over paved or vegetated surfaces during or after rainfall plays an important role, attention has been focused on the study of flow resistance for such surfaces. The early work as well as the most recent developments on this subject were extensively reviewed and are discussed briefly.

REVIEW OF LITERATURE

Presence of grass or vegetation in channels causes considerable loss of energy and retardance of flow [Chow, 1959]. The U.S. Soil Conservation Service conducted a series of experiments in channels with various kinds of grass and then computed Manning's n (retardance coefficient) for each of the measured mean velocity, V, and hydraulic radius, R, of flow. They discovered that the retardance coefficient, n, holds a certain relationship with the product, VR, of the mean velocity and hydraulic radius, but this relationship was found to be practically independent of channel slope and shape. A number of experimental curves for the relationship were developed for five degrees of retardance [Palmer, 1946; Stillwater Outdoor Hydraulic Laboratory, 1947; Ree and Palmer, 1949; Ree, 1958]. For details of the five retardance curves and the corresponding kinds of grass, the readers are referred to Chow [1959].

For many years engineers have used these n versus VR curves for the design of vegetated channels without knowing their implications and validity. It is interesting to note, however, that the retardance coefficient, n, can be expressed in terms of the Darcy-Weisbach coefficient, f, as

$$n = \frac{1.49}{\sqrt{8g}} f^{1/2} R^{1/6} \quad . \quad . \quad . \quad . \quad . \quad . \quad . \quad . \quad . \quad (1)$$

in which g is the gravitational acceleration and R is the hydraulic radius of flow. If the Reynolds number, $\mathbf{R}$, is defined as

$$\mathbf{R} = \frac{VR}{\nu} \quad . \quad . \quad . \quad . \quad . \quad . \quad . \quad . \quad . \quad . \quad . \quad . \quad . \quad (2)$$

in which ν is the kinematic viscosity of water, then the product, VR, is actually the product, $\nu\mathbf{R}$, from Eq. 2. Therefore, the n versus VR curve is equivalent to the $f^{1/2} R^{1/6}$ versus $\nu\mathbf{R}$ curve with the only difference being a constant scale factor between the two curves. A close inspection of the n versus VR curves, especially ones for Bermuda grass plotted by Ree and Palmer [1949], reveals that three distinctive flow regimes exist in the plot. The three flow regimes seemingly correspond to those for laminar, transition, and turbulent flows in the f versus $\mathbf{R}$ plot. Because the retardance coefficient, n, and the product, VR, all have dimensions, the plots of the n versus VR curve does not seem to be unique for any species of grass (or degree of retardance). The previous investigators' claim that the n versus VR relationship is practically independent of channel slope and shape may only be true in the turbulent flow regime, but not in the other flow regimes. Given sufficient data points, if the $n/R^{1/6}$ versus $\mathbf{R}$ (which is essentially the same as f versus $\mathbf{R}$) relationship is plotted instead of the n versus VR curve, one may readily discover that the relationship, even in terms of f and $\mathbf{R}$, is not independent of channel slope and shape. This along with other findings will be discussed further in this report.

Factors Affecting Flow Resistance in Vegetated Channels

The importance of developing valid flow equations for the various flows regimes has also been recognized by engineers in surface irrigations [Myers, 1959]. Myers has stated that flow in surface irrigation commonly occurs at low R and a valid equation in this flow regime must include a viscosity factor. This means that the flow under consideration is in the laminar flow regime. Relative roughness is also of extreme importance in shallow flow or furrow flow. Many difficulties encountered in attempts to characterize Manning's n for various conditions of irrigation flow have quite probably resulted from the fact that Manning's equation is not valid for such shallow flow conditions. In large open channel flow, however, turbulence in flow through vegetation is undoubtedly more closely related to diameter, spacing, and flexibility of plant stems and leaves than to the depth of flow or hydraulic radius. Unfortunately, critical Reynolds number for such irrigation flows has not been satisfactorily determined.

In order to develop the more suitable expressions for flow resistance in vegetated channels, Fenzl [1962] investigated the effect of density of the vegetation on the flow characteristics, using a dimensional analysis for conditions of uniform flow in a simulated vegetated channel. A similar dimensional analysis has been applied by Wessels and Strelkoff [1968] to the solution of established surge on an impervious vegetated bed.

Kouwen and Unny [1973], using flexible plastic strips to simulate a vegetative channel lining, studied the variation of the relative roughness with the stiffness of the vegetation. Three basic flow regimes (erect, waving, and prone) corresponding to laminar, transitional, and turbulent flow were observed by Kouwen and Unny [1973] and also by Gourlay [1970] for Kikuyu grass. Kouwen and Unny's plot of the Darcy-Weisbach friction coefficient versus the Reynolds number showed the friction factor to be a function primarily of the relative roughness for the erect and waving regimes. Phelps [1970] also found that the relative roughness was one of the factors that influence the friction coefficient at low Reynolds number, based on laboratory data obtained from experiments on steady uniform flows over a simulated turf surface. However, Gourlay [1970], after reevaluating Kouwen, Unny, and Hill's [1969] data, concluded that the channel slope would also be a parameter in defining the retardance of flow in laminar and transitional flow regimes.

For the prone roughness such as tall grass submerged under deep flow conditions, the flow boundary in effect becomes a smooth wavy surface and the friction factor appears to be a function of the Reynolds number [Kouwen and Unny, 1973]. However, if the plant or vegetation is stiff and tall, the roughness size and concentration such as those utilized in fixed-bed formulas play a more important role than the Reynolds number in the determination of the friction factor for turbulent flow. Several researchers have attempted to modify the Kármán-Prandtl logarithmic resistance equation for use in vegetated channels. The

Sayre and Albertson [1961] idea of combining channel geometry and roughness height to a single parameter in the Kármán-Prandtl equation have been adopted by Kruse et al. [1965], Heermann et al. [1969], Kouwen et al. [1969], Nnaji and Wu [1973], and Li and Shen [1973] for turbulent flow in vegetated channels. Furthermore, Kouwen et al. [1969, 1973] suggested that in practice, use of the ratio of the total cross-sectional area and the area of the cross section blocked by vegetation might be more convenient than that of the relative roughness.

In fixed, rigid-bed, open channel, Koloseus and Davidian [1966b], after experimentally investigating roughness concentrations for different forms of irregularities, concluded that the ratio of the sum of the upstream projected areas to the total floor area was, within some range of density, a satisfactory measure of roughness concentration. They have also found that a simple relation between the resistance coefficient and the roughness concentration, which is independent of the roughness shape (and, possibly, the pattern as well), pertains over some range of concentration. No similar study in this regard has been conducted for flow in vegetated channels.

Unstable flow as manifested by the presence of roll waves and increased channel resistance exists in both laminar and turbulent flows as well as in both subcritical and supercritical flows. Koloseus and Davidian [1966a] proposed that the regimes of open-channel flow should include the stable and unstable, in addition to the laminar, turbulent, subcritical, and supercritical. Because of the potential instability of ultra-rapid, open-channel flow, the usual relation between the resistance coefficient, relative height, and Reynolds number cannot be extrapolated indefinitely. In other words, when the flow is unstable, channel resistance in a uniform open channel is a function of the Froude number. To the writer's knowledge, no data on unstable flow in the field have been collected so as to show an increase in the channel resistance over that for stable flow. Because of rather small increase in the friction coefficient due to instability, it would be very difficult, if not impossible, to differentiate it from that brought about by variations in such other factors as channel roughness, channel shape, and channel size [Koloseus and Davidian, 1966a].

Most shallow flows over plane surfaces, smooth or rough, fixed or movable, porous or impervious, are believed to be in the laminar flow regime. However, laminar flow in a wide channel has been classified as unstable when Froude number is greater than 0.5, which is about one-third of that for a comparable state in turbulent flow. Thus, sheet flows, according to Koloseus and Davidian's [1966a] new classification, may fall in one of the following laminar flow regimes: Stable-subcritical, unstable-subcritical, and unstable-supercritical. Among them, only the study of the stable-subcritical flow regime has been extensively conducted with success for several flow conditions. In the following, previous findings on shallow flows over various existing surfaces such as glass, masonite, cement, concrete, sand, and grass (natural or simulated) with or without rainfall are reviewed.

Shallow Flows Over Various Existing Surfaces

The earlier studies on this subject were concerned with various kinds of smooth surfaces. It was shown by many previous investigators that the theoretical value of C(=24) in the laminar flow equation with the Darcy-Weisbach friction coefficient, f,

$$f = \frac{C}{R} \quad \ldots\ldots\ldots\ldots\ldots\ldots\ldots\ldots \quad (3)$$

was valid for flow on smooth surfaces. For example, Hopf [1910] examined the theoretical C value for laminar flow on polished brass, unfinished brass, and glass surfaces. Jeffreys' [1925] experimental results also confirmed the theoretical C value. Other experiments such as Horton's et al. [1934] on white pine surfaces, Allen's [1934] on painted wood and paint-mixed sand surfaces, Parsons' [1949] on troweled mortor surfaces, Owen's [1954] on polished brass surfaces, and Straub's et al. [1958] on smooth surfaces (constructed of rolled structural shapes) all checked very well with the theoretical C value. All the aforementioned experiments were performed in rectangular channels with small bed slopes.

Discrepancies from the theoretical C value were observed on some previous experiments in rough steep channels with cross-sectional shapes other than a rectangle. For instance, Parsons' [1949] experiments on a rough surface of a mixture of sand and cement gave the increasing C values with increasing surface slopes. Straub's et al. [1958] experimental results obtained from a 90° triangular channel with a rough surface of sand cloth showed clear differences from the theoretical C value. Chow [1959] noted the general trend of the variation of the C value, i.e., being higher for rougher channels as well as higher for rectangular than for triangular channels.

Izzard [1944], after conducting a series of experiments under rainfall, concluded that the C value for shallow flows over paved and turf surfaces departed significantly from the theoretical 24. With a paved surface, he found the C value other than 24, such as 27, 40, and 58, for various bed slopes and rainfall intensities tested while with a turf (Kentucky Blue grass) surface, he obtained the C value as high as 10,000 which was a few hundred times higher than that for the paved surface.

Woo and Brater [1961] studied the effect of channel slope on the C value. For a masonite surface, despite for all 11 channel slopes ranging from 0.001 to 0.06 being tested, the C value obtained from their experiments was about the same, equal to 30.8. However, for a glued-sand surface, they found that the C values increased with increasing channel slopes. Woo and Brater [1961] also analyzed Vicksburg data [U.S. Waterways Experiment Station, 1935] for various packed-sand and cement surfaces. They found that the finest sand surface acted as a very smooth surface having the C value of 24, whereas the C values for other six sand surfaces were larger than 24 with the largest C

values being obtained from the roughest sand surface. The C values for the intermediate sand surfaces obtained from the Vicksburg data were of the same order of magnitude as those determined by Woo and Brater [1961] on the masonite and glued-sand surfaces having the same slopes. The C value for a cement surface with different slopes was found to be 31.6.

In a recent experimental study conducted by Phelps [1975] on a granular surface having spherical roughness elements with a diameter of 0.046 in., he found that a relationship existed between the Darcy-Weisbach friction coefficient, Reynolds number, and relative roughness in the laminar flow range. The f-R relationship, according to his analysis of his data and Woo and Brater's data [1961], follows a similar trend as represented by Eq. 3 with the value of C constant for a given relative roughness instead of channel slope. However, close examination of his experimental data reveals that the relationship would more likely vary with both the relative roughness and channel slope than just the relative roughness alone. Woo and Brater [1961] already recognized this functional relationship when they experimentally studied the flow resistance for a given surface.

Woo and Brater [1962] also studied the additional effect of raindrop impact on the friction coefficient and hence on the C value for shallow flows over the masonite and glued-sand surfaces. They found that the effect of raindrop impact on the C value was much greater for small slopes than for large slopes. However, for channel slopes being greater than 0.01, according to their experimental results, the effect became negative (or reversed). The negative effect on the C value did not agree with Yoon and Wenzel's [1971] study in which a glass surface with slope ranging from 0.001 to 0.03 was tested under various rainfall conditions. Yoon and Wenzel's study showed that the C values increased with both increasing channel slopes and increasing rainfall intensities. In Yoon and Wenzel's experiments, roll waves which occurred at the slope of 0.03 reduced the accuracy of the depth measurements.

Wenzel [1970] further analyzed Los Angeles airfield data [U.S. Army Engineer District, 1954] for five types of rough surfaces: Concrete, simulated turf, roughened simulated turf, excelsior turf, and actual grass. Wenzel's analysis of the Los Angeles airfield data revealed that rainfall did not significantly affect the friction factor in the range of Reynolds numbers studied. A close examination of the simulated turf data [Wenzel, 1970] indicated that the rainfall had actually lowered the value of f, a similar negative effect of rainfall impact on the C value as discovered by Woo and Brater [1962]. Whether or not this negative effect is caused by erroneous depth measurements should be investigated further. Because data points for the excelsior turf, actual grass, and concrete surfaces all fell in either transition or turbulent flow ranges, no definite conclusion from the analysis could be drawn as to the effect of raindrop impact on f as well as on C in the laminar flow range.

Laboratory experiments similar to Yoon and Wenzel [1971] were conducted on a smooth surface of stainless steel by Shen and Li [1973] in

order to find the effect of rainfall on the friction factor, f. Using multiple linear regression analysis, Shen and Li [1973] found that the f value varied with both the Reynolds number and the rainfall intensity for a Reynolds number less than 900, but depended on the Reynolds number only for a Reynolds number greater than 2,000. Additional statistical tests performed by Li [1972] using his and Yoon's [1970] data showed that the C value in Eq. 3 was not highly correlated with the channel slope under a constant rainfall condition. For a Reynolds number between 900 and 2,000, the relationship between the friction coefficient and the rainfall intensity was found to be very complicated, though the linear interpolation of the relationships between the two end points of the upper and lower regimes was still possible. Details of these investigations are also included in Shen's [1972] report.

Other investigations on the Darcy-Weisbach friction coefficient, f, for sheet flow as affected by one or some important parameters such as the Reynolds number, roughness, bed slope, and rainfall intensity are those conducted by Yu and McNown [1964], Emmett [1970], Brutsaert [1971], and Kisisel et al. [1971].

In light of the recent developments and findings in this field, a general function relationship between the Darcy-Weisbach friction coefficient, f, and the relevant parameters such as the relative roughness, channel slope, channel cross-sectional shape, and rainfall intensity for stable-laminar-subcritical shallow flows in vegetated channels can be formulated and then tested by using the unique equipment built at the Utah Water Research Laboratory.

THEORETICAL CONSIDERATIONS

Parameters Describing Flow Resistance

Consider a free surface flow under a rainstorm in a vegetated channel with arbitrary channel section and slope. The resistance coefficient for open-channel flow is well known to hydraulicians. It is a function of all the relevant parameters that describe the characteristics of flow, roughness, channel geometry, and rainfall [Chow, 1959; Rouse, 1965]. Some of the parameters involved are insignificant in rather restricted particular cases, and others are not, depending on the type of flow under study. The major parameters that describe the flow characteristics in open channels are the Reynolds number and the Froude number. As indicated in the previous section, if the flow is very shallow, it becomes either laminar-subcritical or laminar-supercritical. In this case, both the Reynolds number and the Froude number should be considered in the analysis. Unfortunately, laminar-subcritical flow for a Froude number greater than 0.5 and laminar-supercritical flow are extremely unstable. Because of the lack of knowledge in the analysis of instability in the laminar flow range, we may have to confine ourselves to the study of the stable-laminar-subcritical flow conditions only. Within this rather restricted flow regime, the Froude number may be ignored.

The second important group of parameters related to the friction coefficient are those which describe the roughness characteristics. There are many properties which can be used to define the roughness characteristics of a surface, as mentioned in INTRODUCTION. In general, they can be classified into two categories: Geometric and physical. The geometric characteristics of the vegetation in the channel can be best described by use of lengths defining the height and spacing of plants, such as used by Kouwen and Unny [1973], as well as shape, pattern, and concentrations of plants. The physical (or particularly mechanical) characteristics of plants are more difficult to be defined. Kouwen and Unny [1973] have adopted the flexural rigidity of plants in their dimensional analysis. The deflected height of grass, as defined by Kouwen et al. [1969] and later adopted by Gourlay [1970], can be regarded as a sort of the combination of both geometric and physical characteristics of roughness. Whether the resistance coefficient is a function of all the parameters involved in describing the roughness characteristics of the vegetation is a relative matter. In many practical cases, for example, the concentration of plants is considerably small, but important because such roughness can no longer be described by the height of a protrusion (i.e., plant) or by the corresponding relative measure only. However, if the flow resistance is due chiefly to the drag on the roughness elements, such as grass stems which are planted with maximum density, then the roughness concentration, shape, and pattern seem no longer important. Furthermore, if the flow is very shallow, the grass is not, or barely, submerged and the flexural rigidity of grass may not be so important. The most significant roughness parameter for a shallow flow in a grassed channel is thus the relative roughness.

The third important group of the parameters related to the friction coefficient are those which describe the channel geometry. Unless there exists the nonuniformity of the channel in both profile and plan, the important parameters in this group are channel cross-sectional shape and channel slope. In a wide open channel, the shape of channel section is, of course, no longer a variable.

The final group of the parameters which are significant in determining the value of the friction coefficient are related to those which describe the rainfall characteristics. Application of dimensional analysis to a shallow flow under a rainstorm by Yoon [1970] and Wenzel [1970] revealed that there appeared several parameters which might affect the flow resistance. However, after conducting extensive experiments on a smooth surface of glass, they concluded that the terminal velocity and spacings of raindrops were not significant enough to affect the flow resistance. Although some indication of the effect of raindrop size on the flow resistance was reported by Kuhlemeyer and Warner [1963] in their discussion of Woo and Brater's [1962] paper, their experimental results did not seem to give a definite conclusion to the magnitude of its effect. The most significant parameter in this group is thus the raindrop Reynolds number, $\mathbb{R}_d$, defined as

$$\mathbb{R}_d = \frac{rd}{\nu} \quad . \quad . \quad . \quad . \quad . \quad . \quad . \quad . \quad . \quad . \quad . \quad . \quad . \quad . \quad . \quad . \quad . \quad (4)$$

in which r is the rainfall intensity, d is the raindrop size, ν is the kinematic viscosity of water. If d is fixed and the variation of ν with respect to temperature is ignored, the value of $\mathbb{R}_d$ is proportional to r [Yoon, 1970; Wenzel, 1970; Yoon and Wenzel, 1971; Shen and Li, 1973].

From what we just discussed, the resistance coefficient, f, for a stable, shallow flow under a rainstorm over a turf surface with infinite width may be assumed to take the following functional relationship:

$$f = f(\mathbb{R}, k/y_o, S_o, \mathbb{R}_d) \quad . \quad . \quad . \quad . \quad . \quad . \quad . \quad . \quad . \quad . \quad . \quad . \quad (5)$$

in which $\mathbb{R}$ is the Reynolds number [i.e., Eq. 2 after specifying for a wide open channel $R = y_o$ (flow depth measured perpendicular to the bed)], k/y_o is the relative roughness, k is the roughness size for turf, S_o is the bed slope, and $\mathbb{R}_d$ is the raindrop Reynolds number defined by Eq. 4. Although Gourlay [1970] found that both the relative roughness, k/y_o, and channel slope, S_o, were closely related to the resistance coefficient, f, for short Kikuyu grass and also with Kouwen's et al. [1969] data, his analysis seemingly raised a question regarding the necessity of including both parameters in the functional relationship. Phelps [1970; 1975] considered only k/y_o. Although Woo and Brater [1961] took only S_o into account for a given surface, they recognized the importance of including both parameters in Eq. 5. Whether both parameters should be included in a functional relationship for f, such as shown in Eq. 5, merits a comment from the theoretical point of view.

Functional Relationships for Laminar Flow Resistance Coefficient

First, consider shallow steady, uniform flow with depth, y_o, in a wide open channel having a smooth bed surface with slope, S_o. If the flow is stable and laminar,

$$S_o = \frac{3\nu V}{g y_o^2} \quad \ldots\ldots\ldots\ldots\ldots\ldots \quad (6)$$

in which g is the gravitational acceleration, V is the mean velocity of flow, and ν was already defined. Also the boundary shear, τ_o, of the flow can be expressed in the following forms:

$$\tau_o = \frac{f}{4}\frac{\rho V^2}{2} = \rho g y_o S_o \quad \ldots\ldots\ldots\ldots \quad (7)$$

in which f is the Darcy-Weisbach friction coefficient, ρ is the mass density of water, and the other symbols in Eq. 7 were already defined. Immediately, from Eq. 7,

$$S_o = \frac{f}{8g}\frac{V^2}{y_o} \quad \ldots\ldots\ldots\ldots\ldots\ldots \quad (8)$$

the well-known Darcy-Weisbach formula for flow in a wide open channel is obtained. A combination of Eqs. 6 and 8 gives

$$f = \frac{24}{R} \quad \ldots\ldots\ldots\ldots\ldots\ldots \quad (9)$$

in which $R = V y_o/\nu = q/\nu$ is the Reynolds number for flow. Equation 9 is the theoretical expression of laminar flow in a wide open channel and $q = V y_o$ is the discharge per unit width.

Effect of bed roughness

Next, if the original smooth bed surface is roughened artificially by using a roughness size, k, and concentration, λ, but keeping the same bed slope, S_o and discharge q, the flow is retarded, resulting in smaller velocity, V_r, and larger depth, y_r. Under this situation, the flow is supposedly still subcritical with the same Reynolds number because $V_r < V$ and $y_r > y_o$. If y_r is still very small, about of the same order of magnitude as k, the corresponding velocity of flow, V_r, is proportional to S_o in a way analogous to porous media flow, as long as the flow is laminar. Therefore, a general laminar flow equation for a rough surface similar to Eq. 6 may be assumed as

$$S_o = \frac{C\nu}{8g}\frac{V^2}{y_r^2} \quad \ldots\ldots\ldots\ldots\ldots\ldots \quad (10)$$

in which C is a constant for given S_o, k, and q. A comparison of Eq. 10 with Eq. 6 leads to

$$C = 24 \left(\frac{y_r}{y_o}\right)^3 \quad \ldots\ldots\ldots\ldots\ldots\ldots \quad (11)$$

It can readily be seen from Eq. 11 that the C value must be greater than 24 because physically $y_r > y_o$. A slight increase in depth from y_o to y_r will result in a big increase in the C value by a factor of $(y_r/y_o)^3$. Evidently the new flow depth y_r depends primarily on the bed slope, S_o, the original depth, y_o, and some measure of the roughness characteristics such as the size, k, and concentration, λ, if other factors are kept invariable. The discharge, q, is fixed by S_o and y_o through Eq. 6, thus it cannot enter the function if both S_o and y_o are already included. Application of dimensional analysis to this laminar flow on the rough surface leads to

$$F_1 \left(\frac{y_r}{y_o}, \frac{k}{y_r}, \lambda, S_o\right) = 0 \quad \ldots\ldots\ldots\ldots \quad (12)$$

or

$$C = F_2 \left(\frac{k}{y_r}, \lambda, S_o\right) \quad \ldots\ldots\ldots\ldots \quad (13)$$

Woo and Brater [1961] experimentally proved that for flow on a glued-sand surface (k = 1mm or 0.04 in., λ = maximum similar to Nikuradse's experiments), the value of C varies with S_o. Gourlay [1970] used both k/y_r and S_o as reference parameters in his analysis of data points for all flow regimes, but did not elaborate specifically on the analysis of the C value as affected by both parameters within the laminar flow regime. Meanwhile Phelps [1970; 1975] took only the relative roughness, k/y_r, into consideration in his analysis of shallow flows over a simulated turf surface (k = 0.01 ft assigned) and later over a granular surface. In practice, as Phelps [1970] noticed, the measurement or assignment of k posed a problem. Without accurate measurement of k, the effect of k or k/y_r on the C value cannot be studied.

Effect of raindrop impact

Instead of roughening the smooth bed, let raindrops act on the free surface to the same effect that the smooth bed is roughened. The steady uniform flow with discharge q on the smooth surface with slope S_o is now changed to the spatially varied flow due to adding mass from rain. Also, the flow is retarded by additional resistance caused by adding momentum (or energy) from rain. Because the disturbance of the water surface caused by raindrops is physically equivalent to that caused by the roughness of the bed surface, the preceding discussions in connection with the surface roughness also apply here. It is at once evident that the C value is also a function of r, or a dimensionless form thereof, R_d, as defined by Eq. 4, in addition to those parameters shown in Eq. 13; namely

$$C = F_3\left(\frac{k}{y_r}, \lambda, S_o, R_d\right) \quad . \quad . \quad . \quad . \quad . \quad . \quad . \quad . \quad . \quad . \quad . \quad (14)$$

Whether the effect of r on the C value is greater or smaller than that of k is simply a relative matter. It was judged from laboratory observations [Wenzel, 1970; Yoon, 1970; Yoon and Wenzel, 1971] that the effect of r on the C value would be maximum for flow on the horizontal smooth surface (i.e., $S_o = 0$ and $k = 0$), but would decrease as both k and S_o increase. Because turf surfaces are very rough and highway side slopes are usually steep, from 0.5 percent to 1.5:1, the effect of r on the C value is believed to be insignificant. Furthermore, because the roughness concentration of the turf surface, similar to that of the Nikuradse sand surface, is constant and is fixed at the maximum value, the variation of the parameter representing the roughness concentration, λ, in Eq. 14 can be neglected. Removing λ and R_d from the functional relationship for C, Eq. 14, yields

$$C = F_4\left(\frac{k}{y_r}, S_o\right) \quad . \quad . \quad . \quad . \quad . \quad . \quad . \quad . \quad . \quad . \quad . \quad . \quad (15)$$

The hardest to determine with regard to the measurement of the relative roughness, k/y_r, is probably the bed level of the rough surface over which k and y_r are measured. The geometric mean bed level first suggested by Schlichting [1936] and later adopted by Koloseus and Davidian [1966a] may be used. The adoption of the equivalent Nikuradse sand-grain size, k_s, as a roughness standard for the rough surface has merit because the surface roughness is then put in terms of a single type of roughness that is easily visualized and appreciated. It has the further advantage that k_s is independent of concentration considerations because Nikuradse's roughness concentration is constant and is fixed at the maximum value. However, adding to the difficulty in the measurement of k is the measurement of y_r which usually amounts to merely a fraction of an inch for very thin flow. An error, say by a small fraction of an inch, in the demarcation of the mean bed level or flow depth measurement can easily result in the over- or under-estimation of the f and hence C values.

To measure k accurately for different species of turf is a formidable task. For simplicity in the present analysis, only the functional relationship between C and S_o for each species of turf was considered without further determining k or k/y_r; namely

$$C = F_5(S_o) \quad . \quad . \quad . \quad . \quad . \quad . \quad . \quad . \quad . \quad . \quad . \quad . \quad . \quad . \quad (16)$$

Experiments were conducted to investigate this functional relationship for each species of turf and a special piece of equipment was developed for this purpose.

DEVELOPMENT OF EXPERIMENTAL EQUIPMENT

In the present study, tests on the effect of raindrop impact on the flow resistance were not contemplated due mainly to the limit in time to perform such tests, aside from some theoretical considerations, as discussed in the preceding section. If this is the case, the major equipment needed in the flow-resistance experiments is a tilting test bed which can simulate different urban highway sideslopes covered with various species of turf. For use with the test bed a rainfall simulator was built to aid in investigating the infiltration characteristics of slant turf surfaces overlying various topsoils and subsoils. Because some features of the test bed constructed were decided in conformity with the design criteria of the rainstorm simulator, the concurrent description and discussion of the whole stormflow experimentation system including the rainstorm simulator and the test bed are desirable. Although it is beyond the scope of the present study, the rainstorm simulator might be used to study the effect of raindrop impact on the flow resistance.

The stormflow experimentation system that is capable of reproducing the natural conditions of rainstorms (moving or stationary), soil, and vegetation with sufficient dimensional fidelity for prototype testing of surface and subsurface stormflows has recently been completed at the Utah Water Research Laboratory (UWRL). The system consists of computer-controlled rainstorm simulator, a forcibly-drained tilting test bed, a computer, a console for manual control, and a sunlight simulator for plant growth, as schematically shown in Figure 1. Each of the equipment in the system is briefly described below:

Computer-Controlled Rainstorm Simulator

An extensive review of rainfall simulators and a critical evaluation of their strengths and weaknesses had been made before a new one with versatile features was designed and built at the UWRL. Design criteria as well as construction, operation, and performance of the new rainstorm simulator will be given in detail in a separate report. Reported herein is simply the present configuration of the rainstorm simulator developed.

The rainstorm simulator consists of 100 drip modules. Each module, as shown in Figure 2, consists of a rectangular box 24 in. (60.96 cm) square and an inside depth of 3/4 in. (1.90 cm). The bottom side of this box is drilled with 3/8 in. (0.95 cm) diameter holes spaced one inch apart in a triangular pattern. Each hole is filled with a rubber stopper which contains a brass tube 2 in. (5.08 cm) long with an inside diameter of 0.032 in. (0.81 mm) and an outside diameter of 0.082 in. (2.1 mm). These brass tubes make the drop-formers when the box is filled with water under constant pressure and produce drops approximately 0.177 in. (4.5 mm) in diameter. Each module contains 672 tubing tips.

Water under constant pressure enters the box through an orifice plate which controls the flow into the box and through the tubing tips.

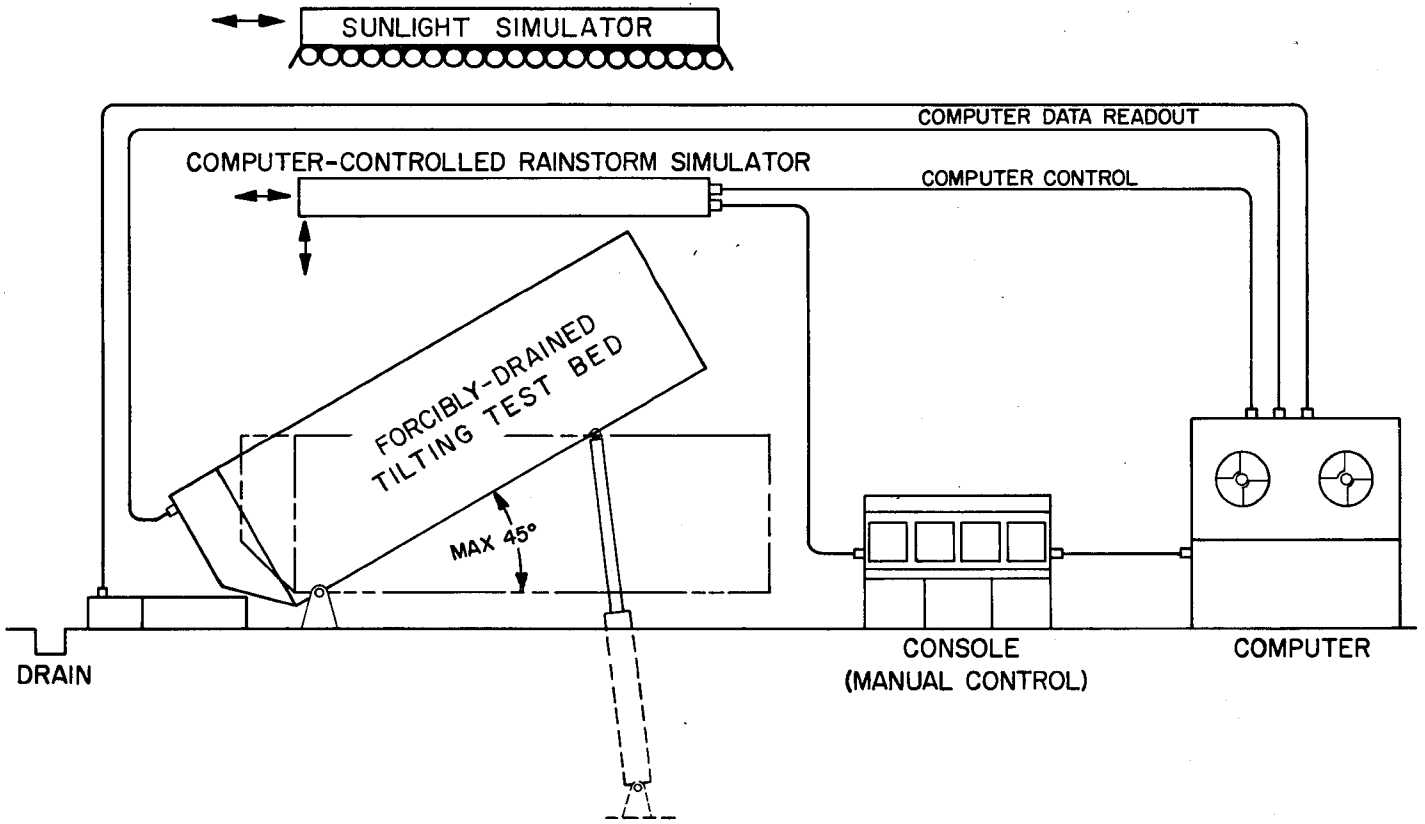

Figure 1. Block diagram of stormflow experimentation system.

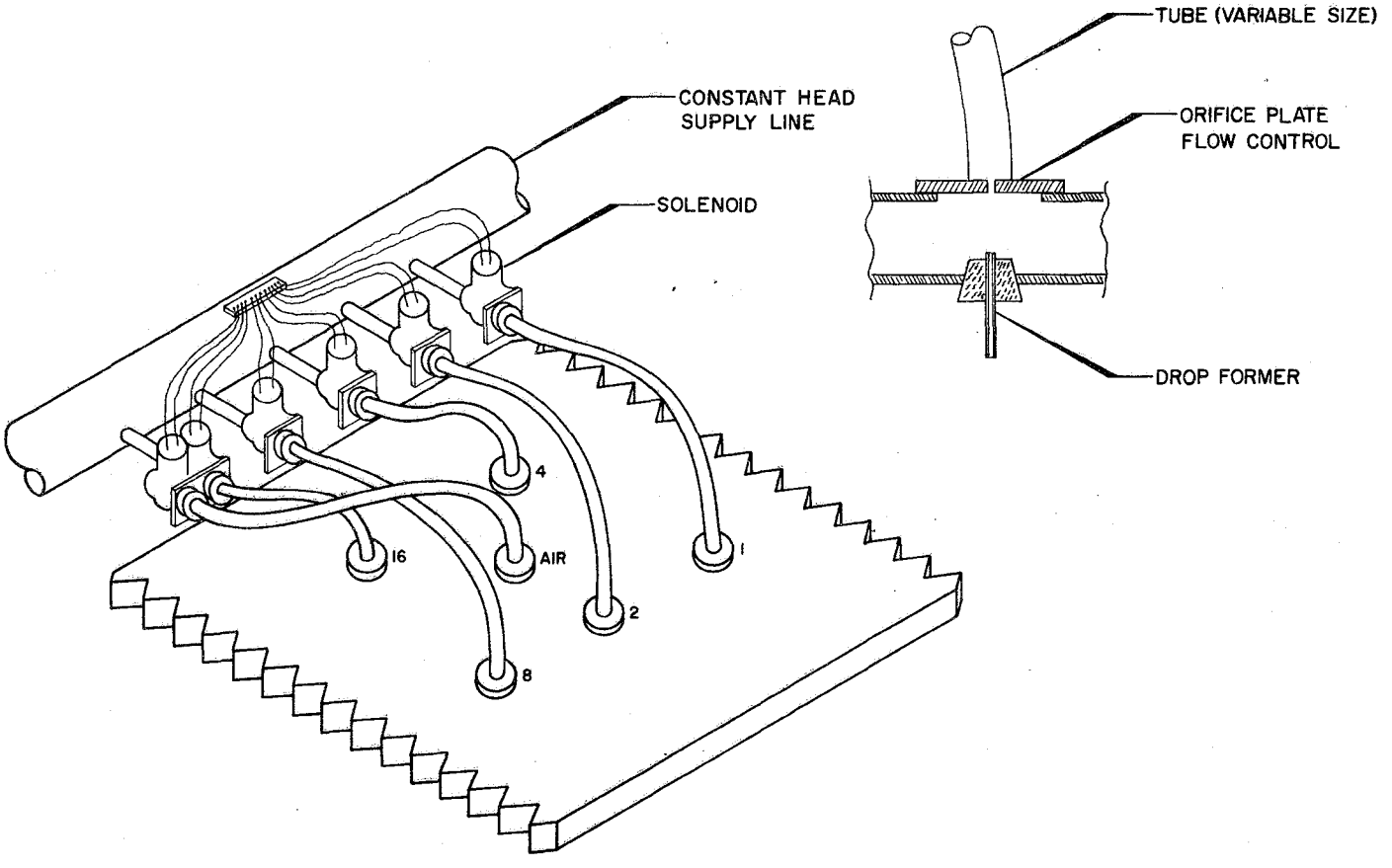

Figure 2. Typical rainstorm simulator module.

There are five different orifice plates leading into each module and the flow through these plates is controlled, either on or off, with a d.c.-operated solenoid valve. The areas of the orifices in each of the five plates have been determined to give approximately a ratio of 1:2:4:8:16 (the same code numbers shown in Figure 2), the areas doubling with each increase in size of orifice. Flow rates into the box can thus be controlled by opening or closing the five solenoid valves with 31 possible combinations, which permit rainfall intensities to vary from 0 to 31 in./hr (787.4 mm/hr) in 1 in./hr (25.4 mm/hr) increments. Each solenoid is controlled either manually at a console or by a computer kept at a distance from the console. During initial filling of the box, a sixth opening on the top (marked AIR in Figure 2) is opened to allow air to escape. As soon as the box is completely filled with water, the air opening is closed by using another d.c. solenoid valve.

Each module was cast in two halves in silicone rubber molds with a polyester resin filled with chopped glass fibers and solid glass spheres. The two halves were then cemented together. Rubber stoppers and brass tubing tips were inserted in the openings after casting was complete. The orifice plates were constructed of 0.005 in. (0.127 mm) thick stainless steel by a photoetching process and were cemented over openings cast in the top of the module. A brass tubing insert connector was attached to the orifice plate and provided a means of attaching the plastic supply tubes.

The full scale rainfall simulator consists of 100 modules arranged in a square pattern to cover a 400 sq. ft (37.16 sq. m) area. Storm patterns can be reproduced in temporal and areal increments of 1 in./hr (25.4 mm/hr) with a spatial resolution of 2 ft (60.96 cm) square. The modules are supported on a structural system which can position the modules over the test bed with a maximum 16-ft (4.88 m) raindrop falling distance.

The support rack for the modules was constructed of 3 in. (7.62 cm) diameter nickel steel pipe which also serves as the water supply manifold to the modules (see Figure 3). The pipes are spaced 24 in. (60.96 cm) apart and are connected at each end to a larger 6-in. (15.24 cm) pipe which in turn is connected with flexible plastic hose to an 8-in. (20.32 cm) supply pipe coming from the constant head tank (see Figure 4). All pipes and hoses from the constant head tank to the modules were sized large enough to keep head losses as minimal as possible. The constant head supply tank was provided with a weir having an equivalent overflowing length equal to 14 ft (4.27 m). The rated maximum flow is 0.287 cfs (0.00813 cms) (31 in./hr x 20 ft x 20 ft) which gives a total variation in head over the weir less than 3/8 in. (9.53 mm). The constant head tank is adjustable vertically so that a constant head, 3.53 ft (1.08 m), can be maintained at any elevation above the rainfall simulator.

The combined water supply-structural system is supported at each corner on pedestals so that the system rests on the ground when servicing is required. As shown in Figure 5, a block and tackle hoist system,

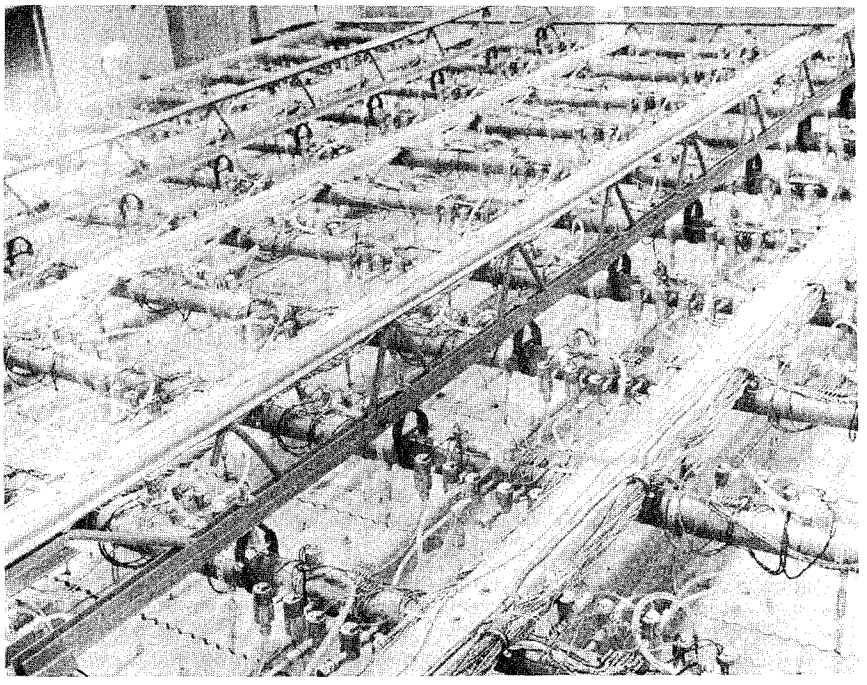

Figure 3. A top view of combined water supply-structural system for 100 modules. The photo shows that each module has 5 solenoid valves for intensity control and 1 solenoid valve (at top of 3-in. pipe) for air release.

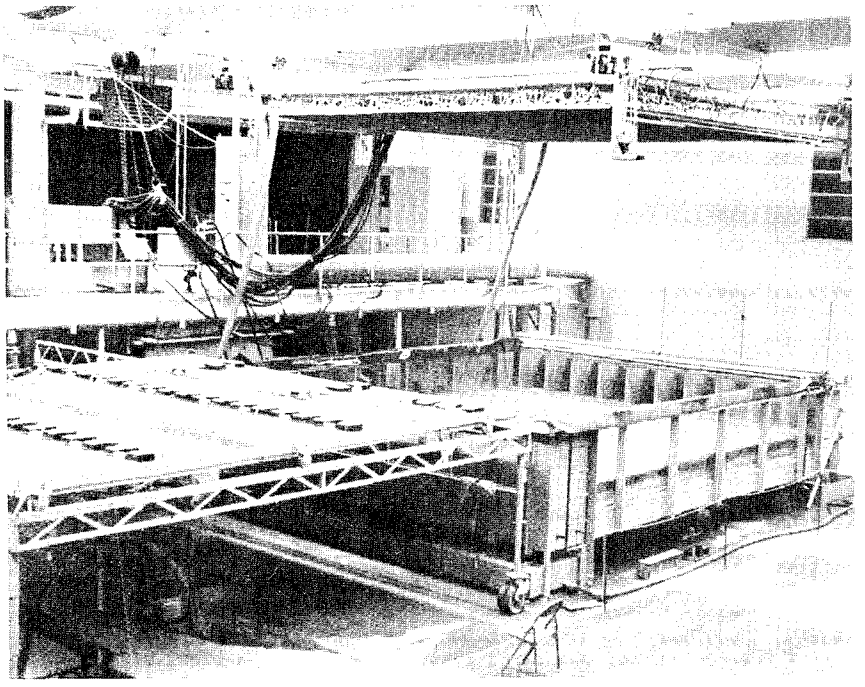

Figure 4. A photographic view of rainstorm simulator positioned over test bed, with combined water supply-structural system. Sitting beside test bed (left front) is a sunlight simulator which can be slid over test bed when rainstorm simulator is not in operation.

mounted on horizontal rails fastened to the roof beams, raises the rainstorm simulator to the desired vertical height and also moves horizontally over the test bed. The individual modules hang from the pipe-support structure on turnbuckles (see Figures 3 and 5) which further support horizontal cables placed under the modules (see Figure 6). The turnbuckles permit the modules to be leveled. As shown in Figures 2 and 3, the five solenoid valves for intensity control are mounted directly on the 3-in. (7.62 cm) pipes by means of a welded length of 3/8-in. (9.53 mm) pipe nipple. A various diameter, flexible plastic tubing connects each solenoid valve to the module. The wiring to the solenoids lies on top of the pipe structure and the 600 wire pairs terminate in a console box (Figure 7) where a manual control system has been constructed with cables transmitting control signals to a remote computer interface. The console also contains control switches to operate the four lifting hoists. A 500-amp d.c. power supply operating at 28 volts operates the solenoid valves as well as the d.c. motor drives on the lifting hoists.

Forcibly-Drained Tilting Test Bed

The tilting test bed is essentially a 20 ft (6.096 m) square box hinged at the downstream side and supported upon hydraulic cylinders near the upstream tank. The telescope-type cylinders can be extended to tilt the test bed from the horizontal. The test bed in its present form is built to support a 1 foot (30.48 cm) deep soil layer, but with slight modification can accommodate a soil layer 2 feet (60.96 cm) deep. The soil is supported on a porous floor over a suction chamber which is divided in the tilt direction into ten 2-ft (60.96 cm) wide compartments, as shown in Figure 8. The suction chamber is connected to a vacuum pump to permit the application of suction pressures to the bottom of the soil layer as a quick solution to the poor drainage problem in the soil. It is found that the performance of the present suction chamber is most efficient when the soil moisture content is above field capacity. As the soil moisture content decreases, soil pores essentially become the media to leak air from atmosphere to the suction chamber to such a degree that suction created in the chamber can no longer be effective to suck water out of the soil. Water infiltrated into the chamber can be measured in each separate compartment.

Water can be applied as a constant flow through a head tank at the upstream end of the test bed and/or can be applied anywhere to the soil surface by means of the rainfall simulator. The present capacity of the head tank with the test bed in a horizontal position is 20 cfs (0.566 cms) and the rainfall simulator can produce flows up to 31 in./hr (787.4 mm/hr) over the 20 ft x 20 ft (6.096 m x 6.096 m) area. The runoff from the test bed exists through ten 2-ft (60.96 cm) wide channels at the downstream end of the test bed where the flow is measured. Hinged flaps in the exit channels can be varied to a maximum depth of 24 in. (60.96 cm) for controlling the depth of water flowing over the soil surface. The side walls of the test bed are built of one-inch (2.54-cm) thick plexiglass to permit visual examination of the surface and subsurface flows.

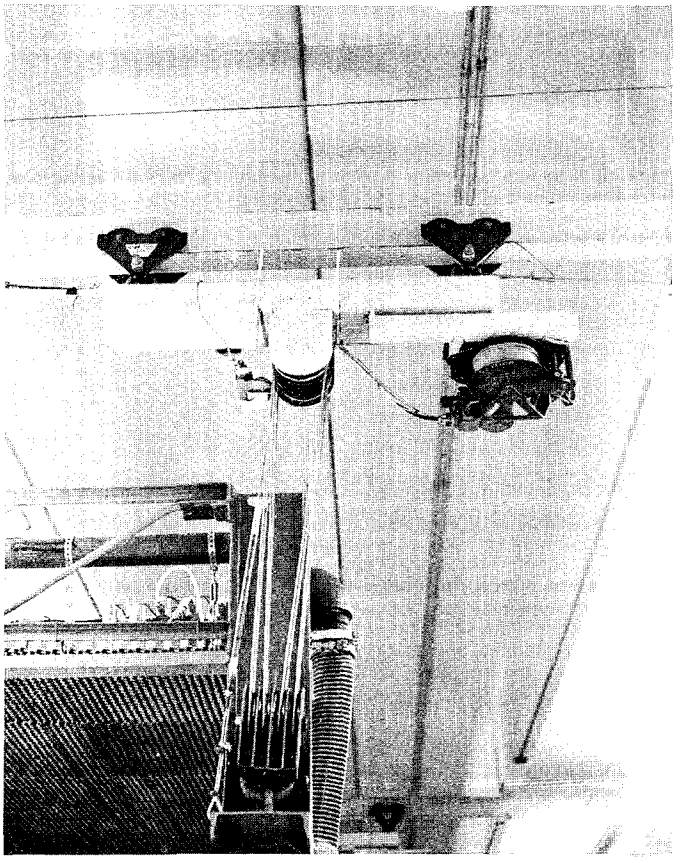

Figure 5. A view of a pedestal and a hoist at each corner of combined water supply-structural system for rainstorm simulator.

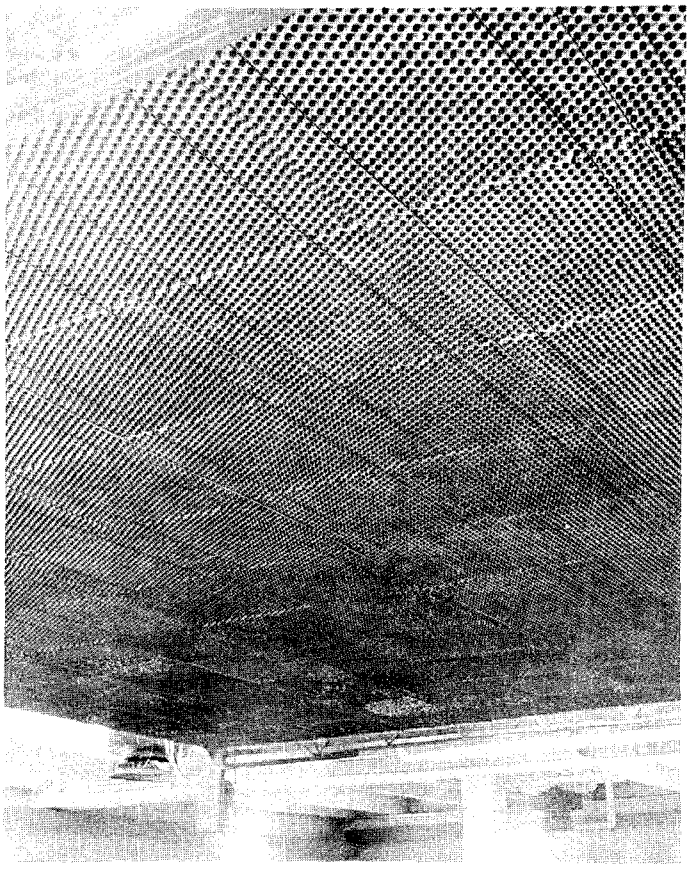

Figure 6. A bottom view of 100 simulator modules supported by horizontal cables.

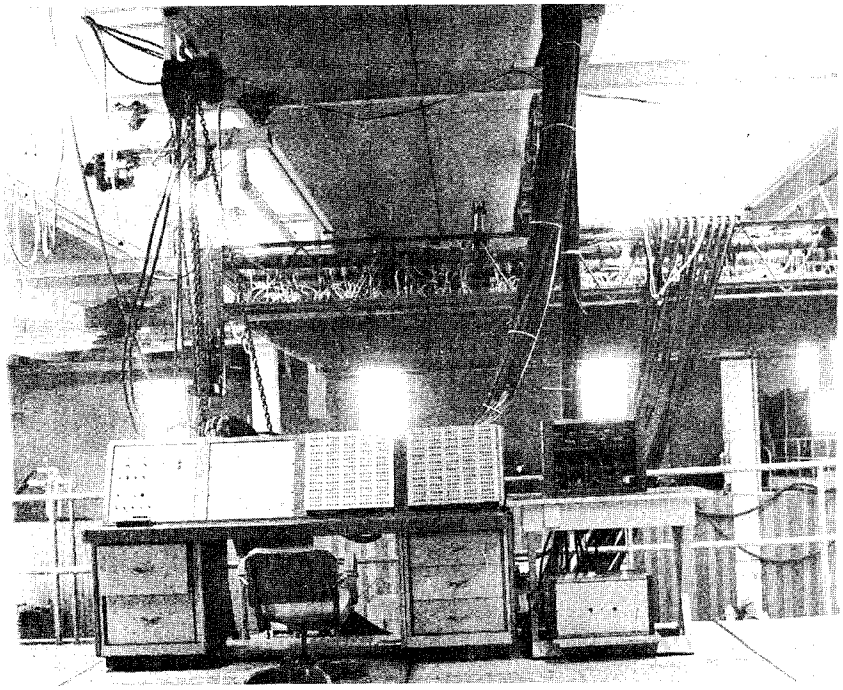

Figure 7. Console for manual control for each of 600 solenoid valves. The console also contains control switches for operating four hoist systems to position rainstorm simulator, two hydraulic cylinders to tilt test bed, and a vacuum pump to drain water from test bed.

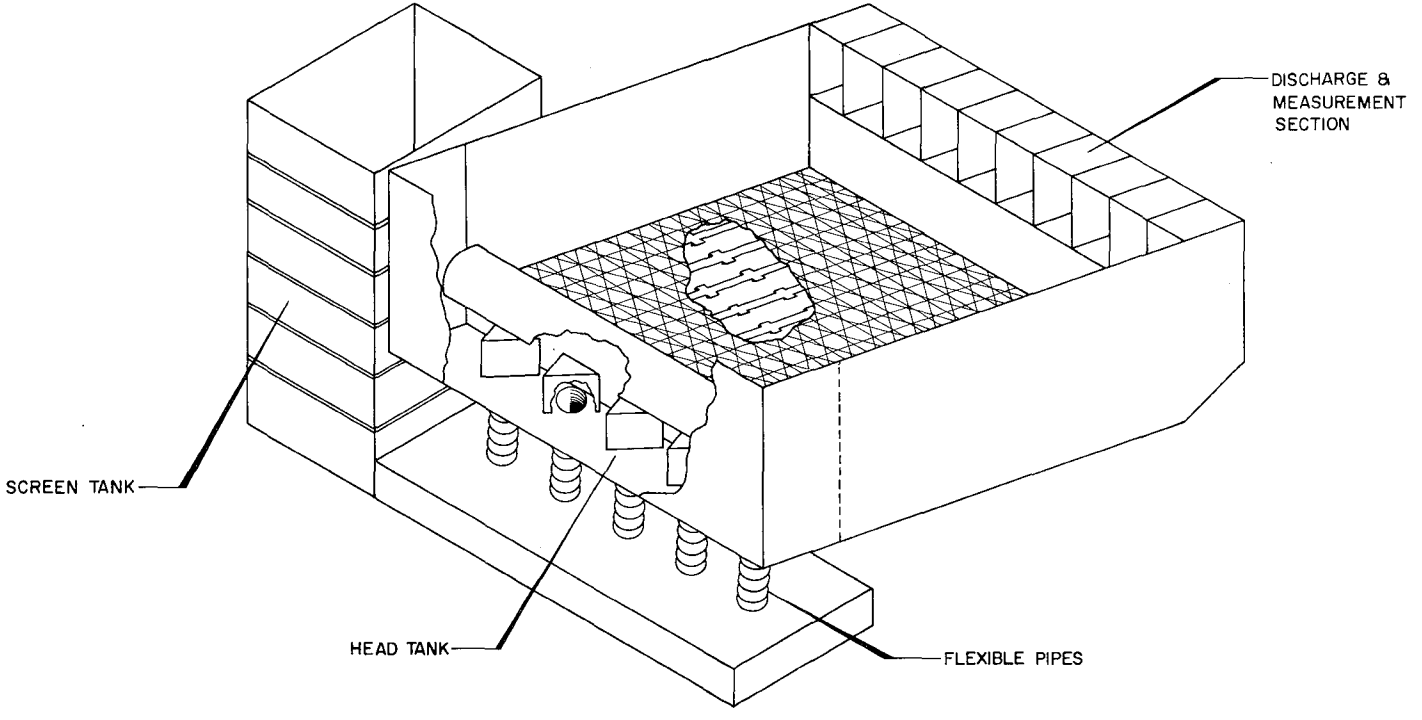

Figure 8. Schematic diagram of forcibly-drained tilting test bed.

Water enters the test bed through a baffled head tank which has dissipated sufficient energy in the water to permit a quiet, smooth approach over the soil surface, as schematically shown in Figure 8. This head tank can be removed from the rest of test bed, if desired, so that the test bed can be tilted to a maximum 45° angle when it is used for rainfall interception only. The head tank is coupled to a supply line with flexible pipes to permit the test bed to be tilted to desired slopes. A screen tank was installed to trap debris and trash entrained in Logan River water which is withdrawn from the reservoir to the laboratory. Two three-stage hydraulic cylinders, as shown in Figure 9, provide the force necessary to tilt the test bed.

A data collection system consists of 10 discharge-measuring flumes, 20 depth-measuring manometers, and 24 soil moisture blocks. Each of the discharge-measuring flumes collect water passing through the 2-ft (60.96 cm) exit section on the test bed and measure the discharge by reading the water stage in a stilling well. In each stilling well located at the end of each flume is a float mechanism which turns an electric potentiometer. The voltage output of the potentiometer changes with the depth of water in the stilling well which in turn gives the discharge proportional to the voltage reading. For covering a wide range of the measured discharge, two sets of the discharge-measuring flumes were built. One set, as shown in Figure 10, which is large and measures the discharge ranging from 0.04 to 1 cfs (0.00113 to 0.0283 cms), was used for friction tests only, while the other set, as shown in Figure 11, was used for measuring smaller discharges ranging from 0.0008 to 0.06 cfs (0.0000227 to 0.00170 cms) for both friction and infiltration tests.

Along the centerlines of the third and eighth 2-ft (60.96 cm) exit sections, two rows of ten depth-measuring manometer tubes were installed on the test bed, spacing 2 feet (60.96 cm) apart, except for the first and last ones that were set 1 foot (30.48 cm) away from the upstream and downstream edges. Each of the 1/2-in. (1.27 cm) aluminum manometer tubes on the bed side is extended through the soil layer and the suction chamber. The top end of the tube capped with fine-mesh brass screen is positioned at the geometric mean level of the soil surface while the bottom end of the tube is clamped to the bottom plate of the suction chamber with a 3/4-in. (1.91 cm) straight, strain relief, liquid-tight connector. Across the bottom of the test bed, as shown in Figure 12, is a flexible plastic tube with a short soft rubber tube which connects the bottom end of the manometer tube (aluminum) on the bed side to the other end of the 1/2-in. manometer tube (plastic) that was pivoted to the side wall of the test bed to maintain in the vertical line when the test bed is tilted. Helical wound resistance wires were inserted in the vertically-hanged manometer tube (plastic) and their voltage output was calibrated individually against the meniscus (water surface) in the tube. Before starting any experiment, the manometer tubes are first filled with water at the soil side and the geometric mean bed level is read automatically by use of the computer. Any appreciable change in the water depth on the soil surface will respond by raising or dropping the meniscus in the manometer tube, where the water depth difference is measured in terms of voltage difference by means of the resistance wires.

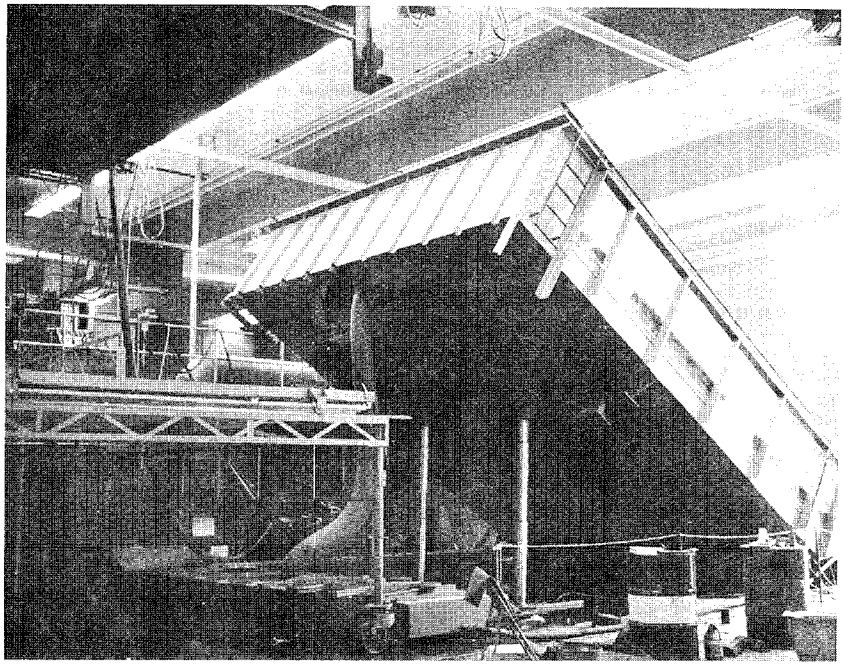

Figure 9. A photographic view of test bed which is tilted with two three-stage hydraulic cylinders. A flexible pipe is used to connect head tank to a rectangular conduit leading to screen tank.

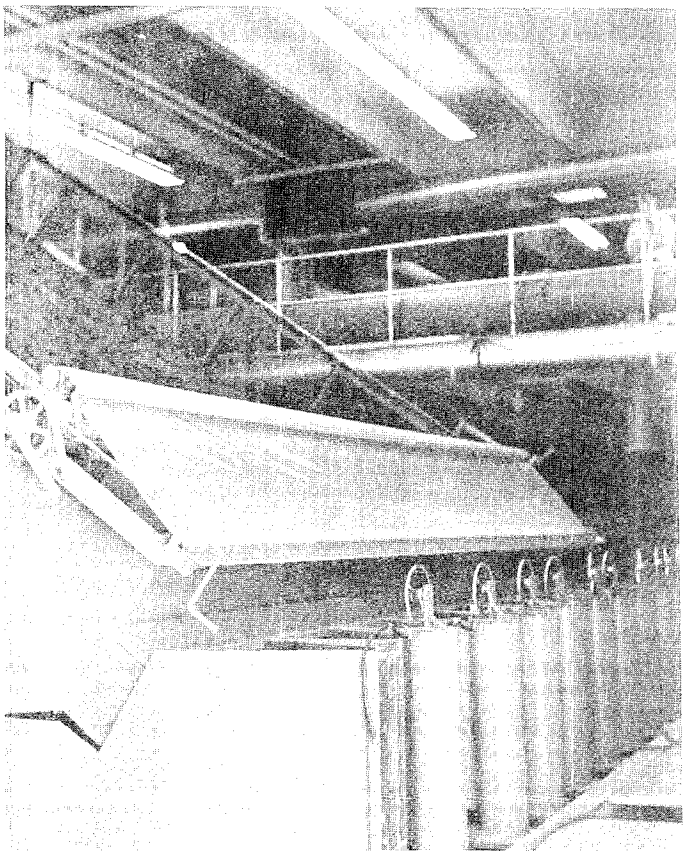

Figure 10. Large discharge-measuring flumes for friction tests. Measurable discharge for each flume ranges from 0.04 to 1 cfs (0.00113 to 0.0283 cms).

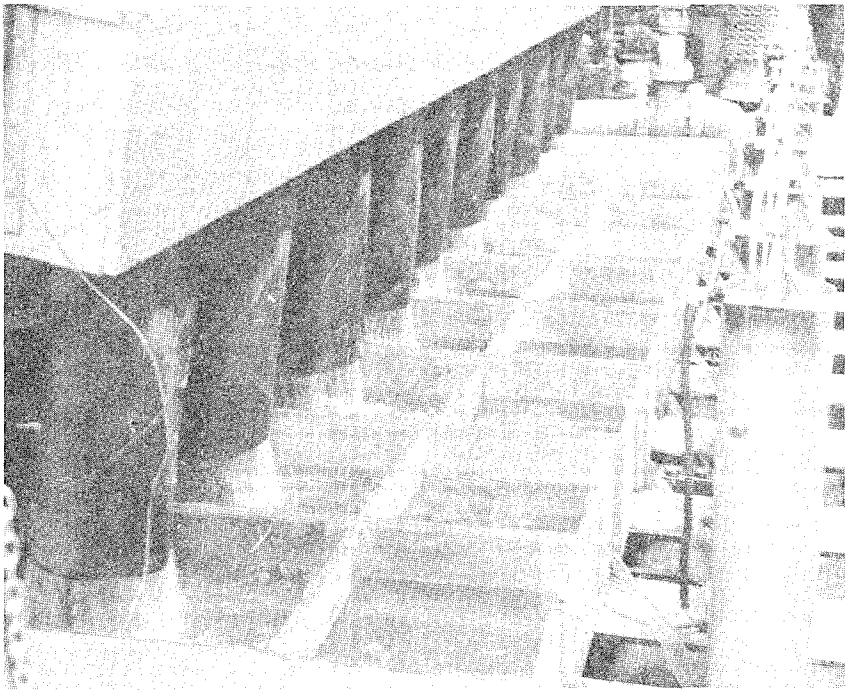

Figure 11. Small discharge-measuring flumes for both friction and infiltration tests. Measurable discharge for each flume ranges from 0.0008 to 0.06 cfs (0.0000227 to 0.00170 cms).

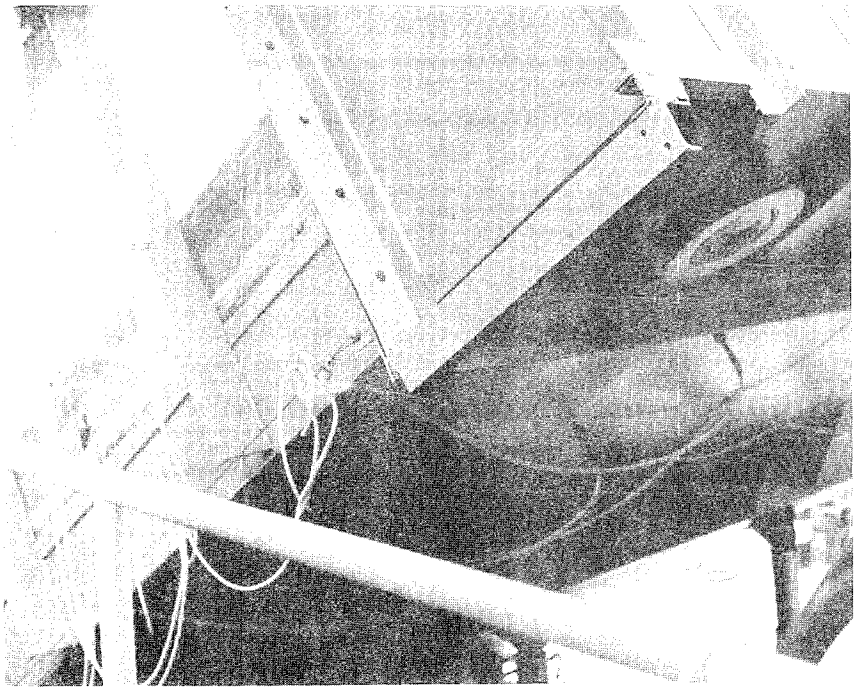

Figure 12. Manometer tubes pivoted on side wall of test bed on one side and connected to bottom of test bed on the other side.

Along the center lines of the third and eighth 2-ft (60.96 cm) exit sections where the manometer tubes were installed, two rows of 12 soil moisture blocks, spaced equally 4 ft (1.219 m) apart, with three moisture blocks at each location are buried inside the soil layer at different depths 2, 5, and 8 inches (5.08, 12.70, and 20.32 cm) deep, respectively. Since the resistance of the soil moisture block varies with the soil capillary potential, the voltage output of the soil moisture block can be converted from the resistance reading and calibrated against the soil capillary potential. The calibration tests were performed in an air-tight pressure container, such as shown in Figure 13, with as many as 24 soil moisture blocks being calibrated at a time. The voltage versus soil capillary potential curve for each moisture block so calibrated is unique, regardless of types of the soils tested.

For illustration, the relative position of the data collection system with respect to the rainstorm simulator and the test bed is schematically drawn in Figure 14.

Console and Computer

For checking the individual performance of all modules of the rainstorm simulator, a manually-controlled console was built in line between the rainstorm simulator and the computer, as shown in Figures 1 and 7. All of the control switches for operating the four hoist systems to position the rainstorm simulator, the hydraulic cylinders to tilt the test bed, and the vacuum pump to drain water from the test bed were also built in the console.

Rainstorm computer control is connected to the console by 1,000 wires. The measurements needed during an experiment are sensed by the appropriate sensors and fed into data conversion (a.c. resistance-measuring) circuits through a precision power supply unit at the console. The data conversion circuits for the water-depth and soil-moisture sensors are housed in a small cabinet, as shown in Figure 15. Briefly, typical discharge, water-depth, and soil-moisture sensors with their electric circuits are schematically drawn in Figures 16, 17, and 18, respectively. The data output proceeds over 256 data lines to a multiplexer, then to an analog-digital converter, and finally to a computer which outputs the data in a digital form. Acting as an interface, controls between the solenoid valves and the computer as well as the multiplexer and analog-digital converters are all accommodated in a big cabinet (Computer Product RIP Interface). The computer used is an EAI 640 digital computer which reads or stores a control program before punching out the test data. The output data from an EAI 640 computer can be directly analyzed through a hybrid computer (EAI PACER 400 system) which consists of an EAI PACER 100 digital computer, an EAI 693 interface controller, and an EAI 580 analog computer.

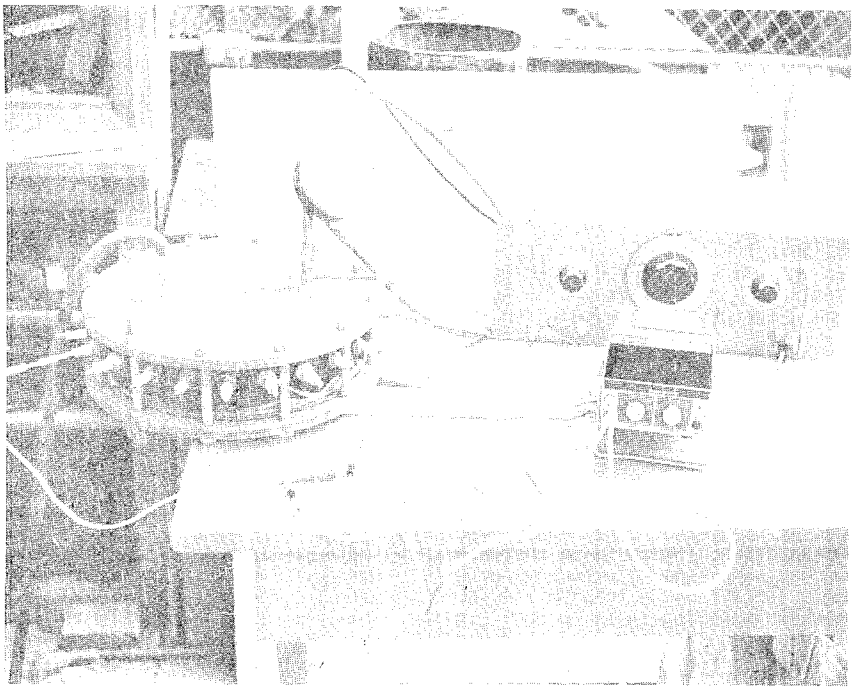

Figure 13. Pressure-controlled, air-tight container for calibration of soil moisture blocks.

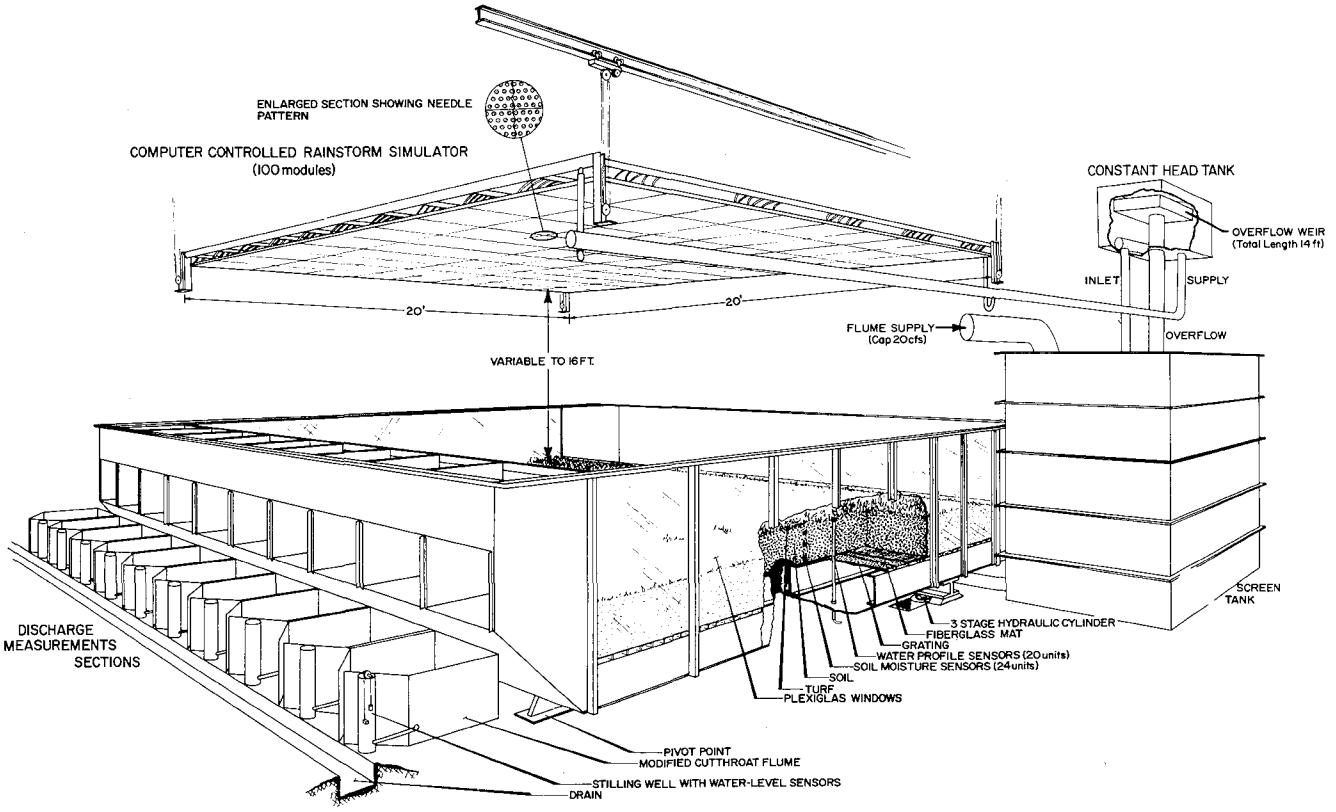

Figure 14. Computer-controlled rainstorm simulator with tilting test bed.

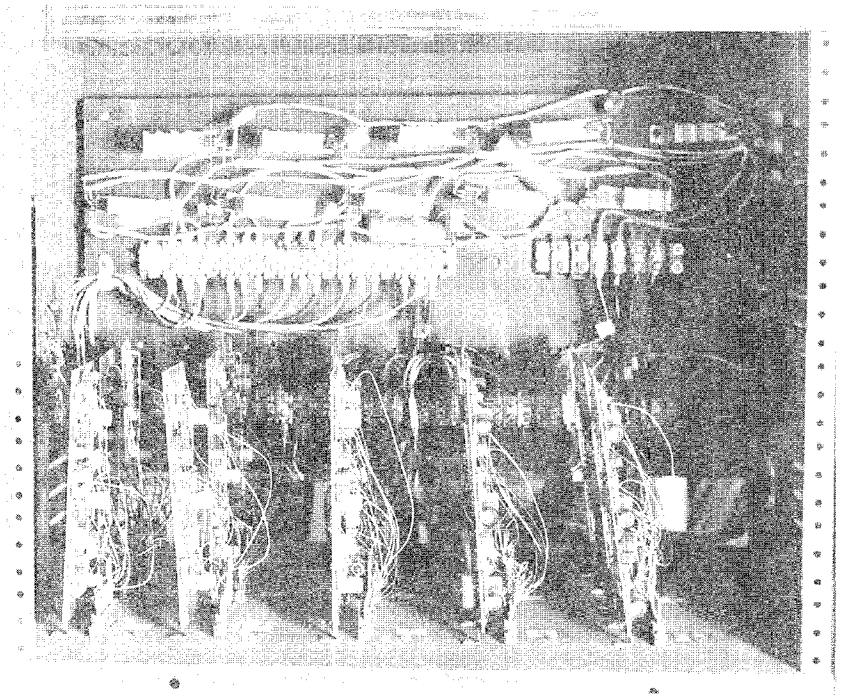

Figure 15. A view of data conversion (a.c. resistance-measuring) circuits for water-depth and soil-moisture sensor at console.

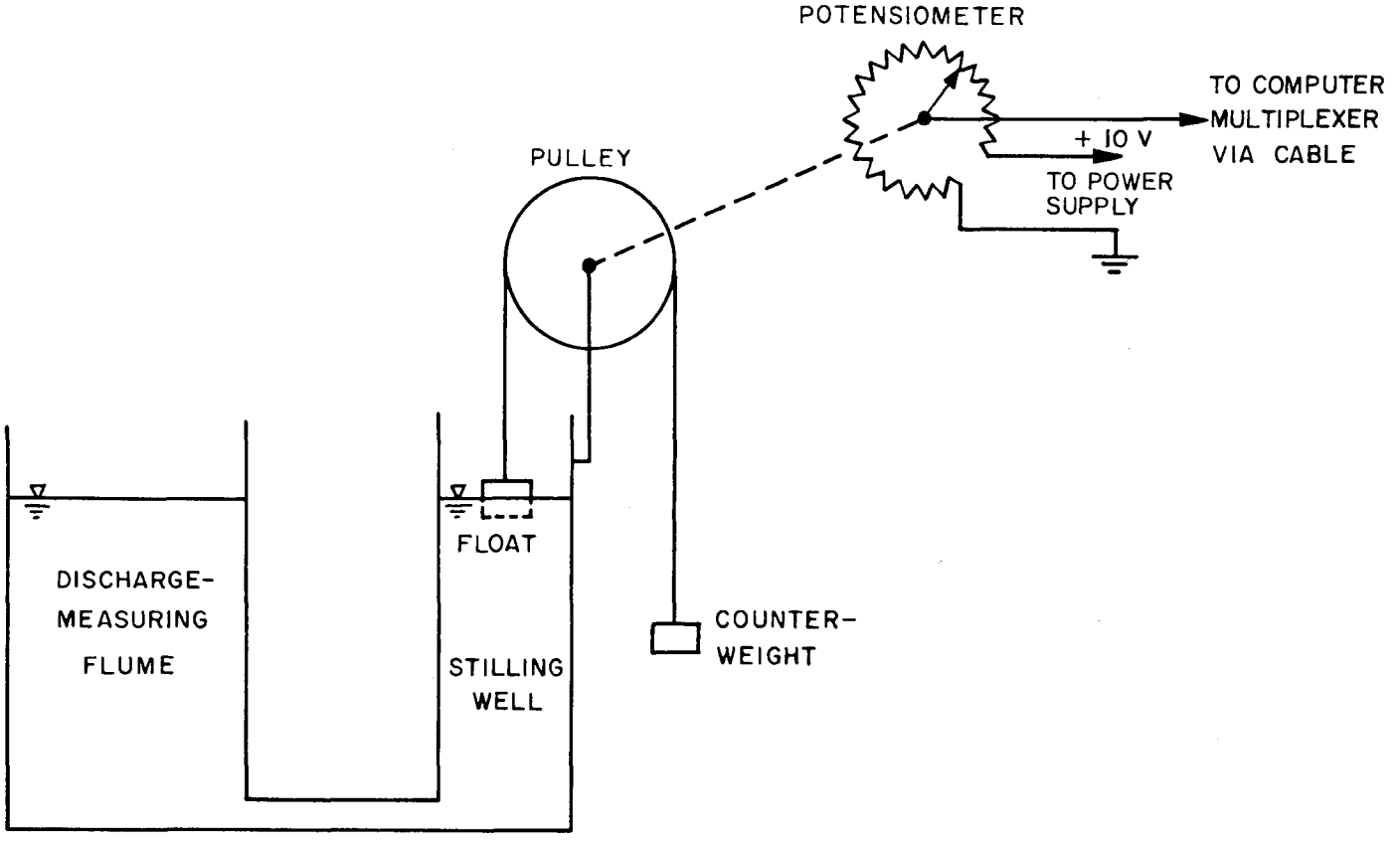

Figure 16. Discharge-measuring flume and electric potentiometer.

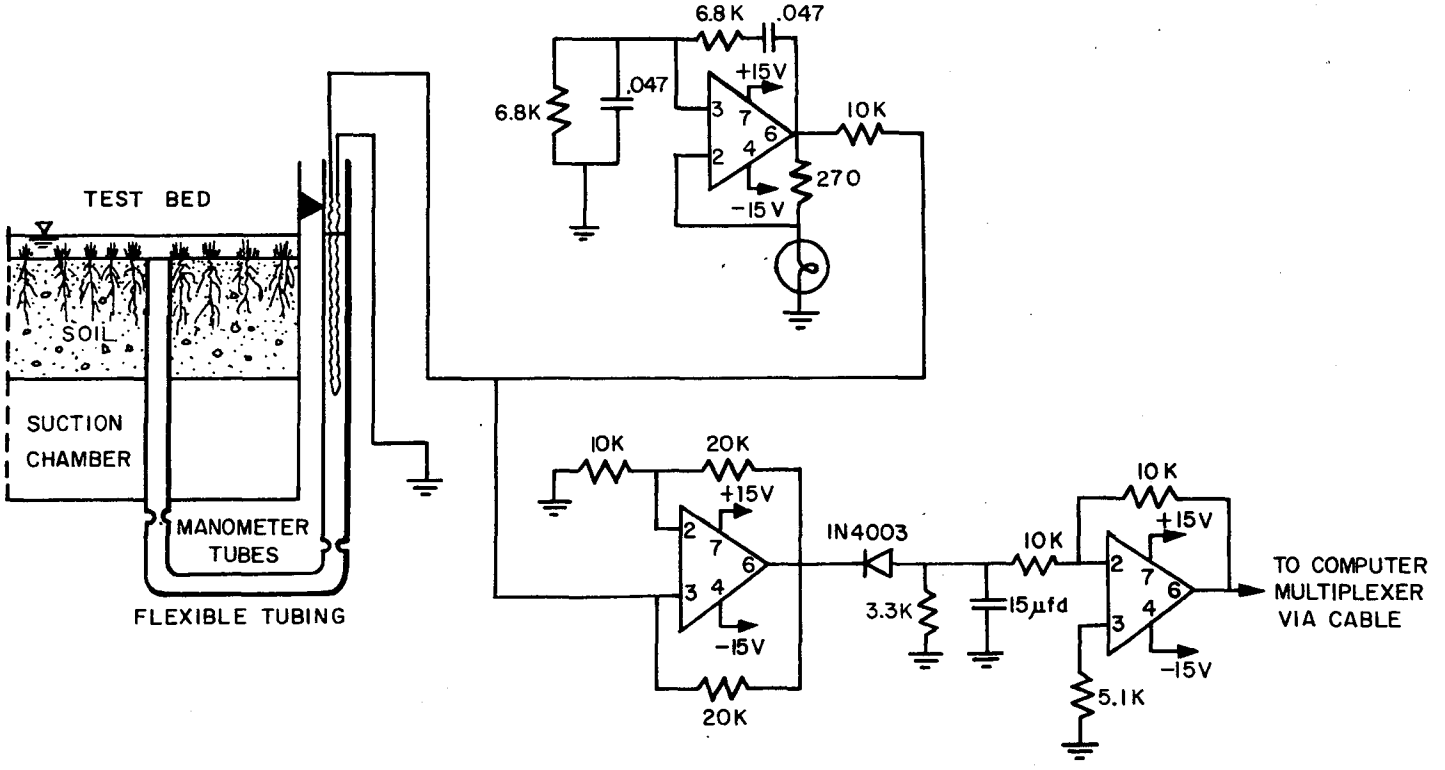

Figure 17. Typical water-depth sensor and a.c. resistance-measuring circuit.

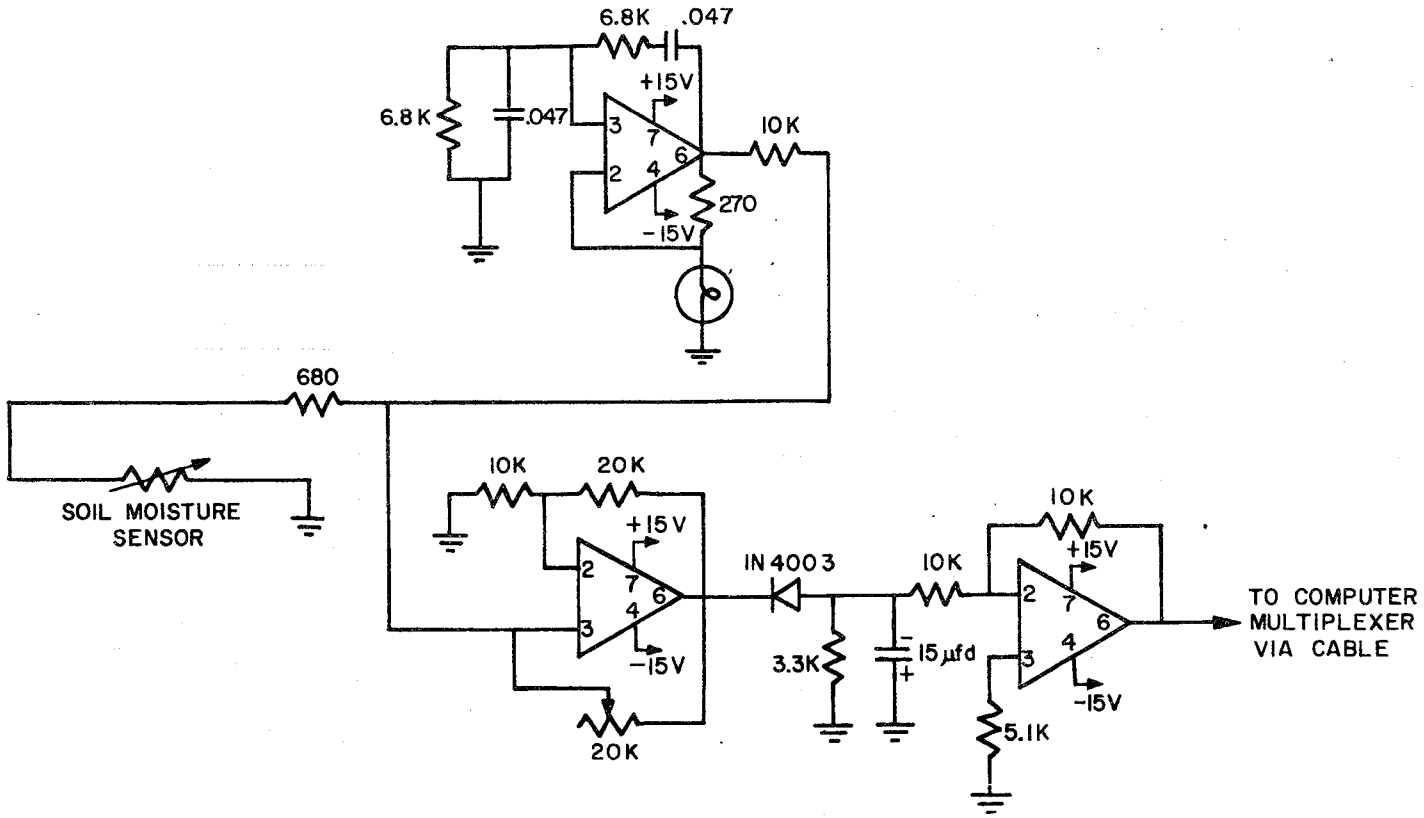

Figure 18. Typical soil moisture sensor and a.c. resistance-measuring circuit.

Sunlight Simulator

Plants cannot survive without light of adequate intensity for photosynthesis. Because the test bed was built in the laboratory which does not have enough light for grass to grow, especially under a prolonged poor drainage condition during an experiment, a sunlight simulator combining light from fluorescent and incandescent lamps was built in order to provide the best balance of radiant energy needed for good grass growth during the experiment.

The efficiency of this lighting system is influenced not only by lamp selection and operation, but also by the size and layout of a supporting frame for the lamps to cover the entire growth area as well as by wall reflectances. It is essential that lamps should be mounted so that light intensity over the grass is high and uniform. This was achieved by arranging lamps in closely spaced banks for high light levels and using high-reflectance metal as a light reflector. For covering a 20-ft (6.096 m) square growth area of grass which is the same area as the test bed, 176 eight-foot (2.438 m) and 14 four-foot (1.219 m) cool-white, high-output fluorescent lamps, 1-3/4 inches (4.45 cm) apart are mounted on the frame, as shown in Figure 4, about 3 feet (91.44 cm) above the grass bed. The light intensity with this type of arrangement gives approximately 1,500 foot candles after 100 hours operation with optimum lamp-cooling conditions. For combined, balanced lighting, 25 incandescent lamps, each covering 4 ft (1.219 m) sq. are added to the fluorescent lamps.

Lamp holders are fastened to the grounded metallic ceiling of the growth area by means of 2 in. x 4 in. (5.08 cm x 10.16 cm) timber beam supports, and the ballasts [88 for 8-foot (2.438 m) lamps and 7 for 4-foot (1.219 m) lamps] were mounted on the other side of the beam supports. Mobile carts were fitted at four footings of the supporting frame so that the entire sunlight simulator is wheeled to move, if necessary, from one place to another, to facilitate the experiments. Horizontal rails were mounted on top of the side walls of the test bed and the supporting frame so that the sunlight simulator can be moved over the test bed when grass needs light (see Figures 19 and 20).

Heat built up around the lamps and ballasts and circulated in the grass growth area could be detrimental to grass. Although heat-producing ballasts were mounted outside the grass growth area, conducted-convected heat from the lamps cannot be removed unless cooled air can be introduced past the lamps. Therefore, the metallic ceiling was made of 1-1/2 in. (3.81 cm) wide strips, placed 1/8 in. (3.2 mm) apart, and an electric fan was used to blow heat off the lamps through the 1/8-in. (3.2 mm) slots.

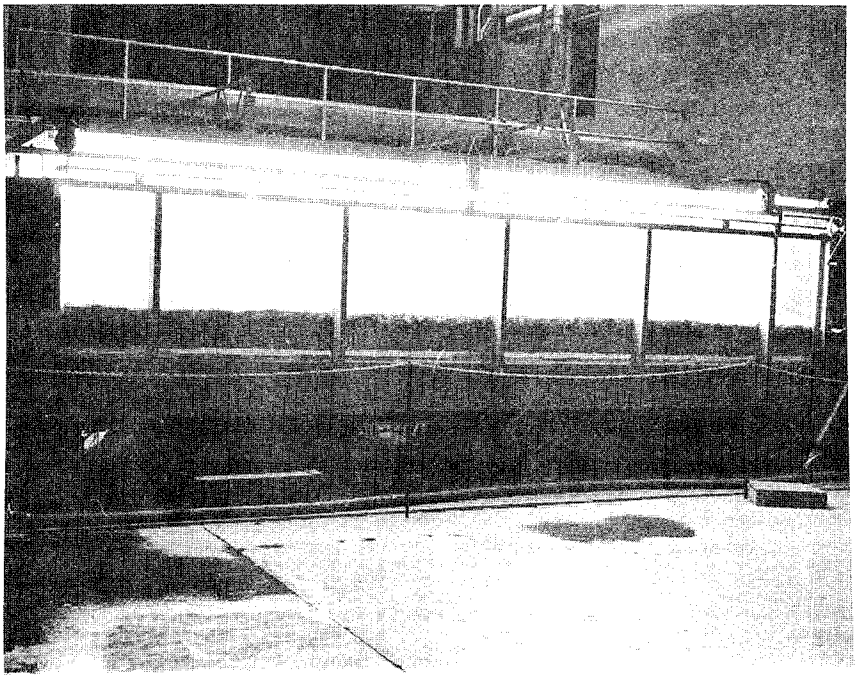

Figure 19. A side view of test bed under sunlight simulator.

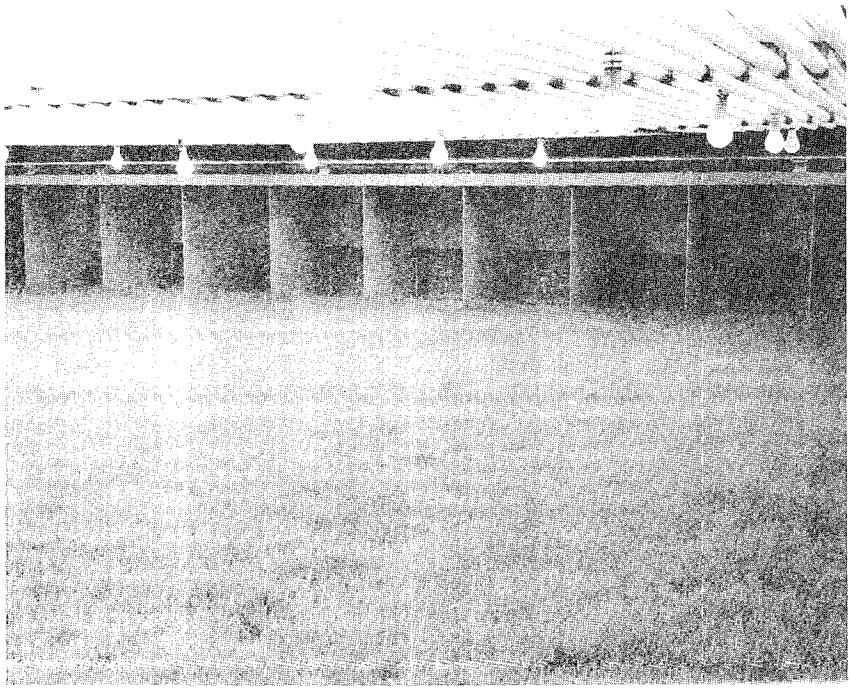

Figure 20. Inside view of test bed, facing downstream, under sunlight simulator.

EXPERIMENTAL PROCEDURES

The preparation of desired soil-and-turf samples for testing is an important task. Whether or not follow-up experiments are successful depends in a great measure upon how well a soil-and-turf sample has been prepared before an experiment. Precaution was taken to avoid excessive leakage and settlement of a soil layer resulting from poor workmanship. This and other related problems which required special attention as well as the specifications of the soil-and-turf samples for realistically simulating a highway sideslope are discussed in the following.

Acquisition of Soils and Turf for Experiments

To simulate an urban and suburban highway side slope as closely as possible in the laboratory one needs to know some special characteristics of the sideslope which are different from the natural or agricultural grassland as follows: (1) The sideslope is composed of disturbed soils; (2) topsoil is needed to grow fine turf; (3) only fine turf species are used; (4) fertilizer is applied, whenever and wherever needed; and (5) the height of turf is maintained at 4 to 6 inches. Usually the sideslope consists of subsoil, topsoil, and turf. Four kinds of subsoil representing four major different drainage conditions can be artificially made according to the Soil Conservation Service (SCS) classification of soil groups A (well drained), B (average or modestly drained), C (poorly drained), and D (very poorly drained). Six species of turf such as Bermuda grass (Cynodon dactylon), Crested Wheat grass (Agropyron desertorum), Fescue grass (Festuca elatior var arundinacea), Kentucky Blue grass (Poa pratensis), Red Top grass (Agrostis palustris; Agrostis alba), and Rye grass (Lolium multiflorum; Lolium perenne) are most commonly used on the urban and suburban highway sideslopes. However, not all of the foregoing turf species are suitable for all types of subsoil. There is a definite relationship between subsoil types and turf species. The following subsoil-turf combinations provided by the Federal Highway Administration represent the major urban and suburban highway sideslope sections in the country.

Subsoil Types	Turf Species
SCS Group A	Bermuda grass Crested Wheat grass
SCS Group B	Kentucky Blue grass Fescue grass Rye grass
SCS Group C	Red Top grass Rye grass
SCS Group D	Red Top grass

Among the six species of turf specified, only Bermuda grass and Kentucky Blue grass can be sodded [Indyk,* 1973, personal contact] while the rest needs to be seeded directly on the test bed. Unfortunately, time did not permit tests to be performed on all of them. Only Bermuda grass and Kentucky Blue grass which can be sodded were tested. Physical (particularly, mechanical) properties and geometric dimensions of subsoil, topsoil, and sodded turf used in the tests are briefly reported herein.

Subsoil

Subsoil representing SCS Group A was simulated by using washed sand which is composed of 71 percent sand particles passing 200 mesh sieve (2 mm). Namely, 29 percent of the sample is coarser than 2 mm (0.079 in.) in diameter. Water holding capacities by weight for this sample are 3.0, 2.6, and 1.3 percent at 1/3, 2/3, and 15 atmospheric suction pressures, respectively. The final infiltration rate varies with the compaction or the bulk density of soil. The final infiltration rates measured at three different bulk densities 98.6 (1.58), 102.4 (1.64), and 112.4 (1.80) lb/cu. ft (g/cu. cm) are 13.1 (332.7), 11.2 (284.5), and 2.9 (73.7) in./hr (mm/hr), respectively.

Subsoil representing SCS Group D was simulated by using a locally available heavy soil composed of 38 percent sand, 46 percent silt, and 16 percent clay. Moisture contents by weight at 1/3, 2/3, and 15 atmospheric suction pressures are 18.5, 13.7, and 6.8 percent, respectively. The final infiltration rates measured at three different bulk densities 79.3 (1.27), 93.6 (1.50), and 102.4 (1.64) lb/cu. ft (g/cu. cm) are 1.50 (38.1), 0.09 (2.3), and 0.05 (1.3) in./hr (mm/hr), respectively.

Subsoil representing SCS Group B was simulated by mixing three parts of washed sand (SCS Group A) and one part of heavy soil (SCS Group D). This soil mixture is composed of 84.5 percent sand, 11.5 percent of silt, and 4.0 percent of clay. Soil moisture contents at 1/3, 2/3, and 15 atmospheric suction pressures are 12.4, 9.5, and 4.1 percent, respectively. The final infiltration rates measured at three different bulk densities 97.4 (1.56), 103.0 (1.65), and 107.4 (1.72) lb/cu. ft (g/cu. cm) are 3.39 (86.1), 1.04 (26.4), and 0.39 (9.9) in./hr (mm/hr), respectively.

Subsoil representing SCS Group C was simulated by mixing one part of washed sand (SCS Group A) and three parts of heavy soil (SCS Group D). This soil mixture is composed of 53.5 percent sand, 34.5 percent silt, and 12.0 percent clay. Soil moisture contents by weight at 1/3, 2/3, and 15 atmospheric suction pressures are 14.7, 12.5, and 5.8 percent respectively. The final infiltration rates measured at three different bulk densities 86.8 (1.39), 90.5 (1.45), and 98.0 (1.57) lb/cu. ft (g/cu. cm) are 1.03 (26.2), 0.66 (16.8), and 0.12 (3.0) in./hr (mm/hr), respectively.

---

*Indyk, H. W., Specialist in Turfgrass Management, College of Agriculture and Environmental Science, Rutgers-The State University of New Jersey, New Brunswick, N.J. 08903.

Subsoil was placed on a porous bed which is made of galvanized grating steel covered with fiberglass, as shown in Figure 8. Fiberglass was glued all the way around the side walls of the test bed for avoiding excessive leakage of water along the side walls. A similar treatment was made on each of the depth-measuring, aluminum manometer tubes that were to be penetrated through the soil layer. Subsoil was placed in layers, not exceeding 1 inch (2.54 cm) in uncompacted depth, properly moistened, and compacted by using a roller before the next layer was placed. Each layer of soil was spread uniformly and raked to uniform thickness prior to compacting. As the compaction of each layer progressed, continuous leveling and manipulating was made to assure uniform density. The thickness of subsoil was kept from 6 to 8 inches (15.24 to 20.32 cm) for a total of 1-foot (30.48-cm) soil layer to be tested. Topsoil was next hauled over the subsoil after subsoil was filled to a desired thickness. During filling work moisture-measuring sensors were buried at predetermined locations and depths and tamped, as necessary.

Topsoil

Locally available topsoil composed of 40 percent sand, 41 percent silt, and 19 percent clay was placed to 4- to 6-in. (10.16- to 15.24-cm) thickness over the subsoil layer. A photographic view of a typical soil profile consisting of 6- to 8-in. (15.24- to 20.32-cm) thick subsoil (SCS Group A) and 4- to 6-in. (10.16- to 15.24-cm) thick topsoil is shown in Figure 21. Soil moisture contents by weight at 1/3, 2/3, and 15 atmospheric suction pressures are 18.4, 16.0, and 10.5 percent, respectively. The final infiltration rates measured at three different bulk densities 60.5 (0.97), 63.0 (1.01), and 69.1 (1.11) lb/cu. ft (g/cu. cm) are 2.50 (63.5), 2.45 (62.2), and 0.61 (15.5) in./hr (mm/hr), respectively. Compaction of the topsoil layer and installation of soil moisture sensors were treated in a similar way as were done to the subsoil layer.

The degree of compaction of a disturbed soil is often measured by soil bulk density which varies with structural condition of the soil, particularly that related to packing. Changes in the degree of compaction thus result in the differences in bulk density that in turn produce the various final infiltration rates for the four subsoils and topsoil used. For brevity in illustration, these soil properties are plotted, as shown in Figures 22 and 23.

Sodded turf

Turf which can be sodded is cut and rolled as a carpet. The common dimensions of each roll are 16 in. (40.64 cm) wide, 6 ft (1.83 m) long, and 1 in. (2.54 cm) thick. To cover a 20 ft x 20 ft (6.096 m x 6.096 m) area of the test bed, at least 50 rolls of sodded turf are required. Every roll of sodded turf was paved side by side on the topsoil. Special care was taken to position the capped ends of the manometer tubes at the geometric mean level of the soil surface. In view of the fact that the thickness of sodded turf acquired from a nursery farm was practically nonuniform, to make the turf surface perfectly level was almost impossible. This nonuniformity in the bed could become the major source of errors in the flow depth measurement.

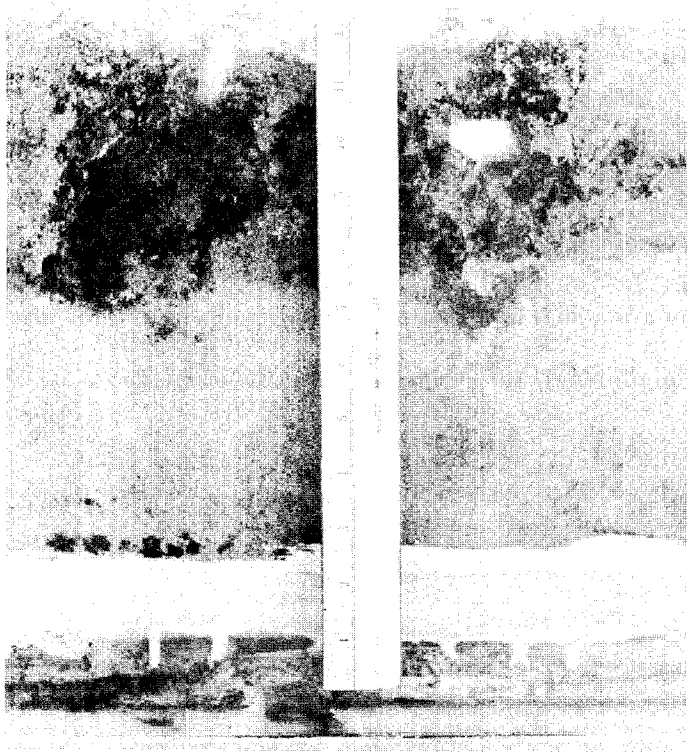

Figure 21. Typical soil profile consisting of 6- to 8-in. thick subsoil and 4- to 6-in. thick topsoil.

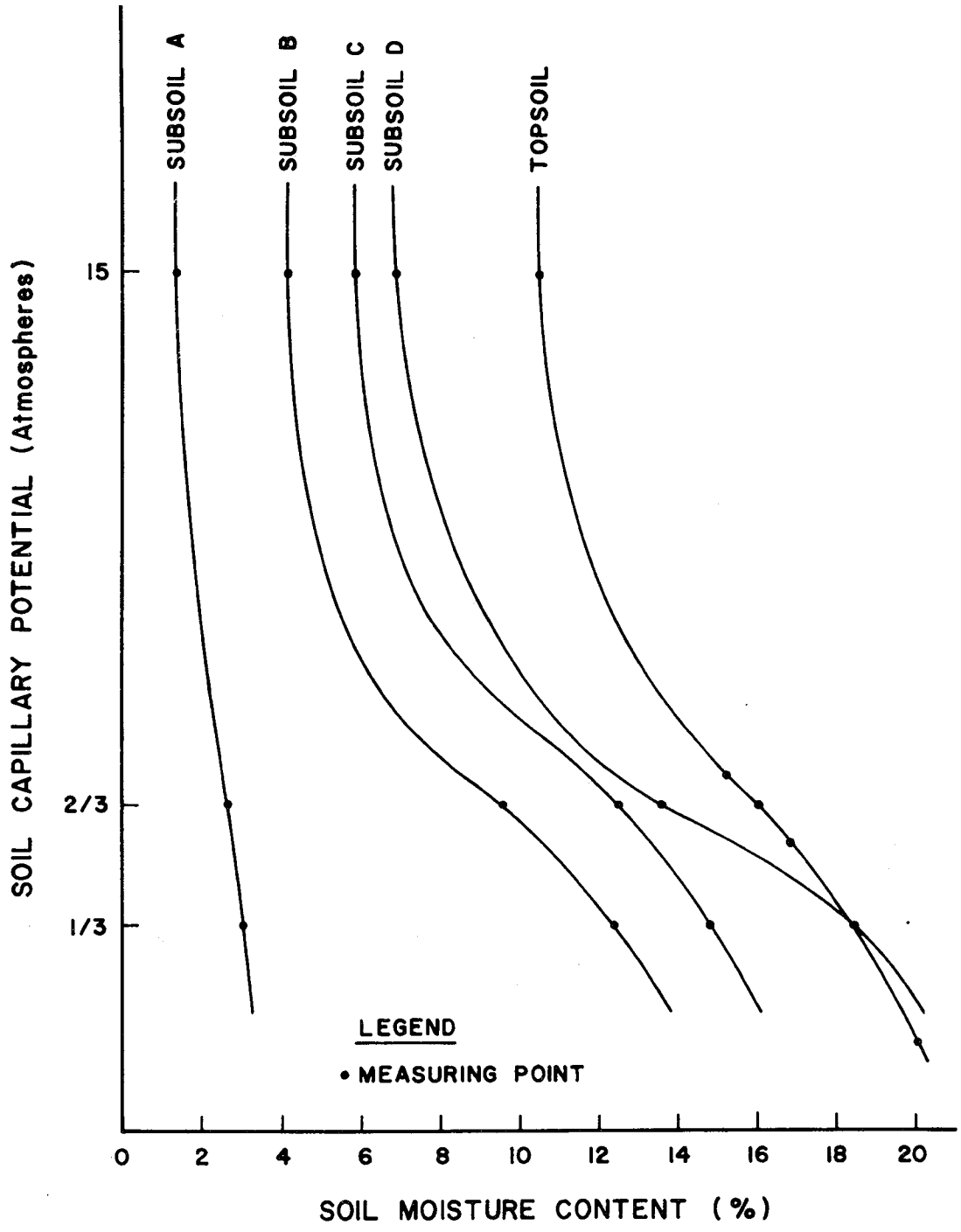

Figure 22. Functional relationships between soil moisture content and soil capillary potential for four subsoils and topsoil.

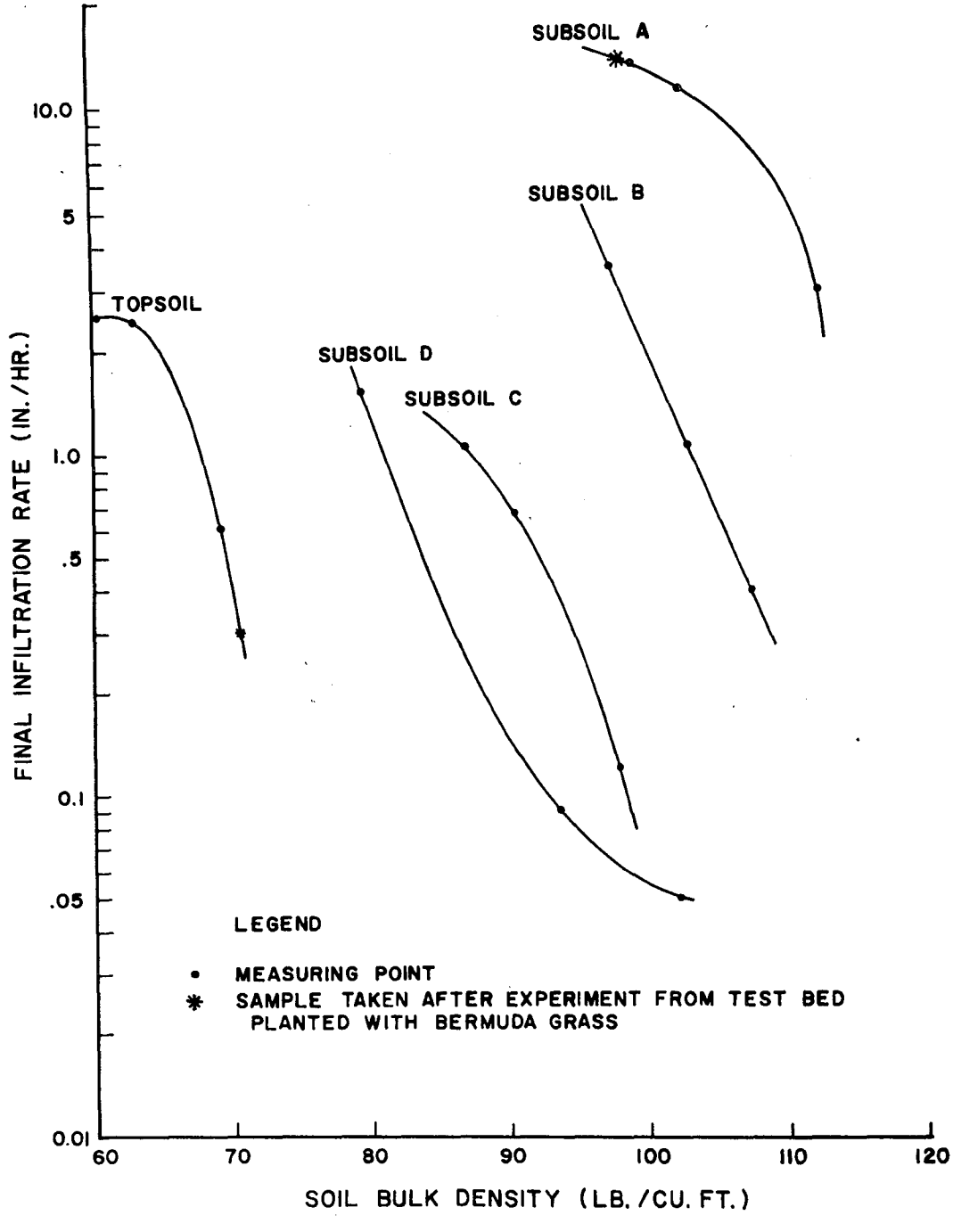

Figure 23. Soil bulk density as a measure of degree of compaction as related to final infiltration rate for four subsoils and topsoil.

Before testing was started, approximately two weeks were allowed for sodded turf to establish its own root system deep into the topsoil and, possibly further into the subsoil. In this transplanting period of time, an adequate amount of water and liquid fertilizer was applied to the turf to keep its optimum growing condition under the sunlight simulator.

Tall turf tends to become prone by its own weight, even though there is no external force acting on it. Thus, for simplicity in the analysis, turf was cut shorter than specified 4 to 6 inches (10.16 to 15.24 cm) with the hope that the effect of roughness stiffness on the flow resistance was small enough to be neglected. Average turf height, as shown in Figure 24, was approximately maintained at 3 inches (7.62 cm) during experiments. The grass was cut by using a hand mower and clippings were raked and collected for dumping.

Kentucky Blue grass sod was locally available so that it was tested first. Bermuda grass sod was obtained from California through a nursery farm in Las Vegas, Nevada. Bermuda grass sod tested was Hybrid Bermuda grass because Common Bermuda grass could not be sodded. It was noticed that Hybrid Bermuda grass had a deeper root system than Kentucky Blue grass. Nevertheless, both are good, solid, dense turf which can stand against erosion. No salient erosion from the turf surfaces was observed during experiments, even on a slope as steep as 1.5:1. No soil or chemical measurements were conducted in this study.

Experiments began in the third week after turf was sodded. It was found that no more than one infiltration test could be conducted every day in addition to a number of friction tests because for the infiltration test the average initial soil moisture content should be reestablished before starting any further experiment. With the present facility including use of both suction pump and sunlight simulator, excess gravitational water in the soil cannot be removed faster than within a half day by means of forced drainage (suction pump) and evapotranspiration (sunlight simulator). It was desired that the initial soil moisture content could be held at field capacity or less before an infiltration test. Time did not permit the initial soil moisture content to be held at wilting point. However, it should be remembered that there was no such need for having a limitation in the initial soil moisture content as far as the friction tests were concerned.

Before an experiment was started, water was introduced into the discharge-measuring flumes and depth-measuring manometer tubes to have the reference levels or zero readings of both discharge and depth sensors checked by a portable voltmeter (Digitec Digital Multimeter S/N 3164) or a computer (EAI 640). These reference levels were used in the later analysis when the computer output data in the form of voltage were reduced to the usable units, such as cfs (cms) and inches (cm), through the calibration curves or relationships.

Measurements of Flow Rates and Depths

The fluid used for the friction tests was Logan River water from a reservoir which supplies the laboratory. The test bed was first tilted

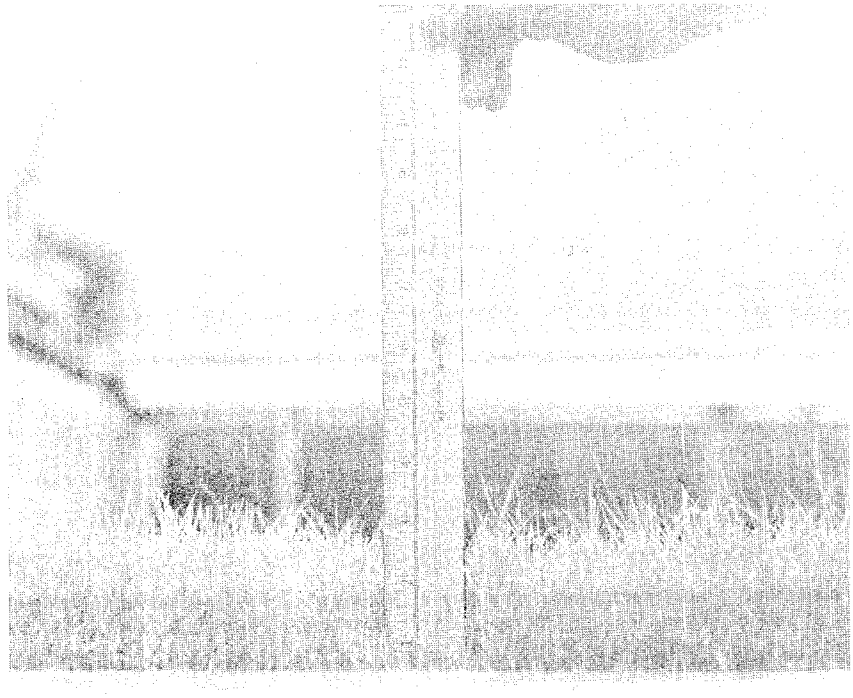

Figure 24. Average turf height maintained during experiments.

to a desired angle of inclination by operating the two hydraulic cylinders (Figure 9). Although both hydraulic cylinders connected to an oil reservoir in parallel were designed to support the total load equally, a slight discrepancy in the telescoped length between them (even within the manufacture's tolerance) has compelled us to use a hand-operated hydraulic jack for leveling the tilted bed more precisely. Once the test bed was properly set, water was delivered through the head tank (Figure 8) over the turf surface.

Seven bed slopes for each turf were tested. The slopes tested were 0.1 percent (0.001), 0.5 percent (0.005), 2° (0.035), 5° (0.087), 6:1 (0.164), 3:1 (0.316), and 1.5:1 (0.555). The rate of water introduced onto the turf surface was varied by adjusting a gate valve which was installed in line connecting either to the screen tank or directly to the head tank in case that the test bed was tilted more than 5° in angle. The discharges and depths for each test were measured in voltage through the sensors and printed instantaneously with the teletype of an EAI 640 computer.

As described previously, two sets of the flumes were used in the discharge measurement. One set of the relatively large flumes, as shown in Figure 10, was made of sharp-crested weirs, each of which is capable of measuring the discharge ranging from 0.04 to 1 cfs (0.00113 to 0.0283 cms). Another set of the relatively small flumes, as shown in Figure 11, was made of V-notched weirs, each of which is capable of measuring the discharge ranging from 0.0008 to 0.06 cfs (0.0000227 to 0.00170 cms).

For each slope, ten or more different flow rates were tested. Although the maximum discharge needed to be tested for a standard highway cross-section within the right of way may not exceed 0.129 cfs/ft (0.0120 cms/m) (= 31 in./hr x 180 ft) which is tantamount to the equilibrium overland flow rate for a foot wide, 180-ft (54.86-m) long drainage area under a 31 in./hr (787.4 mm/hr) rainstorm, the friction tests were conducted for discharge as high as 0.45 cfs/ft (0.0418 cms/m) in the case that the bed slopes were less than 5° in angle. The flow for such high discharges would probably fall in the turbulent or transition flow region that is of course beyond the scope of this study. However, such experimental data would indeed be valuable in bridging the missing information on the flow resistance between the laminar and turbulent flow regimes.

Immediately after an experiment, the sunlight simulator was pulled over the turf surface and lamps were lit for about 12 to 16 hours per day before the next experiment was started. Meanwhile, the vacuum pump was turned on to suck excess gravitational water out of the soil layer. The operation of the vacuum pump might continue until there was no apparent excess water dripping at the bottom of the soil layer. Unfortunately, since there was difficulty in keeping this vacuum pump running satisfactorily, the practice of forcibly draining water out of the soil layer by means of the vacuum pump was discontinued.

Although the soil layer under investigation was only one foot thick, consolidation took place during experiments. Note that subsoils for

Bermuda grass and Kentucky Blue grass are respectively SCS Groups A and B which consist mainly of coarse-grained sand, as described previously. Because coarse-grain soils are relatively pervious, it can reasonably be assumed that they are compressed as rapidly as loads can be applied. Consequently, consolidation is judged to result mainly from the compression of topsoil which was composed largely of fine-grained silts and clays, as exemplified on Bermuda grass tests as shown in Figure 23. The uneven consolidation of the soil layer made the flow depth measurement extremely difficult, especially for very low flow on a steep slope.

Also noted is an apparent difference between the turf sodded on the test bed which is tilted and the naturally growing turf on the highway sideslope. Natural grass always grows vertically, regardless of the slope, whereas grass simulated in the laboratory grows perpendicular to the test bed. It was hoped that this difference would not affect significantly the flow resistance results.

Accuracy of Measurements

Errors involved in the measurements of the flow variables such as the discharge and depth can be attributed to three major sources: (1) Defects in the discharge and depth-measuring devices, (2) unevenness of the soil surface due to poor workmanship, consolidation, and local erosion, and (3) instability and channelization of a thin flow. Some, but not inherent, problems associated with the measuring devices were readily corrected or improved by adopting some unique experimental procedures, but others which were inherent in nature could not be remedied without partial or entire modification of the instrumentation systems. Each of the aforementioned sources of errors and its possible remedies is discussed in the following.

The discharge in the flume can be calibrated against the depth of water in the stilling well, which in turn can be measured by using an electric potentiometer, as shown in Figure 16. However, the discharge was actually measured directly by reading voltage in the potentiometer without taking data on the depth of water in the stilling well. The potentiometer was built for measuring the water depth to the accuracy of 0.001 ft (0.3 mm). The discharge, Q, in cfs was thus calibrated against the potentiometer voltage reading, V, in volts for the large flume (Figure 10) as

$$Q = 0.0845\ V^{1.61} \qquad 0.04 < Q < 1.0 \qquad (17)$$

and that for the small flume (Figure 11) as

$$Q = 0.0055\ V^{2.025} \qquad 0.0008 < Q < 0.06 \qquad (18)$$

The measurement of the discharge by means of Eqs. 17 and 18 was highly accurate (within 1 percent error) in the mid-range of the specified discharges, but the accuracy became poor, probably with an error as high as 10 percent, as the measured discharge approached to the extreme values

of the range. The causes of inaccuracy, if any, in the discharge measurement may be twofold. Either defects in the potentiometers or nonuniformity in the flumes, or in both, could cause serious errors in measuring the discharges, using Eqs. 17 and 18. Because all the potentiometers were carefully checked before an experiment, the potentiometers seldom, if ever, gave us any trouble in this aspect. Each of the sharp-crested weirs for the large flumes and V-notched weirs for the small flumes was repeatedly calibrated so that nonuniformity, if any, in the fabrication of the weirs was already corrected before its application. Consequently, errors in the discharge measurements were believed to be small unless the discharge-measuring flumes were wrongly selected to measure extreme values.

Helical wound resistance wires in the manometer tubes, as shown in Figures 12 and 17, were used to measure to 0.001-ft (0.3-mm) accuracy the flow depth on the soil surface. Many problems were encountered, however, in connection with the use of such resistance wires and manometer tubes. First, each resistance wire needed to be calibrated individually and since there were 20 manometer tubes, 20 calibration curves were required. Second, the calibration curves changed in a short period of time for unknown causes (probably evaporation causing mineral deposit on the resistance wires). Third, there was a time lag for the meniscus in the manometer tube to change in response to a change in the flow depth on the soil surface; the situation aggravated in the receding stage of the surface runoff. (Of course, as long as the friction test was concerned, this time lag did not constitute a problem because the uniform flow was maintained during the test.) Finally, air bubbles easily got trapped in the line connecting to both sides of the manometer tube so that the depth measurement became erroneous. Among these four problems, only the second one could be corrected by draining the manometer tube immediately after a test and then filling it up again before another test. The other three problems are inherent in nature with this type of instrumentation system and thus cannot be corrected without resorting to another type of depth-measuring device.

Although the soil layer had been well compacted prior to experiments, consolidation continued in the repeated wetting and drying processes under the compression of its own load and additional water pressure. Furthermore, local erosion took place at several spots where soil particles were loosely packed and eventually detached from grass roots while high-speed water was flowing over them. As a result, the soil surface gradually became uneven with the time during which experimental data were taken. The fact that the degrees of unevenness (i.e., variations from the geometric mean bed elevation) was almost of the same order of magnitude as the thin flow depth or higher made the accurate measurement of the depth extremely difficult.

To sod rather than seed grass directly on the test bed has several advantages, as mentioned previously, but also has disadvantages which should be carefully examined. For example, topsoil which came with 1-inch (2.54-cm) thick sod would not be the same type of topsoil used in the test; this in effect would add one more dimension of unknown factors in

the later analysis. In addition, supposedly the sod acquired was very uniform in thickness; however, it (especially Bermuda grass) did not arrive in such a perfect shape, and extra efforts and time were spent on the adjustment of the previously-leveled topsoil surface on which sod was laid. Unfortunately, poor workmanship on this type of patching work caused the turf surface to become more uneven. Therefore, if time and situation permitted, it would be more advisable to seed grass directly on the test bed than use sod.

If the test bed was tilted with a slope as steep as 1.5:1, inherent instability in flow coupled with the unevenness of the soil surface might cause the channelization of flow over the turf surface, as shown in Figures 25 and 26. Since there were only two rows of 10 depth-measuring manometer tubes installed along the centerlines of the third and eighth 2-ft (60.96-cm) exit sections in the test bed, as illustrated before, it is possible that some or all of the tubes were not covered by the flow at all when the flow became channelized. It appears that the only way to overcome the inaccuracy of the flow-depth measurement due to flow channelization is to install more manometer tubes on the test bed. However, the more manometer tubes installed, the more would be the preceding inherent instrumentation problems associated with the adoption of helical wound resistance wires and manometer tubes for flow-depth measurements. Thus, this and other related problems should be carefully studied and solution alternatives to the problems compared before any further improvements on the present instrumentation system are initiated.

Water temperature was not taken for each experimental run. Water temperature measured on the daily basis was found to be fairly constant during experiments, ranging from 45° to 50°F (7.2° to 10.0°C). For simplicity, the average water temperature, 47°F (8.3°C), was used in the analysis.

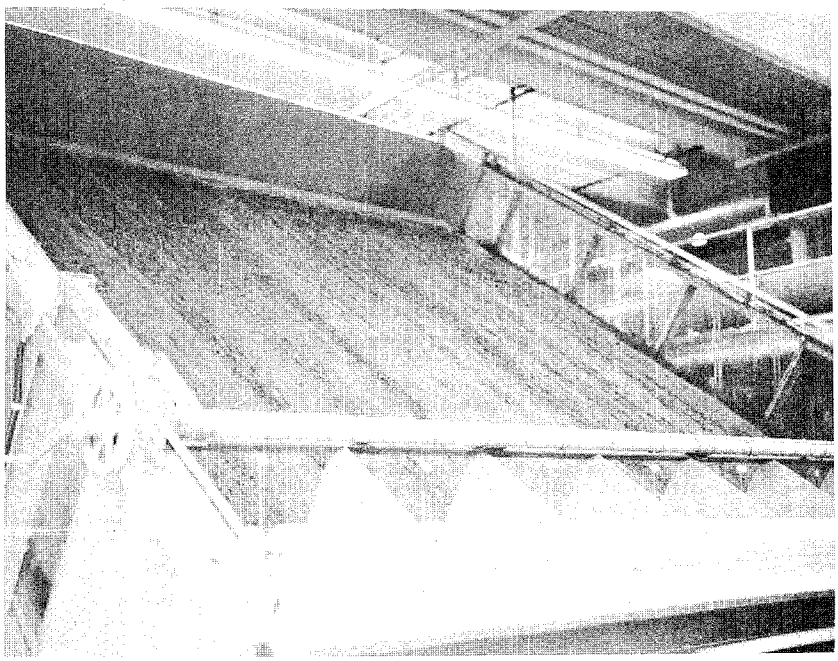

Figure 25. Front view of a channelized thin flow over a turf surface with 1.5:1 bed slope.

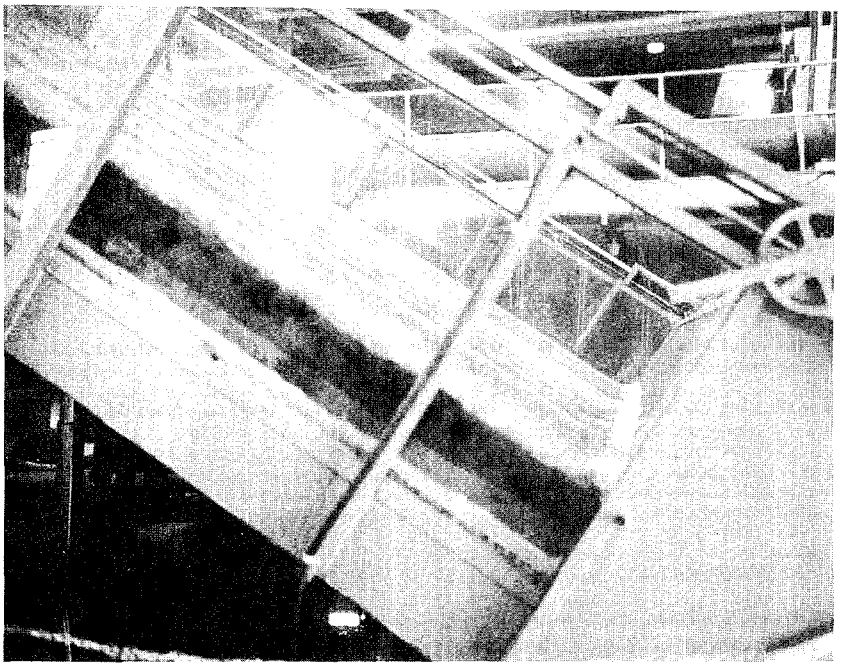

Figure 26. Side view of a channelized thin flow over a turf surface with 1.5:1 bed slope.

ANALYSIS OF RESULTS

For the friction tests, water was introduced from the head tank over the turf surface to the downstream exit sections where water overfell into the discharge-measuring flumes. The depth of flow for a given constant discharge over the infiltrating turf surface varied with the entire test-bed length (i.e., 20 ft). This is a typical case of the so-called spatially varied flow which may be subcritical, critical, or supercritical, depending upon whether the bed slope under test is mild, critical, or steep. Theoretically speaking, a given slope can be classified as mild or steep, depending solely on the given discharge at the time of test if the hydraulic roughness of the turf surface is given. For gradually varied flow (if infiltration is ignored) on both mild and steep slopes, the flow depth at the upstream end of the test bed is much higher than the normal depth, but it gradually approaches the normal depth as the flow moves downstream. The flow depth may or may not attain the normal depth at the downstream end. However, if the flow is shallow, the flow on the downstream side of the test bed is virtually at the normal state (i.e., uniform flow) despite its relatively short test-bed length. For simplicity, such a gradually varied flow is treated as a uniform flow and the uniform flow equation such as Eq. 8 is applied to the computation of the friction coefficient. This simplification in the analysis of the shallow flow on the turf surface is justified for the following reasons.

For analyzing gradually varied flow, strictly speaking, the gradually varied flow equations must be used. However, if the depth is very thin, say in the order of magnitude of the roughness size or the height of random variations from the geometric mean bed elevation, the flow profile measured by means of the manometer tubes at 10 different locations on the test bed did not represent the flow characteristics of the gradually-varied flow. In other words, if the flow depth is less than the roughness size or the height of random variations from the mean bed elevation, the consideration of the flow as a gradually varied flow over the entire test-bed length is meaningless unless the one over each small length of a random variation from the mean bed elevation is microscopically treated as a gradually varied flow. The microscopic treatment of the thin flow in a sense needs hundreds more depth-measuring devices which, nevertheless, do not warrant higher accuracy in the analysis. Consequently, unless the flow was deep enough to be able to measure the difference in the depth, the flow was assumed uniform and the average value of the manometer-tube readings was used to represent the average depth of overland flow. Given the discharge per unit width and the average measured depth of overland flow, the value of the Darcy-Weisbach friction coefficient was then calculated from Eq. 8.

Determination of Friction Coefficient

Substituting the expression of the mean velocity of flow, $V = q/y_o$, into Eq. 8 yields

$$S_o = \frac{f}{8g} \frac{q^2}{y_o^3} \quad . \quad . \quad . \quad . \quad . \quad . \quad . \quad . \quad . \quad . \quad . \quad . \quad . \quad . \quad . \quad (19)$$

$$f = \frac{8gS_o y_o^3}{q^2} \quad . \quad . \quad . \quad . \quad . \quad . \quad . \quad . \quad . \quad . \quad . \quad . \quad . \quad . \quad . \quad (20)$$

Note that y_o is the depth of uniform flow which is different from the depth measured by the manometer tube, d_m, as shown in Figure 27. The

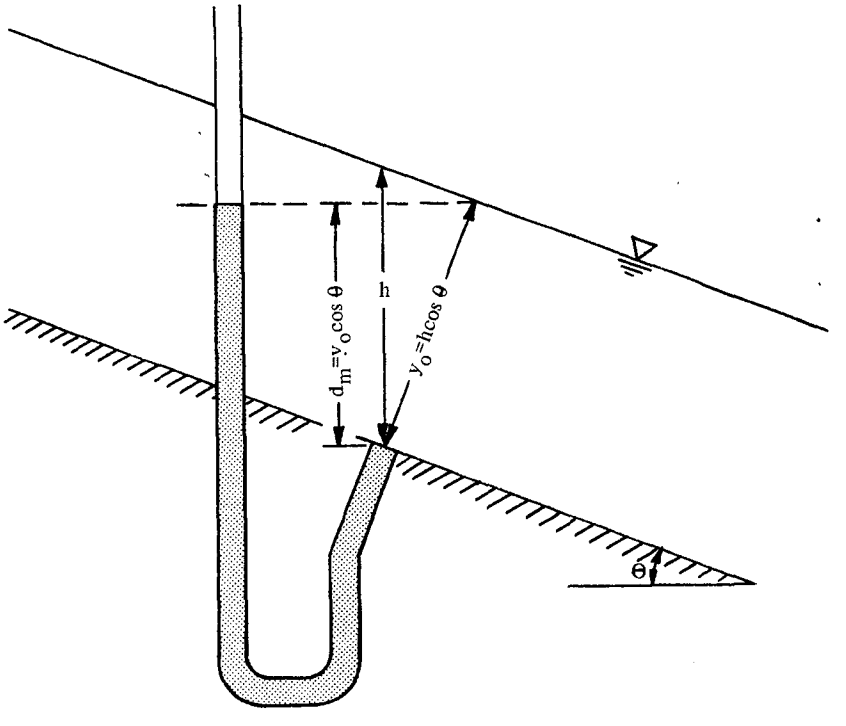

Figure 27. Manometer reading of flow depth on a sloping bed.

relationships between y_o, d_m, and h (i.e., the depth in the vertical direction) for uniform flow on a sloping bed with a slope angle, θ, are as follows:

$$y_o = h \cos\theta \quad . . . . . \quad (21)$$

$$d_m = y_o \cos\theta = h \cos^2\theta \quad . . . . . \quad (22)$$

Expressing f in terms of d_m by incorporating Eq. 22 with Eq. 20 yields

$$f = \frac{8g S_o d_m^3}{q^2 \cos^3\theta} \quad . . . . . \quad (23)$$

The Darcy-Weisbach friction coefficient, f, was computed by using Eq. 23.

The Reynolds number for flow in the wide open channel was calculated from Eq. 2 as

$$\mathbb{R} = \frac{q}{\nu} \quad . . . . . \quad (24)$$

in which ν is the kinematic viscosity of water taken at 47^oF (8.3^oC).

Measured and computed data for flow on the Kentucky Blue grass surface are tabulated in Tables 1 through 7 in the Appendix and those for the Bermuda grass surface are tabulated in Tables 8 through 14 in the Appendix. In these tables, the Froude number, $\mathbb{F}$, was calculated from

$$\mathbb{F} = \frac{V}{\sqrt{g y_o \cos\theta}} \quad . . . . . \quad (25)$$

Although the Froude number was not used in the subsequent analysis, it was computed and listed in the tables for those who may be interested in understanding the various flow regimes, as classified before.

Because no manometer-tube problems were detected prior to the experiments of the flow on Bermuda grass, such as discussed in the previous section, the corrections on the experimental procedures for flow-depth measurements could not be made in time to test the flow on Kentucky Blue grass properly. It is the writer's judgment that the accuracy of data points, especially flow depths, on Kentucky Blue grass is questionable.

Friction Coefficient Versus Reynolds Number Relationships

The calculated values of the Darcy-Weisbach friction coefficient, f, in Tables 1 through 14 were plotted against the corresponding Reynolds numbers, R, as shown in Figure 28. An inspection of Figure 28 reveals that in the laminar-flow range (approximately for $R < 1,000$) a relationship between f and R appears to exist for each of the bed slopes tested. A best-fitting line can be drawn through data points for Bermuda grass on each slope. In Figure 28, there are a total of seven solid lines which can be drawn for seven slopes in parallel with the theoretical line representing Eq. 9. A few comments on the f-R relationships for flow on the turf surface may be appropriate at this stage of analysis.

1. Since the physical appearance of Kentucky Blue grass is similar to that of Hybrid Bermuda grass, data points for Kentucky Blue grass on the corresponding slope should not differ very much from the best-fitting line for Bermuda grass. As a matter of fact, data points for Kentucky Blue grass, though their reliability is still in question as far as the depth measurements are concerned, scatter closely around the corresponding best-fitting lines for Bermuda grass; fitting better especially with smaller slopes. This experimental result proves that the roughness sizes, k, for both species of turf are about equal and Eq. 16 should be valid.

2. The f values for flow on the turf surface are much higher than expected. The f value increases with the bed slope but decreases with the Reynolds number (or discharge if the water temperature is constant). The range of laminar flow on a small slope is larger than that on a large slope. For example, the flow appears to be still laminar on the 0.1 percent slope for R as large as 10^4, but would probably not be laminar on the 1.5:1 slope for R exceeding 10^3.

3. Because of the limit in the flow capacity of the present facility in the laboratory, the full ranges of transition and turbulent flow on the turf surface could not be tested. Of course, the friction tests can be readily extended in the future with a slight modification of the present facility to the inclusion of large flows within the full ranges of transition and turbulent flow. Before such time comes, for the sake of completeness in characterizing the f-R relationships for a full range of the flow on the turf surface, previous investigators' field data on Bermuda grass [Palmer, 1946; Ree and Palmer, 1949] were analyzed, as listed in Tables 15 and 16 in the Appendix, and then plotted accordingly, as shown in Figure 28. Note that Palmer's [1946] field data points, though mostly falling in the range of laminar flow, tend to underestimate the friction coefficient as the flow rate (or Reynolds number) and hence the flow depth decreases. The plot of his data points clearly demonstrates how difficult the depth measurements are with thin flows in the field which are as bad as, if not worse than, in the laboratory.

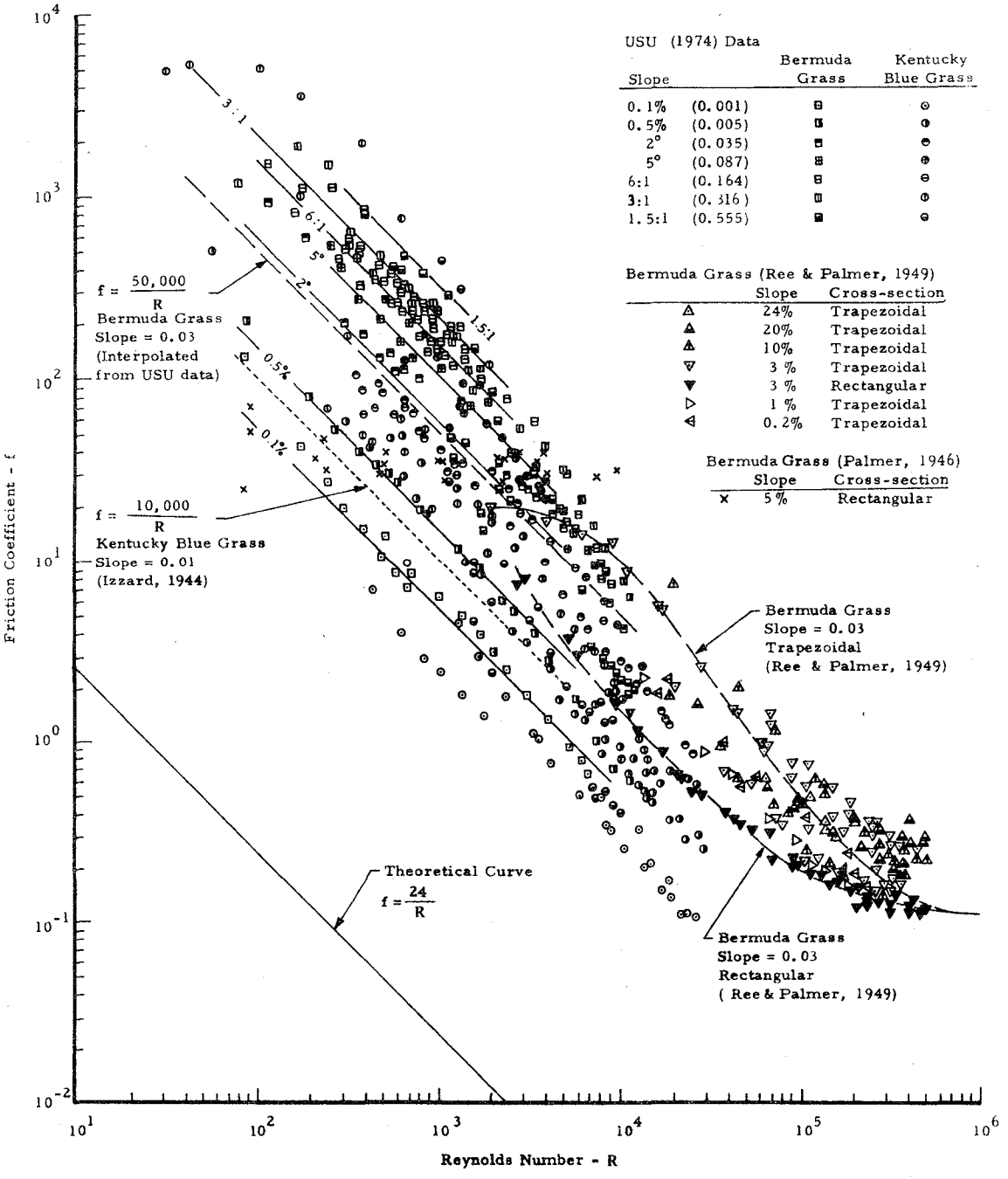

Figure 28. Relationships between the Darcy-Weisbach friction coefficient and Reynolds number for flow on natural turf surfaces.

4. Ree and Palmer's [1949] field experiments on Bermuda grass had two different channels cross-sectional shapes: Trapezoidal and rectangular. The Reynolds number in Table 15 was computed by using Eq. 2 rather than using Eq. 24. A plot of their data points on Figure 28 reveals three interesting results. First, their data points mostly falling in the range of transition and turbulent flow tend to converge to a fixed f value at a high Reynolds number. From Figure 28, the fixed f value for turbulent flow in Bermuda-grassed channels was found to be about 0.11 which in turn gave the relative roughness, y_o/k, equal to 2.17 by means of the Karman-Prandtl logarithmic resistance equation for free-surface turbulent flow on the rough surface. Second, the f values for flow on the same slope may differ due mainly to various channel shapes. For instance, in Figure 28, two broken curves were drawn to connect two groups of data points on the same 3 percent channel slope: One is for flow in trapezoidal channel and the other in a rectangular channel. The f values along the former broken curve are greater than that along the latter broken curve, but both broken curves seem to meet at a point where the R value is approximately equal to 2,000. Finally, the point of intersection between the two broken curves may be the critical point where the flow on the 3 percent slope starts to deviate from the laminar flow region to the transition. The last statement was confirmed by plotting by interpolation on Figure 28 a broken line representing the f-R relationship for laminar flow on the Bermuda grass surface with a 3 percent slope.

The consequence of the foregoing analyses using experimental data obtained from the present study and previous investigators [Palmer, 1946; Ree and Palmer, 1949] is strikingly useful. In the laminar flow regime, a simple expression for the friction coefficient such as Eq. 3 is valid and the C value in Eq. 3 is a function only of bed slope, S_o, for each species of turf tested (see Eq. 16). Since Kentucky Blue grass has physical appearance similar to Bermuda grass, the C value for both species of turf should be about equal. However, Izzard's [1944] experimental results on the Kentucky Blue grass surface with 1 percent slope, as depicted by a dotted line in Figure 28, gave the lower f values than those interpolated by the present sets of experimental data on the corresponding bed slope. Because we had an instrumentation problem at the time of testing Kentucky Blue grass, as indicated before, a definite conclusion with regard to such a comparison cannot be drawn at this moment without analyzing further experimental data points. For verification, another set of tests on Kentucky Blue grass should be run in the future.

Modeling the Friction Coefficient for Shallow Flows Over Turf Surfaces

The C value in Eq. 3 for each of the bed slopes tested can be read directly from Figure 28. The C values versus bed slopes, S_o, for Kentucky Blue grass and Bermuda grass tested in the present study are listed in Table 17 in the Appendix and plotted on log-log paper, as shown in Figure 29. It can readily be seen from Figure 29 that a straight-line (linear) relationship on log-log paper appears to exist between the

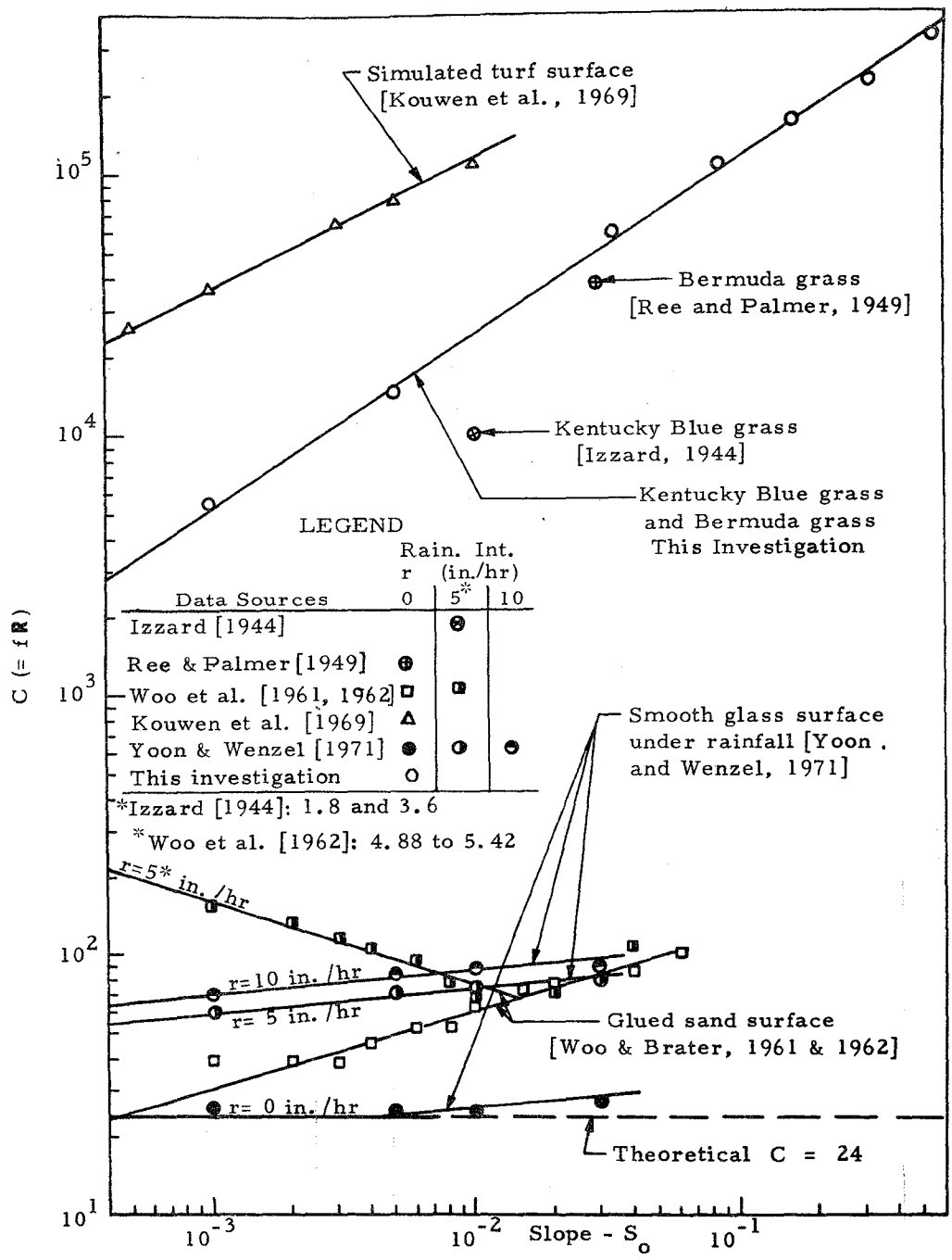

Figure 29. The C-S_o relationships for flow on various surfaces with or without raindrop impact.

C value and S_o for the two species of turf tested. This result implies that Eq. 16 can be simplified by use of an algebraic equation of this type:

$$C = aS_o^b \quad . \quad . \quad . \quad . \quad . \quad . \quad . \quad . \quad . \quad . \quad . \quad . \quad . \quad . \quad . \quad . \quad . \quad (26)$$

in which a and b are the parameters, the values of which seemingly depend on both the roughness size, k, and the rainfall intensity, r, if under rain. The dependence of the parameter values, a and b, on the k and r values was clearly demonstrated in Figure 29 by using other investigators' results such as Woo and Brater's [1961; 1962] data for a glued-sand surface, Kouwen's et al. [1969] data for a simulated turf surface, and Yoon and Wenzel's [1971] data for a smooth glass surface under rainfall or no rainfall. An inspection of the linear relationships between C and S_o for the aforementioned smooth and rough surfaces with or without raindrops reveals that there is a general trend in the variations of the a and b values with the values of k and r, as follows:

Without raindrop impact (i.e., r = 0), the a value approaches to the theoretical 24 while the b value approaches to zero for a perfectly smooth surface (k = 0). As the surface roughness increases, both a and b values increase with the magnitudes of their increases depending upon the surface roughness characteristics such as size, geometry, concentration, mobility, and stiffness, as classified previously. For rough surfaces which have the maximum density such as Woo and Brater's [1961] glued-sand surface and the turf surfaces, the b values that are the slopes of the C-S_o lines on log-log paper appear to be in the same order of magnitude, but the a values differ greatly from each other, depending upon the ''water holding capacity'' (i.e., detention or y_r in Eq. 11) on the surfaces. For example, from Figure 29, the a value is approximately 235 for Woo and Brater's [1961] glued-sand surface, but it becomes as high as 510,000 for Kentucky Blue grass and Bermuda grass surfaces. The corresponding b value for the former surface was determined to be 0.296 and that for the latter surfaces 0.662. Thus, for Woo and Brater's [1961] glued-sand surface, the C value can be calculated from

$$C = 235\, S_o^{0.296} \quad \text{for} \quad S_o \geq 0.00045 \quad . \quad . \quad . \quad . \quad (27a)$$

$$C = 24 \quad \text{for} \quad S_o \leq 0.00045 \quad . \quad . \quad . \quad . \quad (27b)$$

and for Kentucky Blue grass and Bermuda grass surfaces,

$$C = 510{,}000\, S_o^{0.662} \quad \text{for} \quad S_o \geq 0.00000029 \quad . \quad . \quad . \quad (28a)$$

$$C = 24 \quad \text{for} \quad S_o \leq 0.00000029 \quad . \quad . \quad . \quad (28b)$$

In practical applications, however, Eqs. 27a and 28a may be used without specifying a lower limit in S_o, below which the C value is theoretically 24, because both lower limits in S_o are negligibly small.

With raindrop impact (i.e., $r \neq 0$) acting on the water surface, the value of the parameter a in Eq. 26 increases with the rainfall intensity, r, whereas the b value with Yoon and Wenzel's [1971] data remains approximately constant for flow on a smooth glass surface. The increase in the C value due to r is enhanced by the decrease in the bed slope, S_o [Wood and Brater, 1962]. However, Woo and Brater's [1962] data points indicate that there seems to exist a limit in the bed slope, above which the effect of r on the C value is negligible. In view of Yoon and Wenzel's [1971] data points, it may be concluded that this slope limit goes up with the increasing rainfall intensity, r, and with the decreasing roughness size, k. Therefore, for a smooth surface such as glass tested by Yoon and Wenzel [1971], the slope limit may increase without bound while for a very rough surface such as natural turf, the slope limit may go down all the way to zero. In other words, the effect of raindrop impact on the flow resistance may be insignificant for flow on natural turf surfaces. Physically it is conceivable that raindrops falling on the turf surface tend to be intercepted and their added energy to the flow is broken up by tall dense grass stands before they hit the water surface. In any event, the effect of raindrop impact on the flow resistance of natural turf surfaces should be investigated further in the future.

Ignoring negligible factors such as raindrop impact and the slope limit in Eq. 28, and incorporating Eq. 28a with Eq. 3 yields

$$f = \frac{510{,}000\, S_o^{0.662}}{R} \quad \ldots \ldots \ldots \ldots \quad (29)$$

As long as the flow under study is in the laminar flow range (i.e., approximately $R = 10{,}000$ for $S_o = 0.001$ and $R = 1{,}000$ for $S_o = 0.555$), Eq. 29 can be used to evaluate the friction coefficient for shallow flows over Kentucky Blue grass and Bermuda grass surfaces. However, whether or not Eq. 29 is also applied to those cases with other species of turf rather than Kentucky Blue grass and Bermuda grass needs to be experimentally investigated.

SUMMARY AND CONCLUSIONS

Resistance to sheet flows over natural turf surfaces such as Kentucky Blue grass and Bermuda grass was experimentally investigated. The formulation of a functional relationship between the resistance coefficient and controlling parameters for shallow flows over various turf surfaces is essential to the successful modeling of surface runoff from urban highway side slopes covered with different species of turf. A unique laboratory facility including a computer-controlled rainstorm simulator, a forcibly-drained tilting test bed, a computer, a console for manual control, and a sunlight simulator was developed to conduct such friction tests as well as other required infiltration tests, results of which will be presented in another report. Time did not permit tests to be performed on all species of turf other than Kentucky Blue grass and Bermuda grass which can be sodded. An analysis of results obtained from friction tests on Kentucky Blue grass and Bermuda grass reveals that a functional relationship exists between the Darcy-Weisbach friction coefficient, Reynolds number, and bed slope for shallow flows over natural turf surfaces. A general trend of the functional relationship as affected by roughness and raindrop impact was also qualitatively determined.

The major conclusions that may be drawn from these laboratory studies of sheet flows over natural turf surfaces are summarized as follows:

1. The functional relationship for the friction coefficient formulated in the present study may be applied to any species of turf which has the maximum roughness density with the physical appearance similar to Kentucky Blue grass and Bermuda grass. Since only fine turf species are used on the urban highway sideslopes, it may be assumed that the roughness characteristics of the fine turf species such as size, geometry, concentration, mobility, and stiffness are similar to each other and the functional relationship is applicable.

2. The value of the Darcy-Weisbach friction coefficient, f, for laminar flow of the turf surface is of few orders of magnitude higher than that on the glued-sand (or concrete) surface. In general, the f value increases with the bed slope, but decreases with the Reynolds number (or discharge if the water temperature is constant). The range of laminar flow on the bed with a small slope is larger than that on the bed with a larger slope. A best-fitting line on each slope can be drawn through data points in the laminar flow range to parallel the theoretical line (Eq. 9).

3. An analysis of field data obtained from Ree and Palmer [1949] reveals that in the transition regime the f value for flow on the same slope may differ due mainly to various channel shapes, and that the flow in the Bermuda-grassed channel would not become fully turbulent unless the Reynolds number exceeds 10^6 with the f value about equal to 0.11.

4. A straight-line (linear) relationship on log-log paper appears to exist between the C value of Eq. 3 and the bed slope, S_o, for Kentucky Blue grass and Bermuda grass. The slope and intercept of the C-S_o line on log-log paper depends on the roughness size and the rainfall intensity. Without raindrop impact, the roughness size seems to be the only factor influencing the slope and intercept of the C-S_o line on log-log paper. However, with raindrop impact acting on the water surface, the increase in the C value due to the rainfall intensity is strengthened by the decrease in the bed slope, but is lessened by the increase in the roughness size. In application, for simplicity, the effect of raindrop impact on the resistance to shallow flows over natural turf surfaces may be ignored.

RECOMMENDATIONS

The principal future work recommended for the further investigations of the resistance to shallow flows over natural turf surface is as follows:

1. The functional relationship so formulated in the evaluation of the Darcy-Weisbach friction coefficient for laminar flow over the two sodded turf surfaces could be refined by conducting further tests on the same turf surfaces that will be directly seeded rather than sodded on the test bed. The direct seeding of turf on the test bed, though it will take more time for grass to grow and mature prior to experiments than sodding, has an advantage of producing a more uniform and even soil surface on the test bed because longer preparatory time permits fine-grained soil to consolidate and thus a chance to have the even soil surface fixed before erosion and channelization starts.

2. Many species of turf other than those specified need to be tested for studying the effects of the roughness characteristics on the flow resistance. For convenience in controlling the roughness factors, artificial (synthetic) turf which has a uniform roughness size, roughness density, and roughness stiffness may be used in the future study. In addition, other materials such as concrete and bituminus used on the roadway, paved shoulder, and paved side slope need to be tested. It is expected that testing each material having a different roughness size will produce a unique functional relationship of the friction coefficient for shallow flow over such a material.

3. Although the effect of raindrop impact on the resistance to shallow flows over natural turf surfaces has been qualitatively determined by using previous investigators' experimental data on other smooth and rough surfaces, it is in the best interest of this research to carry some similar laboratory experiments on turf surfaces to determine quantitatively the variation of the friction coefficient as affected by the interaction of the rainfall intensity, bed slope, and roughness size.

4. Instrumentation troubles encountered by the flow depth measuring devices should be corrected in the future experiments. As mentioned previously, use of helical wound resistance wires and manometer tubes in the flow depth measurement has many inherent sources of errors in the measurement which cannot be improved or modified without resorting to development of a new depth-measuring device.

REFERENCES

Allen, J. 1934. Streamline and turbulent flows in open channels. Phil. Mag., 17:1081-1112.

American Society of Civil Engineers, Committee on Hydromechanics of the Hydraulics Division. 1963. Friction factors in open channels. Progress Report of the Task Force on Friction Factors in Open Channels. Jour. Hydraul. Div., Proc. Amer. Soc. Civil Engineers, 89(HY2):97-143.

Brutsaert, W. F. 1971. De Saint-Venant equations experimentally verified. Jour. Hydraul. Div., Proc. Amer. Soc. Civil Engineers, 97(HY9):1387-1401.

Chow, V. T. 1959. Open-Channel Hydraulics. McGraw-Hill Book Co., New York, New York. pp. 7-16, 179-188, 543-549.

Emett, W. W. 1970. The hydraulics of overland flow on hill slopes. U.S. Geol. Surv. Prof. Paper 662-A, Washington, D.C.

Fenzl, R. N. 1962. Hydraulic resistance of broad shallow vegetated channels. Ph.D. Dissertation, Univ. of California, Davis, California.

Gourlay, M. R. 1970. Discussion of flow retardance in vegetated channels by N. Kouwen, T. E. Unny, and H. M. Hill. Jour. Irrig. Drain. Div., Proc. Amer. Soc. Civil Engineers, 96(IR3):351-357.

Heermann, D. F., R. J. Wenstrom, N. A. Evans. 1969. Prediction of flow resistance in furrows from soil roughness. Trans. Amer. Soc. Agr. Engineers, 12(4):482-485.

Hopf, L. 1910. Turbulenz bei einem flusse. Ann. Physik, 337, Vierte Folge, 32:777-808.

Horton, R. E., H. R. Leach, and R. Van Vliet. 1934. Laminar sheet flow. Trans. Amer. Geophys. Union, 15:393-404.

Izzard, C. F. 1944. The surface-profile of overland flow. Trans. Amer. Geophys. Union, 25:959-968.

Jeffreys, H. 1925. The flow of water in an inclined channel of rectangular section. Phil. Mag., 49:293, 793-807.

Kisisel, I. T., A. R. Rao, J. W. Delleur, and L. D. Meyer. 1971. Turbulence characteristics of overland flow--the effect of rainfall and boundary roughness. Tech. Rept. No. 28, Water Resources and Hydromechanics Laboratory, Purdue University, Lafayette, Indiana.

Koloseus, H. J., and J. Davidian. 1966a. Free surface instability correlations, laboratory studies of open channel flow. U.S. Geol. Surv. Water-Supply Paper 1592-C, Washington, D.C.

Koloseus, H. J., and J. Davidian. 1966b. Roughness concentration effects on flow over hydrodynamically rough surfaces, laboratory studies of open channel flow. U.S. Geol. Surv. Water-Supply Paper 1592-D, Washington, D.C.

Kouwen, N., and T. E. Unny. 1973. Flexible roughness in open channels. Jour. Hydraul. Div., Proc. Amer. Soc. Civil Engineers, 99(HY5):713-728.

Kouwen, N., T. E. Unny, and H. M. Hill. 1969. Flow retardance in vegetated channels. Jour. Irrig. Drain. Div., Proc. Amer. Soc. Civil Engineers, 95(IR2):329-342.

Kruse, E. G., C. W. Huntley, and A. R. Robinson. 1965. Flow resistance in simulated irrigation borders and furrows. Conserv. Res. Rept. No. 3, Agr. Res. Serv., U.S. Dept. of Agr., 56 pp.

Kuhlemeyer, R. L., and D. B. Warner. 1963. Discussion of spatially varied flow from controlled rainfall by D. C. Woo and E. F. Brater. Jour. Hydraul. Div., Proc. Amer. Soc. Civil Engineers, 89(HY4):233-240.

Li, R. M. 1972. Sheet flow under simulated rainfall. M.S. Thesis, Colorado State Univ., Fort Collins, Colorado.

Li, R. M., and H. W. Shen. 1973. Effect of tall vegetations on flow and sediment. Jour. Hydraul. Div., Proc. Amer. Soc. Civil Engineers, 99(HY5):793-814.

Myers, L. E. 1959. Flow regimes in surface irrigation. Agr. Eng., 40(11):676-677, 682-683.

Nnaji, S., and I. P. Wu. 1973. Flow resistance from cylindrical roughness. Jour. Irrig. Drain. Div., Proc. Amer. Soc. Civil Engineers, 99(IR1):15-26.

Owen, W. M. 1954. Laminar to turbulent flows in a wide open channel. Trans. Amer. Soc. Civil Engineers, 119:1157-1164.

Palmer, V. J. 1946. Retardance coefficients for low flows in channels lined with vegetation. Trans. Amer. Geophy. Union, 27:187-197.

Parsons, D. A. 1949. Depths of overland flow. SCS-TP-82, Soil Conserv. Serv. Res., U.S. Dept. of Agriculture.

Phelps, H. O. 1970. The friction coefficient for shallow flows over a simulated turf surface. Water Resour. Res., 6(4):1220-1226.

Phelps, H. O. 1975. Shallow laminar flows over rough granular surfaces. Jour. Hydraul. Div., Proc. Amer. Soc. Civil Engineers, 101(HY3):367-384.

Ree, W. O. 1949. Hydraulic characteristics of vegetation for vegetated waterways. Agr. Eng., 30(4):184-189.

Ree, W. O. 1958. Retardance coefficients for row crops in diversion terraces. Trans. Amer. Soc. Agr. Engineers, 1(1):78-80.

Ree, W. O., and V. J. Palmer. 1949. Flow of water in channels protected by vegetative linings. U.S. Soil Conserv. Tech. Bull. No. 967, 115 p.

Robertson, J. M., and H. Rouse. 1941. On the four regimes of open-channel flow. Civil Eng., 11(3):169-171.

Rouse, H. 1965. Critical analysis of open-channel resistance. Jour. Hydraul. Div., Proc. Amer. Soc. Civil Engineers, 91(HY4):1-25.

Sayre, W. W., and M. L. Albertson. 1961. Roughness spacing in rigid open channels. Jour. Hydraul. Div., Proc. Amer. Soc. Civil Engineers, 87(HY3):121-150.

Schlichting, H. 1936. Experimentalle Untersuchungen zum Rauhigkeit's problem: Ingenieur-Archiv., 7(1):1-34. [Translation, NACA Tech. Memo 823, 1937.]

Shen, H. W. 1972. Sedimentation and contaminant criteria for watershed planning and management. Completion Rept. Series No. 31, Environmental Resources Center, Colorado State University, Fort Collins, Colorado.

Shen, H. W., and R. M. Li. 1973. Rainfall effect on sheet flow over smooth surface. Jour. Hydraul. Div., Proc. Amer. Soc. Civil Engineers, 99(HY5):771-792.

Stillwater Outdoor Hydraulic Laboratory. 1947. Handbook of channel design for soil and water conservation. U.S. Soil Conserv. Serv. SCS-TP-61.

Straub, L. G., E. Silberman, and H. C. Nelson. 1958. Open-channel flow at small Reynolds numbers. Trans. Amer. Soc. Civil Engineers, 123:685-706.

U.S. Army Engineer District, Los Angeles. 1954. Data report, airfield drainage investigation.

U.S. Waterways Experiment Station Paper 17. 1935. Studies of river bed materials and their movement, with special reference to the lower Mississippi River, Vicksburg, Mississippi.

Wenzel, H. G., Jr. 1970. The effect of raindrop impact and surface roughness on sheet flow. WRC Res. Rept. No. 34, University of Illinois, Water Resources Center, Urbana, Illinois.

Wessels, W. P. J., and T. Strelkoff. 1968. Established surge on an impervious vegetated bed. Jour. Irrig. Drain. Div., Proc. Amer. Soc. Civil Engineers, 94(IR1):1-22.

Woo, D. C., and E. F. Brater. 1961. Laminar flow in rough rectangular channels. Jour. Geophys. Res., 66(12):4207-4217.

Woo, D. C., and E. F. Brater. 1962. Spatially varied flow from controlled rainfall. Jour. Hydraul. Div., Proc. Amer. Soc. Civil Engineers, 88(HY6):31-56.

Yoon, N. Y. 1970. The effect of rainfall on the mechanics of steady spatially varied sheet flow on a hydraulically smooth boundary. Ph.D. dissertation, Univ. of Illinois, Urbana, Illinois.

Yoon, N. Y., and H. G. Wenzel, Jr. 1971. Mechanics of sheet flow under simulated rainfall. Jour. Hydraul. Div., Proc. Amer. Soc. Civil Engineers, 97(HY9):1367-1386.

Yu, Y.S., and J. S. McNown. 1964. Runoff from impervious surfaces. Jour. Hydraul. Res., Internat. Assoc. Hydraul. Res., 2(1):2-24.

APPENDIX

For compilation of measured and computed data, an electronic digital computer (EAI PACER 100) was used. Tables 1 through 7 are measured and computed data for flow on the Kentucky Blue grass surface and Tables 8 through 14 on the Bermuda grass surface with 0.1 percent (0.001), 0.5 percent (0.005), 2^{o} (0.035), 5^{o} (0.087), 6:1 (0.164), 3:1 (0.316), and 1.5:1 (0.555) bed slopes, respectively.

Table 15 is measured and computed data for flow in rectangular or Trapezoidal Bermuda-grassed channels with various channel slopes ranging from 0.2 to 24 percent [Ree and Palmer, 1949] and Table 16 for flow in a rectangular Bermuda-grassed channel with 5 percent bed slope [Palmer, 1946].

Table 1. Test and computed data on Kentucky Blue grass with 0.1 percent bed slope.

Test Date	Discharge q cfs/ft	Depth y_o in.	Mean Velocity V ft/sec	Friction Coefficient f	Reynolds Number R	Froude Number F
4/25/74	0.1395	3.369	0.496	0.292	9226.71	0.1652
ditto	0.1310	3.353	0.468	0.327	8867.42	0.1563
ditto	0.0946	3.083	0.368	0.487	6257.83	0.1280
ditto	0.0529	2.735	0.232	1.088	3499.43	0.8560
ditto	0.0260	2.346	0.133	2.842	1720.82	0.0530
ditto	0.0100	1.864	0.064	9.549	665.05	0.0289
ditto	0.0551	2.716	0.243	0.981	3647.57	0.0902
ditto	0.1384	3.436	0.483	0.315	9156.08	0.1591
ditto	0.1660	3.619	0.550	0.256	10982.76	0.1766
ditto	0.2041	3.831	0.639	0.201	13500.00	0.1993
ditto	0.2679	4.133	0.777	0.146	17723.69	0.2335
ditto	0.2916	4.255	0.822	0.134	19288.87	0.2433
ditto	0.3442	4.446	0.928	0.110	22766.14	0.2689
4/26/74	0.1227	3.637	0.405	0.475	8121.48	0.1296
ditto	0.1979	4.377	0.542	0.318	13093.79	0.1583
ditto	0.2293	4.202	0.654	0.210	15171.33	0.1950
ditto	0.2790	4.300	0.778	0.152	18453.99	0.2292
ditto	0.3563	4.643	0.920	0.117	23568.22	0.2608
ditto	0.4064	4.840	1.007	0.102	26880.46	0.2795
ditto	0.0660	2.763	0.286	0.720	4369.16	0.1053
ditto	0.0356	2.435	0.175	1.691	2358.33	0.0687
ditto	0.0195	2.189	0.107	4.083	1294.27	0.0442
5/3/74	0.0066	1.263	0.063	6.733	441.77	0.0344
ditto	0.0095	1.319	0.086	3.743	632.12	0.0462
ditto	0.0128	1.454	0.105	2.779	848.92	0.0536
ditto	0.0155	1.554	0.119	2.323	1026.10	0.0586
ditto	0.0210	1.737	0.145	1.770	1389.98	0.0671
ditto	0.0280	1.917	0.175	1.332	1857.20	0.0774

Note: Temperature 47°F (8.3°C) is used in the computation, but water temperature ranged between 45°F (7.2°C) and 50°F (10.0°C) during experiments.

Table 2. Test and computed data on Kentucky Blue grass with 0.5 percent bed slope.

Test Date	Discharge q cfs/ft	Depth y_o in.	Mean Velocity V ft/sec	Friction Coefficient f	Reynolds Number R	Froude Number F
3/20/74	0.0035	1.039	0.040	67.399	232.95	0.0243
ditto	0.0046	1.168	0.047	56.010	304.59	0.0267
ditto	0.0062	1.291	0.058	41.031	413.39	0.0312
ditto	0.0083	1.635	0.061	46.806	551.85	0.0292
ditto	0.0094	1.766	0.064	45.941	625.22	0.0294
ditto	0.0124	1.898	0.078	32.747	824.99	0.0349
ditto	0.0188	2.205	0.102	22.382	1249.43	0.0422
4/22/74	0.1238	2.561	0.580	0.816	8188.99	0.2212
ditto	0.0891	2.446	0.437	1.371	5895.54	0.1706
ditto	0.0644	2.370	0.326	2.387	4263.07	0.1293
ditto	0.0478	2.166	0.264	3.311	3162.90	0.1098
ditto	0.0271	1.994	0.163	8.008	1796.32	0.0706
ditto	0.0100	1.558	0.077	27.859	665.05	0.0378
ditto	0.0008	0.803	0.013	504.549	57.89	0.0089
ditto	0.0116	1.568	0.089	21.056	772.58	0.0435
ditto	0.0389	1.984	0.235	3.847	2572.82	0.1019
ditto	0.0734	2.275	0.387	1.626	4858.66	0.1567
ditto	0.1931	3.029	0.765	0.554	12772.22	0.2683
ditto	0.2028	3.047	0.798	0.511	13418.38	0.2793
ditto	0.2268	3.200	0.850	0.474	15000.88	0.2901
ditto	0.2384	3.207	0.892	0.431	15773.61	0.3042
ditto	0.1011	2.594	0.467	1.270	6690.75	0.1773
ditto	0.1331	2.873	0.555	0.997	8806.00	0.2002
ditto	0.1558	3.078	0.607	0.894	10310.69	0.2113
ditto	0.1835	3.254	0.676	0.762	12138.22	0.2290
ditto	0.2204	3.504	0.754	0.659	14577.97	0.2461
ditto	0.2625	3.768	0.835	0.578	17362.75	0.2628
ditto	0.2930	3.442	1.021	0.353	19382.50	0.3361
ditto	0.3717	3.757	1.187	0.285	24585.55	0.3739
ditto	0.4472	4.037	1.329	0.244	29581.44	0.4039
4/24/74	0.1752	3.003	0.700	0.656	11593.55	0.2466
ditto	0.2345	3.333	0.844	0.501	15514.40	0.2822
ditto	0.3233	3.734	1.039	0.370	21387.96	0.3283
ditto	0.4112	4.104	1.202	0.304	27199.39	0.3623

Note: Temperature 47°F (8.3°C) is used in the computation, but water temperature ranged between 45°F (7.2°C) and 50°F (10.0°C) during experiments.

Table 2. Continued.

Test Date	Discharge q cfs/ft	Depth y_o in.	Mean Velocity V ft/sec	Friction Coefficient f	Reynolds Number R	Froude Number F
4/26/74	0.1373	3.584	0.459	1.817	9085.65	0.1482
ditto	0.1470	3.752	0.470	1.819	9726.89	0.1481
ditto	0.1603	3.812	0.504	1.603	10607.41	0.1578
ditto	0.2557	3.917	0.783	0.684	16915.54	0.2461
ditto	0.3030	4.344	0.837	0.664	20042.66	0.2451
ditto	0.3686	4.850	0.912	0.625	24380.78	0.2528
ditto	0.3952	4.924	0.963	0.569	26141.85	0.2649

Note: Temperature 47°F (8.3°C) is used in the computation, but water temperature ranged between 45°F (7.2°C) and 50°F (10.0°C) during experiments.

Table 3. Test and computed data on Kentucky Blue grass with 2 degree bed slope.

Test Date	Discharge q cfs/ft	Depth y_o in.	Mean Velocity V ft/sec	Friction Coefficient f	Reynolds Number R	Froude Number F
4/17/74	0.0057	0.814	0.084	84.543	380.83	0.0574
ditto	0.0074	0.995	0.089	92.671	491.98	0.0548
ditto	0.0121	1.117	0.130	49.465	800.41	0.0751
ditto	0.0185	1.294	0.172	32.722	1227.71	0.0923
ditto	0.0243	1.430	0.204	25.659	1609.90	0.1042
ditto	0.0306	1.772	0.207	30.716	2030.08	0.0953
ditto	0.0369	1.844	0.240	23.899	2443.28	0.1080
ditto	1.919	0.268	0.268	19.930	2839.43	0.1183
ditto	0.0499	1.988	0.301	16.352	3305.55	0.1306
4/23/74	0.0759	1.928	0.472	6.451	5026.18	0.2079
ditto	0.0589	1.849	0.382	9.457	3899.61	0.1717
ditto	0.0402	1.699	0.284	15.757	2660.58	0.1330
ditto	0.0175	1.289	0.163	36.098	1162.50	0.0879
ditto	0.0936	1.998	0.562	4.723	6196.88	0.2430
ditto	0.1078	2.092	0.618	4.090	7134.57	0.2611
ditto	0.1320	2.178	0.727	3.080	8736.60	0.3009
ditto	0.1536	2.293	0.803	2.656	10163.53	0.3241
ditto	0.1695	2.370	0.858	2.409	11210.34	0.3403
ditto	0.1967	2.473	0.954	2.031	13013.11	0.3706
ditto	0.2178	2.542	1.028	1.799	14410.09	0.3907
ditto	0.2652	2.675	1.189	1.414	17542.87	0.4441
ditto	0.2762	2.671	1.240	1.298	18270.37	0.4635
ditto	0.2790	2.687	1.245	1.296	18453.99	0.4639
ditto	0.3578	2.848	1.507	0.937	23669.22	0.5455
ditto	0.3984	2.922	1.636	0.817	26352.08	0.5844
5/1/74	0.0056	0.875	0.077	110.177	372.39	0.0519
ditto	0.0076	0.976	0.094	82.062	507.57	0.0583
ditto	0.0100	1.142	0.105	76.193	667.20	0.0605
ditto	0.0128	1.143	0.134	47.145	848.92	0.0769
ditto	0.0157	1.253	0.151	41.052	1043.86	0.0824
ditto	0.0208	1.418	0.176	34.049	1379.69	0.0905

Note: Temperature 47°F (8.3°C) is used in the computation, but water temperature ranged between 45°F (7.2°C) and 50°F (10.0°C) during experiments.

Table 4. Test and computed data on Kentucky Blue grass with 5 degree bed slope.

Test Date	Discharge q cfs/ft	Depth y_o in.	Mean Velocity V ft/sec	Friction Coefficient f	Reynolds Number R	Froude Number F
3/7/74	0.0123	1.258	0.117	169.629	817.09	0.0642
ditto	0.0151	1.312	0.138	128.343	999.75	0.0738
ditto	0.0218	1.510	0.173	94.226	1442.01	0.0861
ditto	0.0268	1.698	0.189	88.432	1774.57	0.0889
4/29/74	0.0785	1.768	0.532	11.642	5195.83	0.2451
ditto	0.1040	1.857	0.671	7.695	6879.64	0.3014
ditto	0.1279	1.923	0.798	5.644	8461.12	0.3520
ditto	0.1547	1.991	0.932	4.280	10237.01	0.4020
ditto	0.2004	2.119	1.134	3.078	13255.71	0.4766
ditto	0.0777	1.922	0.485	15.277	5139.04	0.2139
ditto	0.0551	1.755	0.377	23.085	3647.57	0.1740
ditto	0.0436	1.608	0.325	28.421	2884.83	0.1568
ditto	0.0170	1.057	0.194	52.524	1130.40	0.1154
4/30/74	0.0100	0.984	0.122	122.479	665.05	0.0755
ditto	0.0190	1.240	0.184	68.130	1260.82	0.1013
ditto	0.0216	1.318	0.196	63.521	1431.33	0.1049
ditto	0.0283	1.506	0.225	55.393	1873.04	0.1123
ditto	0.0337	1.589	0.254	45.736	2233.06	0.1236
ditto	0.0408	1.669	0.294	36.102	2704.88	0.1391
ditto	0.0478	1.724	0.332	29.110	3162.90	0.1550
ditto	0.0521	1.761	0.355	26.067	3450.57	0.1638
ditto	0.0605	1.805	0.402	20.878	4002.20	0.1830

Note: Temperature 47°F (8.3°C) is used in the computation, but water temperature ranged between 45°F (7.2°C) and 50°F (10.0°C) during experiments.

Table 5. Test and computed data on Kentucky Blue grass with 6:1 bed slope.

Test Date	Discharge q cfs/ft	Depth y_o in.	Mean Velocity V ft/sec	Friction Coefficient f	Reynolds Number R	Froude Number F
3/21/74	0.0059	0.444	0.159	61.570	391.37	0.1470
ditto	0.0067	0.506	0.160	69.253	447.56	0.1386
ditto	0.0086	0.578	0.179	63.507	571.40	0.1448
ditto	0.0101	0.659	0.185	67.478	674.33	0.1404
ditto	0.0113	0.691	0.196	63.363	747.74	0.1449
ditto	0.0128	0.700	0.219	51.086	848.92	0.1614
ditto	0.0188	0.756	0.299	29.704	1249.43	0.2117
5/2/74	0.0295	0.798	0.444	14.258	1953.91	0.3056
ditto	0.0429	1.097	0.469	17.534	2839.43	0.2755
ditto	0.0620	1.289	0.577	13.609	4105.80	0.3128
ditto	0.0891	1.417	0.754	8.777	5895.54	0.3895
ditto	0.1268	1.452	1.048	4.658	8392.77	0.5346
1/21/74	0.0794	0.984	0.967	3.704	5252.85	0.5995
ditto	0.0918	1.015	1.085	3.041	6075.66	0.6617
ditto	0.1059	1.067	1.190	2.655	7006.66	0.7081
ditto	0.1147	1.049	1.311	2.152	7589.10	0.7866
ditto	0.1248	1.068	1.402	1.914	8256.70	0.8341

Note: Temperature 47°F (8.3°C) is used in the computation, but water temperature ranged between 45°F (7.2°C) and 50°F (10.0°C) during experiments.

Table 6. Test and computed data on Kentucky Blue grass with 3:1 bed slope.

Test Date	Discharge q cfs/ft	Depth y_o in.	Mean Velocity V ft/sec	Friction Coefficient f	Reynolds Number R	Froude Number F
1/24/74	0.0092	0.469	0.236	56.726	613.60	0.2166
ditto	0.0294	0.676	0.522	16.784	1950.96	0.3983
ditto	0.0436	0.811	0.644	13.244	2884.83	0.4484
ditto	0.0566	0.808	0.841	7.745	3747.62	0.5864
ditto	0.0751	0.838	1.074	4.923	4970.10	0.7355
ditto	0.0873	0.866	1.209	4.013	5776.60	0.8146
ditto	0.1002	0.901	1.334	3.430	6628.24	0.8812
ditto	0.1167	0.955	1.465	3.018	7720.91	0.9393
ditto	0.1289	0.965	1.603	2.547	8529.67	1.0226
ditto	0.1448	0.969	1.793	2.043	9582.96	1.1416
3/22/74	0.0056	0.319	0.212	47.812	375.26	0.2360
ditto	0.0067	0.343	0.236	41.509	447.56	0.2533
ditto	0.0135	0.415	0.392	18.334	897.81	0.3811
ditto	0.0190	0.538	0.424	20.322	1259.21	0.3620
ditto	0.0245	0.645	0.457	20.960	1626.18	0.3564
ditto	0.0301	1.302	0.277	114.743	1990.88	0.1523
4/19/74	0.0004	0.296	0.020	4931.768	32.92	0.0232
ditto	0.0006	0.372	0.021	5332.226	44.68	0.0223
ditto	0.0015	0.650	0.029	5215.895	104.33	0.0225
ditto	0.0026	0.814	0.038	3650.860	174.58	0.0270
ditto	0.0040	0.989	0.049	2785.620	267.55	0.0309
ditto	0.0057	1.130	0.061	2055.737	380.59	0.0359
ditto	0.0074	1.156	0.077	1297.923	495.26	0.0453
ditto	0.0096	1.158	0.100	784.973	639.06	0.0582
4/30/74	0.1157	0.768	1.806	1.596	7654.90	1.2916
ditto	0.1592	0.741	2.576	0.757	10532.92	1.8749
ditto	0.1919	0.922	2.495	1.004	12692.31	1.6283
ditto	0.2078	0.916	2.720	0.840	13745.97	1.7804
ditto	0.2191	0.920	2.856	0.764	14493.94	1.8663
ditto	0.0408	0.741	0.662	11.462	2704.88	0.4820
5/2/74	0.0026	0.538	0.058	1057.433	174.58	0.0501
ditto	0.0048	0.444	0.130	177.682	319.11	0.1224
ditto	0.0100	0.436	0.277	38.465	667.20	0.2631
ditto	0.0135	0.408	0.398	17.400	897.81	0.3912
ditto	0.0213	0.456	0.560	9.849	1410.68	0.5200
ditto	0.0273	0.554	0.591	10.748	1809.75	0.4978

Note: Temperature 47°F (8.3°C) is used in the computation, but water temperature ranged between 45°F (7.2°C) and 50°F (10.0°C) during experiments.

Table 7. Test and computed data on Kentucky Blue grass with 1.5:1 bed slope.

Test Date	Discharge q cfs/ft	Depth y_o in.	Mean Velocity V ft/sec	Friction Coefficient f	Reynolds Number R	Froude Number F
1/25/74	0.0175	0.436	0.483	22.207	1162.50	0.4898
ditto	0.0248	0.414	0.721	9.457	1646.56	0.7505
ditto	0.0350	0.515	0.814	9.244	2316.29	0.7591
ditto	0.0492	0.512	1.154	4.575	3257.74	1.0791
ditto	0.0660	0.528	1.498	2.800	4369.16	1.3793
ditto	0.0927	0.541	2.056	1.522	6136.15	1.8705
ditto	0.1040	0.564	2.212	1.370	6879.64	1.9716
ditto	0.1167	0.638	2.194	1.577	7720.91	1.8380
ditto	0.1310	0.641	2.452	1.268	8667.42	2.0497
ditto	0.1427	0.674	2.538	1.245	9439.85	2.0685
3/15/74	0.0161	1.134	0.171	460.224	1070.79	0.1075
ditto	0.0208	1.181	0.211	312.736	1379.69	0.1305
5/1/74	0.1438	0.754	2.286	1.718	9511.30	1.7609
ditto	0.1069	0.419	3.057	0.533	7070.51	3.1593
ditto	0.1157	0.419	3.313	0.454	7654.90	3.4256
ditto	0.1268	0.456	3.333	0.488	8392.77	3.3011
ditto	0.1416	0.466	3.644	0.417	9368.60	3.5714
ditto	0.1536	0.474	3.886	0.373	10163.53	3.7754
ditto	0.0294	0.389	0.907	5.630	1950.96	0.1241
ditto	0.0652	0.513	1.525	2.624	4315.99	1.4249
ditto	0.0811	0.535	1.818	1.925	5367.61	1.6636
5/2/74	0.0234	0.309	0.909	4.444	1548.99	1.0949
ditto	0.0304	0.294	1.241	2.274	2015.69	1.5304
ditto	0.0259	0.410	0.758	8.482	1716.72	0.7925

Note: Temperature 47°F (8.3°C) is used in the computation, but water temperature ranged between 45°F (7.2°C) and 50°F (10.0°C) during experiments.

Table 8. Test and computed data on Bermuda grass with 0.1 percent bed slope.

Test Date	Discharge q cfs/ft	Depth y_o in.	Mean Velocity V ft/sec	Friction Coefficient f	Reynolds Number R	Froude Number F
8/28/74	0.0105	1.717	0.073	6.813	695.95	0.0342
ditto	0.0088	1.634	0.064	8.329	584.63	0.0309
ditto	0.0073	1.550	0.056	10.396	483.11	0.0277
ditto	0.0059	1.469	0.047	14.258	391.37	0.0236
ditto	0.0046	1.406	0.039	18.942	309.39	0.0205
ditto	0.0037	1.344	0.033	26.245	245.64	0.0174
ditto	0.0026	1.262	0.025	41.314	178.21	0.0139
ditto	0.0013	1.157	0.013	129.365	88.32	0.0078
9/3/74	0.0077	1.769	0.052	13.567	515.49	0.0242
ditto	0.0112	1.919	0.070	8.296	745.13	0.0310
ditto	0.0156	2.154	0.087	6.068	1036.16	0.0362
ditto	0.0205	2.370	0.104	4.679	1362.14	0.0413
ditto	0.0260	2.575	0.121	3.758	1720.82	0.0461
ditto	0.0313	2.694	0.139	2.975	2070.09	0.0518
ditto	0.0375	2.831	0.159	2.391	2486.17	0.0578
ditto	0.0485	3.027	0.192	1.754	3210.19	0.0675
ditto	0.0636	3.250	0.235	1.261	4210.40	0.0795
ditto	0.0829	3.445	0.288	0.886	5483.30	0.0949
ditto	0.0955	3.587	0.319	0.753	6319.00	0.1030
ditto	0.1069	3.662	0.350	0.639	7070.51	0.1117

Note: Temperature 47°F (8.3°C) is used in the computation, but water temperature ranged between 45°F (7.2°C) and 50°F (10.0°C) during experiments.

Table 9. Test and computed data on Bermuda grass with 0.5 percent bed slope.

Test Date	Discharge q cfs/ft	Depth y_o in.	Mean Velocity V ft/sec	Friction Coefficient f	Reynolds Number R	Froude Number F
8/24/74	0.0012	0.787	0.019	216.076	85.79	0.0135
ditto	0.0029	0.957	0.036	76.655	193.09	0.0228
ditto	0.0041	1.076	0.046	53.173	276.59	0.0274
ditto	0.0053	1.146	0.056	39.126	354.31	0.0319
ditto	0.0067	1.278	0.063	33.947	447.56	0.0343
ditto	0.0080	1.374	0.070	29.832	532.64	0.0366
ditto	0.103	1.571	0.078	27.196	681.49	0.0383
9/7/74	0.0121	1.532	0.094	18.288	800.41	0.0467
ditto	0.0195	1.790	0.131	11.169	1294.27	0.0598
ditto	0.0248	1.951	0.153	8.931	1646.56	0.0668
ditto	0.0350	2.116	0.198	5.759	2316.29	0.0833
ditto	0.0420	2.209	0.218	4.962	2660.58	0.0897
ditto	0.0514	2.384	0.258	3.818	3401.97	0.1023
ditto	0.0660	2.477	0.320	2.593	4369.16	0.1241
ditto	0.0909	2.618	0.416	1.616	6015.39	0.1572
ditto	0.1157	2.551	0.544	0.923	7654.90	0.2080
ditto	0.1459	2.704	0.647	0.691	9654.83	0.2404
ditto	0.1706	2.871	0.713	0.605	11286.59	0.2569

Note: Temperature 47°F (8.3°C) is used in the computation, but water temperature ranged between 45°F (7.2°C) and 50°F (10.0°C) during experiments.

Table 10. Test and computed data on Bermuda grass with 2 degree bed slope.

Test Date	Discharge q cfs/ft	Depth y_o in.	Mean Velocity V ft/sec	Friction Coefficient f	Reynolds Number R	Froude Number F
6/14/74	0.0096	1.281	0.090	117.206	639.13	0.0487
ditto	0.0200	1.799	0.133	75.142	1328.04	0.0609
ditto	0.0369	1.953	0.226	28.394	2443.28	0.0991
ditto	0.0443	2.129	0.249	25.571	2930.50	0.1044
ditto	0.0492	2.259	0.261	24.718	3257.74	0.1062
ditto	0.0551	2.346	0.282	22.075	3647.57	0.1124
ditto	0.0652	2.433	0.321	17.578	4315.99	0.1259
ditto	0.0743	2.482	0.359	14.401	4914.26	0.1392
ditto	0.1352	2.704	0.600	5.620	8945.41	0.2228
ditto	0.1649	2.788	0.709	4.144	10907.29	0.2594
7/7/74	0.0088	1.184	0.089	110.655	584.63	0.0502
ditto	0.0072	1.096	0.078	131.609	477.09	0.0460
ditto	0.0058	1.010	0.069	157.528	385.96	0.0420
ditto	0.0046	0.946	0.058	207.550	304.59	0.0366
ditto	0.0028	0.918	0.036	511.154	185.57	0.0233
ditto	0.0017	0.825	0.025	954.938	115.75	0.0170
8/18/74	0.0083	1.229	0.081	138.873	551.85	0.0448
ditto	0.0121	1.408	0.103	98.920	801.41	0.0531

Note: Temperature 47°F (8.3°C) is used in the computation, but water temperature ranged between 45°F (7.2°C) and 50°F (10.0°C) during experiments.

Table 11. Test and computed data on Bermuda grass with 5 degree bed slope.

Test Date	Discharge q cfs/ft	Depth y_o in.	Mean Velocity V ft/sec	Friction Coefficient f	Reynolds Number R	Froude Number F
6/13/74	0.0161	1.332	0.145	117.886	1067.23	0.0770
ditto	0.0300	1.740	0.207	75.659	1990.37	0.0961
ditto	0.0408	1.709	0.287	38.754	2704.88	0.1343
ditto	0.0529	1.914	0.331	32.523	3499.43	0.1466
ditto	0.0612	1.967	0.373	26.332	4053.88	0.1629
ditto	0.0751	2.014	0.447	18.808	4970.10	0.1928
ditto	0.0891	2.040	0.524	13.877	5895.54	0.2245
ditto	0.1002	2.053	0.585	11.188	6628.24	0.2500
ditto	0.1108	2.063	0.644	9.291	7328.06	0.2743
ditto	0.1217	2.079	0.702	7.868	8054.19	0.2981
8/18/74	0.0038	0.771	0.059	404.085	254.29	0.0416
ditto	0.0054	0.855	0.076	274.946	359.49	0.0504
ditto	0.0072	0.945	0.091	211.224	477.09	0.0575
ditto	0.0092	1.009	0.109	156.253	611.54	0.0669
ditto	0.0109	1.062	0.123	129.491	725.31	0.0734
8/3/74	0.0038	0.851	0.054	542.208	254.29	0.0359
ditto	0.0054	1.023	0.063	471.334	359.49	0.0385
ditto	0.0081	1.119	0.087	274.288	539.01	0.0505
ditto	0.0106	1.206	0.105	201.797	703.23	0.0588

Note: Temperature 47°F (8.3°C) is used in the computation, but water temperature ranged between 45°F (7.2°C) and 50°F (10.0°C) during experiments.

Table 12. Test and computed data on Bermuda grass with 6:1 bed slope.

Test Date	Discharge q cfs/ft	Depth y_o in.	Mean Velocity V ft/sec	Friction Coefficient f	Reynolds Number R	Froude Number F
6/12/74	0.0260	1.415	0.220	102.622	1720.82	0.1139
ditto	0.0369	1.626	0.272	77.184	2443.28	0.1313
ditto	0.0536	1.893	0.340	57.718	3548.55	0.1518
ditto	0.0768	1.976	0.466	31.999	5082.49	0.2040
ditto	0.0918	1.822	0.604	17.566	6075.66	0.2753
ditto	0.1147	1.825	0.754	11.316	7589.10	0.3430
ditto	0.1331	1.821	0.877	8.343	8806.00	0.3995
ditto	0.1459	1.815	0.964	9.426	10090.25	0.3758
ditto	0.0211	1.374	0.184	142.454	1396.57	0.0966
7/7/74	0.0017	0.575	0.036	1520.311	115.75	0.0295
ditto	0.0041	0.694	0.072	469.603	276.59	0.0532
ditto	0.0055	0.743	0.089	330.415	364.71	0.0634
ditto	0.0086	0.929	0.111	263.367	571.40	0.0711
ditto	0.0103	0.914	0.135	176.149	681.49	0.0869
ditto	0.0129	0.997	0.155	144.779	856.97	0.0959
ditto	0.0170	1.117	0.182	117.873	1125.70	0.1062
7/26/74	0.0090	0.963	0.112	267.470	598.00	0.0705
ditto	0.0103	1.124	0.109	328.209	681.49	0.0636
ditto	0.0113	1.039	0.130	215.328	747.74	0.0786
ditto	0.0135	1.136	0.143	195.210	897.81	0.0825
ditto	0.0151	1.311	0.138	241.397	999.75	0.0742
ditto	0.0180	1.361	0.158	190.204	1191.51	0.0836
7/28/74	0.0055	0.866	0.076	524.376	364.71	0.0503
ditto	0.0076	0.974	0.094	384.754	507.57	0.0588
ditto	0.0094	1.071	0.105	337.078	625.22	0.0628
ditto	0.0111	1.135	0.118	286.119	740.22	0.0682
ditto	0.0129	1.214	0.128	261.170	856.97	0.0714
ditto	0.0152	1.299	0.140	231.115	1008.49	0.0759
ditto	0.0187	1.413	0.159	196.888	1239.68	0.0822
8/3/74	0.0024	0.585	0.049	836.494	160.45	0.0399
ditto	0.0044	0.756	0.070	533.275	295.10	0.0499
ditto	0.0053	0.837	0.076	501.479	354.31	0.0515
ditto	0.0069	0.934	0.089	413.855	459.26	0.0567
ditto	0.0093	0.998	0.112	279.087	618.36	0.0690
ditto	0.0113	1.076	0.126	238.627	747.74	0.0747
ditto	0.0137	1.160	0.141	203.873	906.09	0.0808

Note: Temperature 47°F (8.3°C) is used in the computation, but water temperature ranged between 45°F (7.2°C) and 50°F (10.0°C) during experiments.

Table 12. Continued.

Test Date	Discharge q cfs/ft	Depth y_o in.	Mean Velocity V ft/sec	Friction Coefficient f	Reynolds Number R	Froude Number F
8/23/74	0.0039	0.907	0.052	1155.106	263.10	0.0339
ditto	0.0084	1.043	0.097	390.817	558.33	0.0583
ditto	0.0107	1.106	0.116	287.433	710.55	0.0680
ditto	0.0125	1.146	0.131	232.515	832.93	0.0756
ditto	0.0160	1.236	0.155	179.348	1061.78	0.0861
ditto	0.0214	1.344	0.191	128.849	1421.08	0.1016
8/25/74	0.0026	0.680	0.046	1108.368	174.58	0.0346
ditto	0.0047	0.795	0.071	544.906	314.23	0.0494
ditto	0.0069	0.885	0.094	351.998	459.26	0.0615
ditto	0.0097	0.981	0.119	242.364	646.04	0.0741
ditto	0.0125	1.062	0.142	185.235	832.93	0.0847
ditto	0.0164	1.153	0.171	138.627	1088.94	0.0980
ditto	0.0224	1.090	0.246	63.002	1484.34	0.1453

Note: Temperature 47°F (8.3°C) is used in the computation, but water temperature ranged between 45°F (7.2°C) and 50°F (10.0°C) during experiments.

Table 13. Test and computed data on Bermuda grass with 3:1 bed slope.

Test Date	Discharge q cfs/ft	Depth y_o in.	Mean Velocity V ft/sec	Friction Coefficient f	Reynolds Number R	Froude Number F
6/17/74	0.0096	0.687	0.168	163.614	639.13	0.1275
ditto	0.0237	1.006	0.283	84.715	1573.55	0.1773
ditto	0.0429	1.254	0.410	50.487	2839.43	0.2296
ditto	0.0612	1.502	0.489	42.495	4053.88	0.2503
ditto	0.0785	1.586	0.594	30.492	5195.83	0.2955
ditto	0.0955	1.601	0.716	21.180	6319.00	0.3546
ditto	0.1117	1.600	0.838	15.454	7393.00	0.4151
ditto	0.1300	1.601	0.974	11.438	8598.43	0.4825
ditto	0.1637	1.600	1.227	7.202	10832.02	0.6081
ditto	0.1788	1.589	1.350	5.910	11825.83	0.6713
7/29/74	0.0019	0.777	0.029	5936.334	127.77	0.0211
ditto	0.0049	0.701	0.085	658.074	328.97	0.0636
ditto	0.0074	0.838	0.107	495.101	495.26	0.0733
ditto	0.0103	0.911	0.135	335.348	681.49	0.0891
ditto	0.0138	1.015	0.163	257.697	914.41	0.1016
ditto	0.0185	1.082	0.206	172.583	1229.97	0.1242
ditto	0.0259	1.181	0.263	115.357	1716.72	0.1519
8/4/74	0.0024	0.629	0.047	1912.662	163.93	0.0373
ditto	0.0047	0.640	0.089	547.837	314.23	0.0697
ditto	0.0075	0.608	0.149	184.899	501.40	0.1200
ditto	0.0094	0.735	0.154	209.870	625.22	0.1126
ditto	0.0122	0.804	0.182	164.023	809.23	0.1274
ditto	0.0173	1.003	0.206	158.917	1144.31	0.1294
ditto	0.0211	1.027	0.247	114.099	1400.31	0.1527
8/26/74	0.0038	0.792	0.058	1583.515	254.29	0.0410
ditto	0.0069	0.736	0.113	390.015	459.26	0.0826
ditto	0.0100	0.825	0.146	259.998	667.20	0.1012
ditto	0.0138	0.773	0.214	113.816	914.41	0.1529

Note: Temperature 47°F (8.3°C) is used in the computation, but water temperature ranged between 45°F (7.2°C) and 50°F (10.0°C) during experiments.

Table 14. Test and computed data on Bermuda grass with 1.5:1 bed slope.

Test Date	Discharge q cfs/ft	Depth y_o in.	Mean r Velocityr- V ft/sec	Friction Coefficient f	Reynolds Number R	Froude Number F
7/30/74	0.0184	0.528	0.419	35.720	1220.29	0.3862
ditto	0.0266	0.500	0.639	14.547	1762.93	0.6052
8/4/74	0.0059	0.708	0.100	838.192	391.37	0.0797
ditto	0.0101	0.803	0.152	412.302	674.33	0.1136
ditto	0.0133	0.708	0.225	165.793	881.36	0.1792
ditto	0.0157	0.786	0.240	161.431	1043.86	0.1816
ditto	0.0170	0.845	0.241	172.175	1125.70	0.1759
ditto	0.0227	0.966	0.282	143.691	1505.73	0.1925
ditto	0.0327	0.823	0.477	42.911	2167.82	0.3523
8/27/74	0.0295	0.968	0.366	85.865	1953.95	0.2491
ditto	0.0216	0.905	0.286	130.917	1431.53	0.2017
ditto	0.0171	1.020	0.201	297.962	1134.98	0.1337
ditto	0.0127	0.905	0.168	379.661	840.90	0.1184
ditto	0.0098	0.821	0.144	470.430	653.05	0.1064
ditto	0.0057	0.706	0.097	880.628	380.59	0.0777
8/31/74	0.0221	0.643	0.413	44.830	1466.40	0.3447
ditto	0.0337	0.694	0.583	24.257	2233.06	0.4686
ditto	0.0457	0.896	0.611	28.477	3022.65	0.4325
ditto	0.0536	0.906	0.709	21.407	3548.55	0.4988
ditto	0.0620	0.998	0.745	21.363	4105.80	0.4994
ditto	0.0726	1.050	0.829	18.143	4803.30	0.5419
ditto	0.0794	1.050	0.907	15.193	5252.85	0.5922
ditto	0.0873	1.111	0.942	14.885	5776.60	0.5982
ditto	0.0964	0.907	1.276	6.625	6380.40	0.8967
ditto	0.1069	0.750	1.709	3.052	7070.51	1.3211
ditto	0.1187	1.183	1.204	9.706	7853.58	0.7409
ditto	0.1279	0.794	1.924	2.562	8461.12	1.4419
ditto	0.1384	0.835	1.987	2.515	9156.08	1.4552
ditto	0.1514	0.851	2.134	2.223	10017.18	1.5481
ditto	0.1592	0.859	2.223	2.068	10532.92	1.6051
ditto	0.1718	0.895	2.302	2.009	11363.04	1.6283
ditto	0.1764	0.879	2.406	1.807	11670.79	1.7167
ditto	0.1799	0.903	2.390	1.880	11903.63	1.6832
9/9/74	0.0092	0.750	0.147	408.776	611.54	0.1141
ditto	0.0187	0.584	0.385	46.884	1239.68	0.3371
ditto	0.0264	0.530	0.599	17.586	1751.32	0.5504
ditto	0.0337	0.932	0.434	58.832	2232.87	0.3009

Note: Temperature 47°F (8.3°C) is used in the computation, but water temperature ranged between 45°F (7.2°C) and 50°F (10.0°C) during experiments.

Table 15. Test and computed data on Bermuda grass with various channel slopes ranging from 0.2 to 24 percent [Ree and Palmer, 1949].

Test Date	Discharge Q cfs	Cross-Sectional Area A ft^2	Mean Velocity V ft/sec	Effective Slope S	Water Temp. °F	Friction Coefficient f	Reynolds Number R	Froude Number F
Trapezoidal shape, bed slope 24 percent.								
10/23/36	0.95	0.307	3.09	0.2345	60	0.921	37300	1.450
10/26/36	1.85	0.430	4.30	0.2308	60	0.607	67200	1.770
10/27/36	2.90	0.547	5.30	0.2276	60	0.469	98600	2.000
ditto	3.75	0.672	5.58	0.2346	60	0.481	114000	2.000
10/28/36	4.90	0.790	6.20	0.1932	60	0.356	141000	2.100
ditto	2.90	0.545	5.32	0.2262	60	0.461	98500	2.010
10/30/36	5.02	0.758	6.62	0.2135	60	0.321	140000	2.330
2/11/38	3.03	0.536	5.66	0.2350	56	0.447	103000	2.080
2/14/38	5.32	0.706	7.54	0.2287	55	0.291	161000	2.540
2/24/38	7.32	0.947	7.73	0.2307	54	0.346	202000	2.340
Trapezoidal shape, bed slope 20 percent								
9/02/38	4.200	0.838	5.01	0.1926	71	0.567	139000	1.660
9/07/38	6.500	0.976	6.66	0.1944	72	0.357	205000	2.110
ditto	9.850	1.270	7.77	0.1954	72	0.316	286000	2.240
9/08/38	13.400	1.550	8.64	0.1931	73	0.294	377000	2.310
9/12/38	17.300	1.820	9.48	0.1974	66	0.276	419000	2.410
9/13/38	21.600	2.190	9.88	0.1964	68	0.281	493000	2.390
9/16/38	21.300	2.130	10.00	0.2049	68	0.277	485000	2.460
2/12/40	27.300	2.930	9.31	0.1940	50	0.362	415000	2.090
9/19/41	0.951	0.449	2.12	0.1954	70	1.530	27400	1.020
9/20/41	3.020	0.733	4.12	0.1979	67	0.541	67500	1.730

Table 15. Continued.

Trapezoidal shape, bed slope 20 percent (cont.)

Test Date	Discharge Q cfs	Cross-Sectional Area A ft^2	Mean Velocity V ft/sec	Effective Slope S	Water Temp. °F	Friction Coefficient f	Reynolds Number R	Froude Number F
9/23/41	4.680	0.930	5.04	0.1961	66	0.415	94000	1.960
9/24/41	9.400	1.400	6.72	0.1994	66	0.299	158000	2.340
ditto	14.260	1.790	7.98	0.2012	66	0.252	226000	2.560
9/26/41	19.170	2.170	8.85	0.1990	68	0.225	279000	2.690
9/29/41	23.650	2.390	9.89	0.2062	70	0.194	337000	2.951
10/04/41	29.310	2.910	10.08	0.1977	68	0.204	378000	2.810
ditto	4.570	1.120	4.08	0.1978	68	0.728	89800	1.490
8/19/38	4.650	1.140	4.09	0.0916	71	0.509	141000	1.200
8/20/38	7.120	1.430	4.97	0.0906	70	0.380	192000	1.380
8/22/38	10.000	1.770	5.66	0.0907	74	0.333	257000	1.480
8/23/38	13.500	2.110	6.40	0.0906	74	0.288	322000	1.590
8/24/38	17.900	2.530	7.07	0.0884	74	0.246	381000	1.700
8/25/38	23.000	2.950	7.80	0.0874	73	0.216	449000	1.800
8/27/38	28.100	3.490	8.06	0.0845	73	0.217	512000	1.770
2/13/39	26.100	3.070	8.51	0.0842	48	0.187	362000	1.900
2/14/39	25.900	2.960	8.74	0.0872	48	0.178	363000	1.980
2/15/39	26.300	3.020	8.70	0.0880	49	0.184	372000	1.960
2/16/39	26.300	2.980	8.82	0.0846	48	0.171	369000	1.990
2/17/39	26.100	2.930	8.90	0.0857	45	0.168	349000	2.030
9/21/39	1.040	1.110	0.94	0.1024	67	7.150	20300	0.339
9/22/39	2.960	1.520	1.94	0.1009	60	1.970	46200	0.642
ditto	4.940	1.860	2.65	0.0988	66	1.120	73900	0.843
9/25/39	9.840	2.520	3.90	0.0985	65	0.606	126000	1.140
ditto	15.210	3.050	4.98	0.0982	67	0.411	183000	1.390

Table 15. Continued.

Trapezoidal shape, bed slope 20 percent (cont.)

Test Date	Discharge Q cfs	Cross-Sectional Area A ft^2	Mean Velocity V ft/sec	Effective Slope S	Water Temp. °F	Friction Coefficient f	Reynolds Number R	Froude Number F
9/26/39	20.820	3.520	5.93	0.0966	68	0.304	234000	1.600
9/28/39	25.840	3.940	6.56	0.0974	70	0.266	284000	1.720
10/03/39	30.440	4.310	7.07	0.0964	67	0.237	306000	1.810
10/04/39	35.460	4.720	7.51	0.0980	68	0.214	333000	1.920
11/08/40	0.979	0.620	1.58	0.1010	51	1.770	19300	0.677
11/12/40	2.820	0.953	2.96	0.1012	52	0.649	47100	1.120
ditto	4.710	1.210	3.90	0.1000	54	0.432	74300	1.360
11/15/40	9.930	1.750	5.67	0.0984	47	0.241	117000	1.810
ditto	14.700	2.240	6.56	0.0980	46	0.204	151000	1.970
11/18/40	19.800	2.660	7.44	0.0999	45	0.173	180000	2.160
ditto	24.60	3.050	8.06	0.0977	47	0.155	217000	2.250
11/22/40	29.80	3.420	8.74	0.1002	57	0.145	292000	2.360
Trapezoidal shape, bed slope 3 percent.								
7/26/38	4.090	2.510	1.630	0.0324	71	1.370	68300	0.436
7/27/38	4.090	2.420	1.690	0.0322	75	1.230	72600	0.457
7/29/38	6.870	2.930	2.340	0.0319	74	0.729	114000	0.592
8/01/38	9.760	3.500	2.790	0.0318	70	0.575	145000	0.665
8/02/38	14.000	4.000	3.500	0.0318	70	0.397	198000	0.800
8/03/38	18.800	4.590	4.100	0.0318	68	0.314	244000	0.900
8/04/38	23.300	5.140	4.540	0.0323	68	0.279	289000	0.963
8/05/38	29.000	5.770	5.030	0.0312	71	0.235	358000	1.030
5/13/39	0.093	0.412	0.226	0.0319	56	18.400	1990	0.118
5/14/39	0.215	0.715	0.301	0.0320	56	16.000	4100	0.126

Table 15. Continued.

Trapezoidal shape, bed slope 3 percent (cont.)

Test Date	Discharge Q cfs	Cross-Sectional Area A ft^2	Mean Velocity V ft/sec	Effective Slope S	Water Temp. ^oF	Friction Coefficient f	Reynolds Number R	Froude Number F
3/15/39	0.356	0.982	0.363	0.0327	52	14.700	6090	0.133
3/16/39	0.561	1.300	0.432	0.0323	56	12.600	9430	0.143
3/17/39	0.748	1.410	0.530	0.0314	51	8.650	11500	0.170
3/27/39	1.040	1.510	0.687	0.0308	56	5.320	17000	0.215
ditto	1.760	1.680	1.050	0.0312	57	2.510	28300	0.315
3/28/39	2.690	1.870	1.440	0.0321	58	1.470	42300	0.418
ditto	4.380	2.160	2.030	0.0329	58	0.845	66500	0.558
10/24/39	3.890	2.060	1.880	0.0337	62	0.949	62500	0.533
10/26/39	1.050	1.060	0.990	0.0322	64	1.940	19800	3.650
10/27/39	2.960	1.420	2.080	0.0328	65	0.560	53100	0.685
10/30/39	4.920	1.740	2.820	0.0332	57	0.362	75300	0.857
11/01/39	9.860	2.380	4.140	0.0352	52	0.223	128000	1.120
11/07/39	14.940	3.040	4.940	0.0356	47	0.187	163000	1.230
11/09/39	20.630	3.670	5.630	0.0355	51	0.161	226000	1.330
11/10/39	25.940	4.270	6.070	0.0354	52	0.151	272000	1.370
11/13/39	28.470	4.550	6.260	0.0354	53	0.148	294000	1.390
11/14/39	35.420	5.280	6.720	0.0348	52	0.137	337000	1.430
8/09/38	3.990	1.720	2.320	0.0359	68	0.753	93900	6.180
8/10/38	6.510	2.220	2.930	0.0361	70	0.546	141000	0.727
ditto	9.910	2.780	3.570	0.0370	70	0.426	193000	0.834
8/11/38	13.700	3.320	4.130	0.0365	72	0.347	253000	0.918
8/12/38	18.500	3.980	4.650	0.0354	73	0.288	313000	0.992
8/15/38	24.200	4.760	5.080	0.0352	73	0.264	377000	1.030
11/14/39	30.300	5.640	5.370	0.0352	73	0.260	439000	1.040

Table 15. Continued.

Trapezoidal shape, bed slope 3 percent (cont.)

Test Date	Discharge Q cfs	Cross-Sectional Area A ft^2	Mean Velocity V ft/sec	Effective Slope S	Water Temp. ^oF	Friction Coefficient f	Reynolds Number R	Froude Number F
10/05/39	3.950	1.600	2.460	0.0350	65	0.618	91300	0.673
10/06/39	1.090	0.634	1.720	0.0318	65	0.693	38000	0.606
10/07/39	2.930	1.030	2.850	0.0335	66	0.346	82700	0.881
10/09/39	4.860	1.450	3.350	0.0346	66	0.312	118000	0.942
10/10/39	9.850	2.200	4.460	0.0340	68	0.217	205000	1.120
10/11/39	15.200	2.940	5.180	0.0341	68	0.192	279000	1.190
10/12/39	20.200	3.560	5.680	0.0344	68	0.179	341000	1.240
ditto	24.600	4.080	6.040	0.0342	68	0.169	389000	1.270
10/20/39	29.800	4.730	6.300	0.0348	58	0.170	379000	1.280
ditto	34.800	5.300	6.570	0.0348	60	0.166	433000	1.300
9/19/41	0.939	1.420	0.660	0.0314	70	5.180	17600	0.220
9/20/41	2.980	2.100	1.420	0.0310	67	1.400	45800	0.420
9/23/41	4.680	2.540	1.840	0.0312	66	0.919	64200	0.521
9/24/41	9.440	3.580	2.640	0.0315	66	0.539	109000	0.684
ditto	14.390	4.370	3.290	0.0312	66	0.384	153000	0.806
9/26/41	19.660	5.210	3.780	0.0312	60	0.315	174000	0.890
Trapezoidal shape, bed slope 1 percent								
11/08/40	0.980	1.62	0.606	0.0098	51	2.080	13100	0.194
11/12/40	2.820	2.64	1.070	0.0097	51	0.845	29700	0.303
ditto	4.740	3.38	1.400	0.0103	53	0.604	46500	0.369
11/15/40	9.920	4.84	2.050	0.0108	47	0.359	74700	0.491
ditto	14.630	5.95	2.460	0.0111	46	0.285	97800	0.558
11/18/40	19.680	6.99	2.820	0.0101	44	0.211	116000	0.618

Table 15. Continued.

Trapezoidal shape, bed slope 1 percent (cont.)

Test Date	Discharge Q cfs	Cross-Sectional Area A ft^2	Mean Velocity V ft/sec	Effective Slope S	Water Temp. ^oF	Friction Coefficient f	Reynolds Number R	Froude Number F
11/18/40	24.670	8.00	3.090	0.0102	46	0.190	140000	0.655
11/22/40	30.000	8.83	3.400	0.0102	56	0.163	189000	0.707
Rectangular shape, bed slope 3 percent								
12/05/40	0.099	0.154	0.643	0.0297	41	2.850	6020	0.289
12/06/40	0.306	0.217	1.410	0.0301	41	0.850	15900	0.532
12/09/40	0.471	0.247	1.910	0.0294	43	0.512	29500	0.678
ditto	0.694	0.286	2.420	0.0290	44	0.364	44500	0.798
12/11/40	1.130	0.339	3.340	0.0278	44	0.218	71900	1.010
ditto	1.430	0.399	3.580	0.0278	44	0.222	91300	1.000
ditto	1.660	0.432	3.840	0.0279	44	0.210	106000	1.030
12/12/40	2.120	0.483	4.400	0.0278	45	0.179	137000	1.110
12/17/40	2.920	0.565	5.170	0.0276	46	0.150	193000	1.210
ditto	4.880	0.758	6.450	0.0267	47	0.126	328000	1.300
12/18/40	6.370	0.905	7.050	0.0264	44	0.124	405000	1.310
ditto	7.810	1.020	7.680	0.0270	45	0.121	505000	1.340
12/05/40	0.900	0.248	0.363	0.0298	41	7.340	2780	0.180
12/06/40	0.304	0.339	0.896	0.0302	41	1.660	9380	0.381
12/09/40	0.689	0.425	1.620	0.0304	44	0.644	22400	0.615
12/11/40	1.440	0.572	2.520	0.0300	44	0.354	46600	0.824
12/12/40	2.120	0.664	3.200	0.0298	45	0.254	69900	0.969
12/17/40	2.900	0.775	3.740	0.0298	46	0.217	97600	1.050
ditto	4.860	1.000	4.840	0.0303	47	0.169	167000	1.200
12/18/40	6.450	1.170	5.490	0.0304	44	0.154	211000	1.260
ditto	7.850	1.300	6.000	0.0309	45	0.145	261000	1.300

Table 15. Continued.

Rectangular shape, bed slope 3 percent (cont.)

Test Date	Discharge Q cfs	Cross Sectional Area A ft^2	Mean Velocity V ft/sec	Effective Slope S	Water Temp. °F	Friction Coefficient f	Reynolds Number R	Froude Number F
12/19/40	10.600	1.560	6.820	0.0310	44	0.138	345000	1.340
ditto	13.400	1.790	7.500	0.0307	44	0.129	435000	1.380
12/06/40	0.300	0.528	0.568	0.0298	41	3.610	5250	0.257
12/09/40	0.686	0.630	1.090	0.0296	44	1.160	12600	0.451
12/11/40	1.440	0.810	1.780	0.0296	44	0.560	26300	0.651
12/12/40	2.120	0.935	2.270	0.0295	45	0.398	39600	0.771
12/17/40	4.860	1.330	3.660	0.0294	47	0.217	93800	1.040
12/18/40	7.790	1.660	4.690	0.0300	46	0.168	148000	1.200
12/19/40	13.450	2.200	6.120	0.0300	44	0.131	248000	1.350
ditto	17.100	2.510	6.840	0.0294	44	0.117	313000	1.420
12/20/40	21.950	2.990	7.360	0.0284	47	0.117	424000	1.400
ditto	24.000	3.210	7.480	0.0270	48	0.115	473000	1.370
12/06/40	0.300	0.828	0.363	0.0292	42	7.910	3090	0.172
12/11/40	1.140	1.140	1.000	0.0294	44	1.390	11700	0.411
12/12/40	2.120	1.340	1.590	0.0293	45	0.669	22800	0.592
12/17/40	4.840	1.800	2.680	0.0294	48	0.315	55400	0.864
12/19/40	10.800	2.540	4.250	0.0305	44	0.184	115000	1.115
12/20/40	19.100	3.110	6.150	0.0332	45	0.118	207000	1.500
ditto	22.000	3.660	6.020	0.0316	48	0.137	251000	1.360
ditto	23.900	3.860	6.200	0.0312	49	0.135	277000	1.360

Table 15. Continued.

Trapezoidal shape, bed slope 0.2 percent

Test Date	Discharge Q cfs	Cross-Sectional Area A ft^2	Mean Velocity V ft/sec	Effective Slope S	Water Temp. °F	Friction Coefficient f	Reynolds Number R	Froude Number F
8/26/40	1.180	3.350	0.353	0.00188	75	2.150	19400	0.0842
9/30/40	1.290	3.480	0.372	0.00174	60	1.780	17100	0.0875
8/27/40	2.750	4.600	0.597	0.00202	73	0.957	39100	0.1290
ditto	4.720	5.800	0.813	0.00208	73	0.624	61300	0.1640
9/30/40	4.750	5.830	0.814	0.00192	60	0.565	51600	0.1640
8/28/40	10.100	8.550	1.180	0.00213	75	0.369	114000	0.2130
ditto	14.900	10.700	1.400	0.00199	79	0.282	157000	0.2380
9/30/40	15.100	10.800	1.400	0.00185	60	0.269	124000	0.2380
8/29/40	20.200	13.000	1.550	0.00178	77	0.229	192000	0.2510
ditto	25.100	15.400	1.640	0.00141	75	0.177	214000	0.2520
9/30/40	24.700	15.300	1.620	0.00144	60	0.179	173000	0.2500
9/03/40	30.400	17.700	1.710	0.00127	78	0.158	251000	0.2560
ditto	34.800	20.300	1.710	0.00111	79	0.144	272000	0.2470
9/20/40	35.700	21.000	1.700	0.00108	60	0.149	214000	0.2430

Table 16. Test and computed data on Bermuda grass with 5 percent bed slope in a rectangular channel [Palmer, 1946].

Discharge q cfs/ft	Average Depth y_o ft	Mean Velocity V ft/sec	Effective Slope S	Water Temp. °F	Friction Coefficient f	Reynolds Number R	Froude Number F
0.0011	0.0168	0.0655	0.0503	60*	50.8	90.9	0.0891
0.0028	0.0304	0.0921	0.0504	60	46.5	231	0.0932
0.0063	0.049	0.129	0.0503	60	38.4	521	0.102
0.0129	0.076	0.170	0.0502	60	34.1	1070	0.109
0.0263	0.124	0.212	0.0502	60	35.6	2170	0.106
0.0428	0.168	0.255	0.0502	60	33.5	3540	0.110
0.0010	0.0124	0.0806	0.0502	60	24.7	82.6	0.128
0.0025	0.026	0.0462	0.0503	60	36.4	207	0.105
0.0062	0.046	0.135	0.0504	60	32.9	512	0.111
0.0124	0.074	0.168	0.0506	60	34.4	1020	0.109
0.0287	0.130	0.221	0.0506	60	34.8	2370	0.108
0.0474	0.186	0.255	0.0506	60	37.3	3920	0.104
0.1200	0.325	0.369	0.0496	60	30.5	9920	0.114
0.0011	0.0186	0.0591	0.0511	60	70.0	90.9	0.0765
0.0029	0.0272	0.107	0.0510	60	31.4	240	0.114
0.0058	0.042	0.138	0.0510	60	28.9	479	0.119
0.0149	0.076	0.196	0.0510	60	26.0	1230	0.125
0.0283	0.117	0.242	0.0510	60	26.3	2340	0.125
0.0493	0.176	0.280	0.0510	60	29.5	4070	0.118
0.0931	0.266	0.350	0.0504	60	28.2	7690	0.120

Note: * 60° F assumed

Table 17. Variation of C values (Eq. 3) with bed slope S_o for Kentucky Blue grass and Bermuda grass.

S_o		C
0.1%	(0.001)	5,300
0.5%	(0.005)	14,800
2^o	(0.035)	58,000
5^o	(0.087)	105,000
6:1	(0.164)	155,000
3:1	(0.316)	218,000
1.5:1	(0.555)	335,000

GPO 910-499